

**TREG RECRUITMENT/INDUCTION FOR THE PREVENTION OF AN
EXPERIMENTAL INFLAMMATORY MODEL OF DRY EYE DISEASE**

by

Michelle Lynn Ratay

B.S., Point Park University, 2010

M.S., Duquesne University, 2011

M.B.A., Point Park University, 2012

Submitted to the Graduate Faculty of
The Swanson School of Engineering in partial fulfillment
of the requirements for the degree of
Doctor of Philosophy

University of Pittsburgh

2017

UNIVERSITY OF PITTSBURGH
SWANSON SCHOOL OF ENGINEERING

This dissertation was presented

by

Michelle Lynn Ratay

It was defended on

November 3, 2017

and approved by

Joel S. Schuman, M.D., Director of NYU Langone Eye Center, Professor of Ophthalmology
at NYU Langone Medical Center, NYU School of Medicine, Electrical and Computer
Engineering at NYU Tandon School of Engineering

Sanjeev Shroff, Ph.D., Gerald E. McGinnis Chair and Distinguished Professor, Department of
Bioengineering, and Medicine

Yadong Wang, Ph.D., McAdam Family Foundation Professor of Cardiac Assist Technology,
Nancy E. and Peter C. Meinig School of Biomedical Engineering

Dissertation Director: Steven R. Little, Ph.D., William Kepler Whiteford Professor,
Department of Chemical and Petroleum Engineering, Bioengineering,
Pharmaceutical Sciences, Ophthalmology, and Immunology

Copyright © by Michelle Lynn Ratay

2017

TREG RECRUITMENT/INDUCTION FOR THE PREVENTION OF AN EXPERIMENTAL INFLAMMATORY MODEL OF DRY EYE DISEASE

Michelle Lynn Ratay, Ph.D.

University of Pittsburgh, 2017

Dry eye disease (DED) affects more than 10 million individuals in the United States. DED originates from disruption of the immunological homeostasis of the lacrimal functional unit (LFU). This disruption stems from persistent infiltration of pro-inflammatory effector CD4⁺ T lymphocytes (Teff) into the LFU, and reduced numbers and/or function of immunosuppressive regulatory T cells (Tregs). Current clinical treatments block pro-inflammatory signaling but do not address the underlying immunological imbalance in DED. Notably, in a healthy state, the body utilizes sophisticated regulatory mechanisms that include Tregs to promote immunological balance. Indeed, *ex vivo* expanded Tregs, adoptively transferred into mice with induced DED, effectively ameliorates disease symptoms. Using living Tregs to dynamically and responsively manipulate the local immunological milieu to treat DED would represent a departure from traditional drug-based treatments. Although Treg cell therapy is an extremely promising treatment for DED, *ex vivo* Treg expansion has significant limitations, such as regulatory hurdles, Treg plasticity, and high costs. For these reasons, we developed several acellular approaches that utilize biodegradable microspheres composed of poly(lactic-co-glycolic acid) to release different factors capable of recruiting endogenous Tregs and/or inducing local Tregs in the ocular tissue to restore immunological homeostasis. To this end, our data suggest that controlled release systems can generate and sustain a biological gradient of the Treg-preferential chemoattractant, CCL22, recruiting endogenous Tregs. In turn, these “Treg-recruiting formulations” reduce the symptoms of DED when placed locally in the lacrimal gland in a

Concanavalin A-induced murine model of DED. Moreover, the local delivery of TGF- β , IL-2, and Rapamycin from similar controlled release systems induces local differentiation of naïve CD4⁺ T cells into FoxP3⁺ Treg, which in turn, prevents DED symptoms such as loss of tear production, maintenance of goblet cell density, and ocular surface damage. As an alternative approach to enhance Treg populations, we also investigated the administration of microspheres containing one factor, which may be more translational than three different factors, and demonstrated the prevention of signs of DED. Taken together, all of these microsphere formulations aim to mimic how the body resolves inflammation and may be a potential modern therapeutic engineered approach for DED.

TABLE OF CONTENTS

ACKNOWLEDGEMENTS	XIX
1.0 INTRODUCTION.....	1
1.1 ROUTES OF OCULAR ADMINISTRATION	3
1.2 ANTERIOR SEGMENT	3
1.2.1 Topical	3
1.2.2 Contact Lenses	6
1.2.3 Punctal Plugs.....	7
1.3 POSTERIOR SEGMENT	9
1.3.1 Topical and Systemic Administration.....	9
1.3.2 Intravitreal Injections	10
1.3.3 Intravitreal Implants.....	11
1.4 ENGINEERED DRUG DELIVERY SYSTEMS: MICROPARTICLES AND NANOPARTICLES	15
1.5 AGE-RELATED MACULAR DEGENERATION.....	17
1.5.1 Background on the Pathology of AMD.....	17
1.5.2 Anti-Inflammatory Therapy Based Treatments for Age-Related Macular Degeneration.....	20
1.5.2.1 Immunosuppressive Agent: Rapamycin	20
1.5.2.2 Doxycycline	21

1.5.3	Anti-Angiogenic Treatments for AMD.....	22
1.5.3.1	Sustained Delivery of a HIF-Antagonist	22
1.5.3.2	Anti-VEGF Therapy	22
1.5.4	Gene Therapy for AMD	23
1.5.5	Complement Inhibition	24
1.5.6	IL-18 Therapy	24
1.5.7	Cellular-Based Therapies.....	26
1.5.7.1	Human Embryonic Stem Cells (hESCs)	26
1.5.7.2	Induced Pluripotent Stem Cells (iPSCs)	27
1.5.7.3	Retinal Progenitor Cells (RPCs)	28
1.6	UVEITIS.....	30
1.6.1	Background on the Pathology	30
1.6.2	Anti-Inflammatory Based Treatments for Uveitis	35
1.6.2.1	Corticosteroids	35
1.6.2.2	Methotrexate.....	35
1.6.2.3	Mycophenolate mofetil	36
1.6.2.4	Cyclosporine	37
1.6.2.5	Tacrolimus	37
1.6.3	Biological Therapeutic Approaches	38
1.6.3.1	Anti-TNF- α	38
1.6.3.2	Anti-IL-2	39
1.6.3.3	Anti-IL-17A	40
1.6.3.4	Anti-CD28 - Abatacept	41

1.6.4	Engineering Approaches to Treat Uveitis	42
1.6.4.1	Fluocinolone acetonide implants – Retisert	42
1.6.4.2	Cyclosporine-Releasing Microparticles	44
1.6.5	Gene Therapy for Uveitis.....	46
1.7	DRY EYE DISEASE	47
1.7.1	Background on the Pathology	47
1.7.2	Anti-Inflammatory Based Treatments for Dry eye Disease	51
1.7.2.1	Lipids and LipiFlow.....	51
1.7.2.2	Corticosteroids	53
1.7.2.3	Doxycycline	53
1.7.2.4	Cyclosporine A	54
1.7.3	Contact Lenses	55
1.7.4	Biological/Small Molecule Antagonist Therapies	57
1.7.4.1	CCR2	57
1.7.4.2	Lifitegrast.....	58
1.7.5	Cell-Based Therapy	58
1.7.5.1	Regulatory T cells.....	58
1.8	CONCLUSION.....	60
2.0	CONTROLLED RELEASE OF TREG-RECRUITING MICROSPHERES FOR THE PREVENTION OF DRY EYE DISEASE.....	62
2.1	INTRODUCTION	62
2.2	MATERIALS AND METHODS.....	65
2.2.1	Fabrication of Microspheres.....	65
2.2.2	Characterization of Microspheres	67

2.2.3	Experimental DED Model and Treatments	67
2.2.4	Measurement of Tear Production	68
2.2.5	Corneal Permeability	68
2.2.6	Histopathology	69
2.2.7	Immunophenotyping Analysis by Flow Cytometry.....	69
2.2.8	Statistical Analysis.....	70
2.3	RESULTS.....	70
2.3.1	Characterization of Treg-recruiting Microspheres.....	70
2.3.2	Treg-recruiting microspheres Prevent Decrease in Tear Production, Corneal Staining, and Goblet Cell Depletion.....	73
2.3.3	Treatment with Treg-recruiting microspheres decreases the frequency of CD4 ⁺ T Cells in Regional Draining Lymph Nodes	78
2.3.4	Treatment with Treg-recruiting microspheres Reduces Infiltration of CD4 ⁺ IFN- γ ⁺ T cells in the Lacrimal Gland.....	80
2.3.5	Administration of anti-GITR Reverses the Effect of Regulatory T-cell Recruiting Formulations.....	82
2.4	DISCUSSION.....	84
3.0	TRI MICROSPHERES PREVENT KEY SIGNS OF DRY EYE DISEASE IN A MURINE, INFLAMMATORY MODEL	90
3.1	INTRODUCTION	90
3.2	MATERIALS AND METHODS.....	92
3.2.1	Fabrication of Microspheres.....	93
3.2.2	Characterization of Microspheres	94
3.2.3	Mice.....	95
3.2.4	Murine DED Model and Treatment	95
3.2.5	Suppression of Tregs via the Administration of Anti-GITR.....	95

3.2.6	Tear Production.....	96
3.2.7	Corneal Fluorescein Staining	96
3.2.8	Ocular Histology	96
3.2.9	qRT-PCR.....	97
3.2.10	Immunofluorescence of the Lacrimal Gland	97
3.2.11	Statistical Analysis.....	98
3.3	RESULTS.....	98
3.3.1	Characterization of TRI MS: IL-2, TGF- β 1 and Rapamycin	98
3.3.2	TRI MS Prevent Loss of Aqueous Tear Production	101
3.3.3	Goblet Cell Density Maintained with the Administration of TRI MS....	102
3.3.4	Corneal Fluorescein Staining Reduced with TRI MS.....	105
3.3.5	TRI MS Decrease Pro-Inflammatory Cytokines	108
3.3.6	TRI MS Increase the Percentage of FoxP3 ⁺ Tregs of overall CD3 ⁺ T cells in the Lacrimal Gland	109
3.3.7	Suppression of Tregs via Administration of Anti-GITR	111
3.4	DISCUSSION.....	112
4.0	CONTROLLED RELEASE OF AN HDAC INHIBITOR FOR REDUCTION OF INFLAMMATION IN DRY EYE DISEASE.....	116
4.1	INTRODUCTION.....	116
4.2	MATERIALS AND METHODS.....	118
4.2.1	Fabrication of HDACi Microspheres.....	119
4.2.2	Characterization of HDACi Microspheres.....	119
4.2.3	Mice.....	120
4.2.4	Murine Model	120

4.2.5	Tear Production.....	120
4.2.6	Corneal Fluorescein Staining	121
4.2.7	Ocular Histology	121
4.2.8	qRT-PCR.....	121
4.2.9	Suppression Assay	122
4.2.10	Statistical Analysis.....	123
4.3	RESULTS.....	123
4.3.1	Characterization of SAHA Microspheres	123
4.3.2	Aqueous Tear Production is Restored by SAHA Microsphere Treatment.....	125
4.3.3	The Administration of SAHA Microspheres Prevents Loss of Goblet Cell Density	126
4.3.4	SAHA Microspheres Decrease Corneal Fluorescein Staining.....	128
4.3.5	mRNA Expression Altered in the Lacrimal Gland with SAHA Microspheres.....	130
4.3.6	Lymphocyte Suppression Assay	132
4.4	DISCUSSION.....	134
5.0	CONCLUSIONS AND FUTURE WORK.....	139
	APPENDIX A	144
	BIBLIOGRAPHY	157

LIST OF TABLES

Table 1. Summary of AMD Treatments.	19
Table 2. Summary of Uveitis Treatments.	34
Table 3. Summary of Dry Eye Disease Treatments.....	50

LIST OF FIGURES

Figure 1. Schematic illustration of the overall structure of the eye.	5
Figure 2. Representative Image of the Anterior Segment of the eye and some examples of different routes of administration.....	8
Figure 3. Illustration of the Posterior Segment of the eye and a few examples of some methods of therapeutic administration.....	14
Figure 4. Characteristic features associated with the pathology of Age-Related Macular Degeneration. (A) Intermediate state of AMD with drusen (B) Loss of retinal pigment epithelial cells and choroidal vessels. (C) Neovascular AMD with retinal hemorrhage. Reproduced with permission. ^[160] Copyright 2009, Elsevier, The Lancet	20
Figure 5. (A) Representative images of fundus fluorescein angiography show a reduction of fluorescein stained lesions in the treatment (IL-18) group (B) The amount of fluorescein lesions were significantly decreased in the IL-18 group suggesting that the immunotherapy, IL-18, can prevent choroidal neovascularization. Modifications / Reproduced with permission ^[180] Copyright 2015, Investigative Ophthalmology and Visual Science.....	26
Figure 6. SEM micrographs of PLGA-based scaffolds fabricated using a phase-inversion technique. (A) Representative image of the water-exposed side. (B) Representative image of the glass side. (C) Representative image of the cross section. Reproduced with permission, can prevent choroidal neovascularization. Modifications/Reproduced with permission. ^[180] Copyright 2015, Investigative Ophthalmology and Visual Science.....	29

Figure 7. Images showing retinal inflammation characterizing EAU in mice at different time periods after immunization using IRPB. (A) Non-immunized mouse retina. (B) Mouse fundus (25 days post immunization) characterized by severe optic disk inflammation and vasculitis (white arrows). (C) Mouse fundus (60 days post immunization) characterized by retinal atrophy, vascular sheathing (white arrows), and small retinal infiltrates. (D) Mouse fundus (80 days post immunization) characterized by inferior vitreous infiltrates (asterisks) and vascular sheathing. (E) Mouse fundus (80 post immunization) characterized by multiple infiltrates. The blue arrow indicates an area of gliosis or scar. (F) Mouse fundus (90 days post immunization) characterized by vascular sheathing (white arrow) and multiple retinal infiltrates (white arrowheads). (G) Mouse fundus (120 days post immunization) characterized by large scars. (H) Mouse fundus (120 days post immunization) characterized by pigment deposition. (I) The retinal inflammation in the images was quantified with a clinical score and grouped according to the time period after immunization. Reproduced with permission.^[207] Copyright 2012, American Society for Investigative Pathology. 33

Figure 8. (A) Schematic and (B) site of implantation of Retisert. 43

Figure 9. Scanning electron microscopy images (SEM) of PLGA microparticles loaded with cyclosporine (A) SEM image of microparticles before the in vitro release assay (B) SEM image after two weeks of in vitro release (C) SEM image taken after two months of in vitro release (10 μ m scale bar). (D) Diagram showing the concentration of cyclosporine released overtime in different ocular tissues and blood subsequently after the cyclosporine microparticles are intravitreally injected for the treatment of uveitis. (\square) Iris-ciliary body; (\square) cornea; (Δ) conjunctiva; (O) aqueous humor; (\square) blood; (\square) vitreous body; (\bullet) choroid-retina; (\bullet) sclera; (\blacktriangle) lens. Reproduced with permission.^[86] Copyright 2006, Association for Research in Vision and Ophthalmology. 45

Figure 10. Representation of the LipiFlow Disposable. Black arrows show the Eye Cup and Lid Warmer. Reproduced with permission.^[114] Copyright 2012, Lippincott Williams & Wilkins. 52

Figure 11. Image of a hyaluronic acid-laden implant contact lens fabricated to enable the sustained delivery of hyaluronic acid while maintaining ideal optical properties over the pupil for accurate vision. Reproduced with permission.^[26] Copyright 2017, Elsevier 56

Figure 12. Synthesis strategy to recruit Tregs and shift T effectors and Treg balance for the prevention of dry eye disease. 64

Figure 13. Schematic of the Double Emulsion Fabrication Process of PLGA Microspheres for the encapsulation of an aqueous protein 66

- Figure 14. Characterization of engineered porous microspheres loaded with the chemokine CCL22 and blank microspheres. (A) Representative SEM image of porous blank microspheres (1000x) (B) Representative SEM image of porous microspheres with CCL22 encapsulated (1000x) (C) A representative particle size distribution obtained using a Coulter Counter shows the Treg-recruiting microspheres. (D) Release Kinetics of CCL22 (Treg-recruiting microspheres) from porous microspheres is shown (n=3). 72
- Figure 15. Treg-recruiting MS for preventing Dry eye Disease (DED) in mice. At Day 0, ConA and Treg-recruiting microspheres (MS) were injected into the lacrimal glands. 74
- Figure 16. Treg-recruiting MS prevent DED symptoms in mice. (A) Phenol red thread wetting measured in millimeters for aqueous tear production (n = 8) shown as mean \pm S.D. (B) A clinical score of the ocular surface staining scored on a scale of (0-4) (n = 8) show the integrity of the epithelial layer of the cornea. Green staining on the cornea is a positive indication of disease (n=8). * $p \leq 0.05$; ** $p \leq 0.01$; *** $p \leq 0.001$, **** $p \leq 0.0001$ 75
- Figure 17. Treg-recruiting MS prevent reduction of goblet cell density in the conjunctiva. Representative images of histological sections of the eyes (20X) were examined to identify differences in the Treg-recruiting MS group compared to the diseased groups (100 μ m scale bar). Goblet cells shown are the pink/purple cells located in the conjunctiva labeled with arrows and the groups are shown as mean \pm S.D. * $p \leq 0.05$; ** $p \leq 0.01$; *** $p \leq 0.001$, **** $p \leq 0.0001$ 77
- Figure 18. Treg-recruiting MS suppress T effector cells in the regional draining lymph nodes. (A) Data from flow cytometry performed on the regional draining lymph nodes in order to examine overall CD4+ T cell percentages (n=8) shown as mean \pm S.D. (B) IFN- γ cytokine expression was examined in the regional draining lymph nodes (n = 8) shown as mean \pm S.D. (C) Activated T effector percentages were analyzed using flow cytometry (n = 8) shown as mean \pm S.D. (D) FoxP3+ Tregs analysis on the regional draining lymph nodes using flow cytometry (n = 8) shown as mean \pm S.D. * $p \leq 0.05$; ** $p \leq 0.01$; *** $p \leq 0.001$, **** $p \leq 0.0001$ 79
- Figure 19. Treg-recruiting MS enhance anti-inflammatory responses in the lacrimal gland. (A) IFN- γ cytokine expression was analyzed in the lacrimal gland (n=8) shown as mean \pm S.D. (B) Analysis of intracellular staining for Tregs (n = 8) shown as mean \pm S.D. (C) The ratio of CD4+ FoxP3+/CD4+IFN- γ + cells in the lacrimal gland (n=8) shown as mean \pm S.D. * $p \leq 0.05$; ** $p \leq 0.01$; *** $p \leq 0.001$; **** $p \leq 0.0001$ 81

- Figure 20. Administration of anti-GITR reverses the prevention signs associated with DED by Treg-recruiting MS. (A) Quantification of corneal fluorescein staining shown as mean \pm S.D. (B) Representative images of corneal fluorescein staining shown as mean \pm S.D. (C) Aqueous tear production was quantified using phenol red threads (D) Goblet cells located in the conjunctiva were counted and data is shown as mean \pm S.D. (E) Representative histology images (20X) indicates arrows pointing to the pink/purple goblet cells (F) Data from flow cytometry was performed on the regional draining lymph nodes shown as mean \pm S.D. (G) Cytokine expression and Treg percentages were analyzed in the lacrimal gland shown as mean \pm S.D. * $p \leq 0.05$; ** $p \leq 0.01$; *** $p \leq 0.001$, **** $p \leq 0.0001$ 83
- Figure 21. Microspheres that release a combination of recombinant proteins and a synthetic drug in order to promote Treg differentiation. 92
- Figure 22. Characterization of Treg-inducing Microspheres (A) Representative Scanning electron microscopy (SEM) image of Rapamycin microspheres (1000x) (B) Representative SEM image of IL-2 Microspheres (1000x) (C) Representative image of TGF- β Microspheres. (D) Release Kinetics of Rapamycin Microspheres is shown (n=3) (E) Release Kinetics of porous IL-2 Microspheres (n=3) (F) Release Kinetics of TGF- β Microspheres (n=3). (G) Size distribution of Rapamycin Microspheres (H) Size distribution of IL-2 Microspheres (I) Size Distribution of TGF- β Microspheres..... 100
- Figure 23. TRI microspheres for the prevention of inflammation associated with Dry eye Disease (DED) in mice. A timeline for the experimental murine model of inflammation induce via Concanavalin A..... 102
- Figure 24. TRI MS prevent clinical signs of inflammation associated with DED (A) Wetting of phenol red threads were measured in millimeters using a dissecting microscope (n=6) shown as mean \pm S.D. (B) Representative images of histological sections of the eyes (20X) were quantified to identify differences in the TRI MS group compared to the diseased groups and non-diseased group (100 μ m scale bar). (C) Goblet cells shown are the pink/purple (Periodic Acid Schiff stained) cells located in the conjunctiva labeled with arrows and the groups are shown as mean \pm S.D. * $p \leq 0.05$; ** $p \leq 0.01$; *** $p \leq 0.001$, **** $p \leq 0.0001$ 103
- Figure 25. Single factors (Rapamycin; IL-2; TGF- β) and combinations of two factors (Rapa + TGF- β ; Rapa + IL-2; TGF- β + IL-2) were utilized to examine goblet cell density in the conjunctiva. (A) Representative images of single and combination factors of PAS stained goblet cells in the conjunctiva (B) Quantification of goblet cell numbers from the histology of the conjunctiva..... 104
- Figure 26. TRI MS reduce ocular surface staining (A) Representative images of corneal fluorescein staining. (B) Clinical corneal fluorescein staining scores of the ocular surface on a scale of (0-4) (n = 6) shown as mean \pm S.D. * $p \leq 0.05$ 106

- Figure 27. (A) Phenol Red Thread testing for the single factor (Rapamycin; IL-2; TGF- β) and combination of two factors (Rapa + TGF- β ; Rapa + IL-2; TGF- β + IL-2) experimental groups (n=6) (B) Ocular Surface Staining score (n=6) (C) Representative images of corneal fluorescein staining 107
- Figure 28. Administration of TRI MS reduces levels of cytokines in the lacrimal gland shown as mean \pm SEM. * $p \leq 0.05$ 108
- Figure 29. Representative lacrimal gland fixed frozen cryosections (10X magnification) stained for T-cells (CD3+ T cells-Cyan), Regulatory T-cells (FoxP3+ T cells - Red), and nuclei (DAPI-blue). Scale bars are 100 μ m. Quantification of lacrimal gland T cells per imaged field and % Treg, based on IHC images with FoxP3 staining (n=5). * $p \leq 0.05$; ** $p \leq 0.01$; *** $p \leq 0.001$ 110
- Figure 30. A tolerogenic antigen presenting cell (APC) can activate a naïve T effector (Teff) and under the treatment of an HDACi this can lead to non-polarizing conditions resulting in the induction of Tregs and can directly enhance the suppressive function of Tregs. 118
- Figure 31. Characterization of SAHA Microspheres. (A) Representative scanning electron microscopy (SEM) images (1000X) (B) Volume Impedance Measurements (Coulter Counter) of Blank Microspheres and SAHA Microspheres. 124
- Figure 32. Cumulative Release of SAHA Microspheres 124
- Figure 33. Tear Production is maintained with the administration of SAHA MS shown as mean \pm S.D (n=4-5 per group) Saline (non-diseased), ConA (diseased), Blank MS (diseased + unloaded microspheres), SAHA MS (diseased + SAHA microspheres). * $p \leq 0.05$ 125
- Figure 34. SAHA MS Preserve Goblet Cell Density in the Conjunctival Epithelial Layer. (A) Quantification of the Number of Goblet Cells per field shown as mean \pm S.D (n=5-8 per group). (B) Representative Histological Images of the goblet cells in the conjunctiva (10X) of Saline (non-diseased), ConA (diseased), Blank MS (diseased + unloaded microspheres), SAHA MS (diseased + SAHA microspheres) * $p \leq 0.05$ 127
- Figure 35. Corneal Fluorescein Staining is Reduced with the Administration of SAHA MS. (A) Corneal Fluorescein Staining scored on a scale of (0-4) shown as mean \pm S.D. (n=6). (B) Representative Corneal Fluorescein Images of Saline (non-diseased), ConA (diseased), Blank MS (diseased + unloaded microspheres), SAHA MS (diseased + SAHA microspheres) * $p \leq 0.05$; ** $p \leq 0.01$; *** $p \leq 0.001$ 129
- Figure 36. mRNA Expression is Altered in the Lacrimal Gland Tissue with the administration of SAHA MS shown as mean \pm S.D (n=4). * $p \leq 0.05$ 131
- Figure 37. Lymphocyte Suppression Assay. (A) Representative Flow Cytometry Histograms of T effector cells only untreated (no SAHA) and cells treated with 50nM and 200nM SAHA and bar graphs shown as mean \pm S.D. (B) Representative Flow Cytometry Histograms of 1:1 Treg: T effector cells untreated (no SAHA) and cells treated with 50nM and 200nM SAHA and bar graphs shown as mean \pm S.D. * $p \leq 0.05$; ** $p \leq 0.01$; *** $p \leq 0.001$. 133

- Figure 38. The reaction scheme of the Single-Walled Carbon Nanotubes reacted with fluorescein in the presence of boron trifluoride etherate. The reaction starting materials are SWNT functionalized with carboxylic acid groups (1.1% atomic weight) and fluorescein free acid (green compound), which is reacted via esterification reaction using a Lewis acid catalyst (boron trifluoride etherate). 147
- Figure 39. FT-IR spectra of functional groups contained on the starting materials and reaction of SWNT and fluorescein (A) (P3) SWNT starting material (B) SWNT mechanically ground with fluorescein as a physical mixture (1:4 ratio), and (C) the reaction product of SWNT and fluorescein (1:4 ratio) after esterification. 149
- Figure 40. Thermogravimetric Analysis (TGA) compares the stability of the (P3) SWNT (black) and the Reaction of SWNT and Fluorescein (green). The (P3) SWNTs have a higher thermal stability compared to the reaction of fluorescein SWNTs. The total weight loss difference between the SWNT and functionalized SWNT is 22% 151
- Figure 41. Raman spectrum examines the inherent structure and possible defects of (P3) SWNT (black) and reaction of SWNT and fluorescein (green). The 1590 cm⁻¹ peak typical of the graphene band (G band) and the 1390 cm⁻¹ peak typical of defect band (D band) are marked as well as the radial breathing mode (RBM) typical of thermal contractile nature of the nanotube, which is also highlighted in the insert..... 153
- Figure 42. UV-vis-NIR spectrum demonstrates the fluorescent properties of the (P3) SWNT (black), fluorescein (red), mixture of SWNT and fluorescein (1:4 ratio) (purple) and the reaction product of SWNT and fluorescein (green). The SWNT exhibit the signatures of the M11 (metallic) and S11 (semiconducting) bands. The fluorescein exhibits a peak corresponding to $\lambda_{max}/496nm$. The reaction of SWNT and fluorescein produces the signature bands of nanotubes and a slight shift in the fluorescence of fluorescein. 155

ACKNOWLEDGEMENTS

First and foremost, I thank my advisor, Dr. Steven R. Little, for the opportunity to pursue my Ph.D. and his tremendous support, patience, and guidance as a mentor. Steve has been an excellent mentor; providing integral direction to enhance my writing, communication, analytical, and problem-solving skills. My dissertation would not have been possible without his guidance. I also want to thank my committee members, Dr. Sanjeev Shroff, Dr. Yadong Wang, and Dr. Joel Schuman for their support and instrumental mentorship throughout my Ph.D. dissertation.

I would also like to acknowledge all the lab members of the Little lab for their support, insightful scientific comments, and assistance over the years. Thank you to the CTSI program for their financial and academic support, which provided me with many opportunities for professional growth and development. My sincere thanks to the ophthalmology core for providing the resources to enhance the research through the imaging, histology and flow cytometry facilities.

On a personal note, I would like to thank my family and friends whom served as a continued motivation and support system, in particular, my growth group and bible study group. I would also like to especially thank my parents, Pat and Sandy, whom their patience, encouragement, and love has helped me throughout my graduate career. I love them so much, and I am incredibly thankful for their unconditional love, prayers, and providing a solid faith

foundation. Also, I would like to thank my sisters, Lori and Sheri, whom are my best friends that have provided support, encouragement and love. I would like to thank my husband, Jeff, for his tremendous support, encouragement and love. There are no words to adequately convey how much I love you and appreciate your support. Most of all, I would like to thank God, whom is my Heavenly Father and the author of salvation.

1.0 INTRODUCTION

This chapter is adapted from Michelle L. Ratay, Elena Bellotti, Riccardo Gottardi, and Steven R. Little. (2017). Modern Therapeutic Approaches for Non-Infectious Ocular Diseases Involving Inflammation. *Advanced Healthcare Materials*. <https://doi.org/10.1002/adhm.201700733>

With the global ophthalmic drug delivery market estimated to grow at two-and-a-half times the overall rate of the pharmaceutical industry, many commercial opportunities exist for the development of new ophthalmic drugs.^[1] Ideal candidates for improved drug delivery treatments are those ocular diseases that drastically affect patients' quality of life including dry eye disease (DED), age-related macular degeneration (AMD), and uveitis.^[2-4] These three common ocular diseases affect different regions of the eye and have immuno-mechanistic characteristics in their disease pathogenesis. For instance, DED affects the ocular surface and is thought to be primarily due to inflammation mediated by T cell infiltration.^[5,6] Although, the disease pathogenesis of uveitis is also thought to be mediated via T cells, inflammation occurs in the uveal tract of the eye. On the other hand, AMD primarily afflicts the macula tissue of the eye, and is thought to be caused by the complement immune system (innate immunity), chronic oxidative stress, and neovascularization.^[7,8] Though, all these diseases affect different regions of the eye and possess different pathology, one common underlying link associated with these ocular diseases is the involvement of inflammation.^[7,9,10] When properly regulated, inflammation is both healthy and essential for the elimination of pathogens and healing. However, excessive, unregulated

inflammation can lead to chronic diseases where immune-mediated damage to the ocular tissues elicits an inflammatory response that causes further damage.^[11-13] In order to either treat the damage caused by unregulated inflammation or halt the inflammatory cycle, current and new therapies have been developed.^[7,14,15] Moreover, these current/new therapies (modern therapeutic approaches) are interdisciplinary in nature, utilizing a combination of synthetic materials, cells, biologics and small molecule based treatments in order to address the underlying inflammatory imbalance. Ultimately, these modern therapeutic approaches can even be inspired by the body's own method of restoring homeostasis. Specifically, some of the methods of administration for these modern therapeutic approaches include: topical administration, injections, contact lenses, and implants.^[16,17] However, there are several limitations associated with these methods of drug administration, such as anatomical barriers, poor bioavailability, and patient compliance issues. For this reason, new treatment strategies intend to address one or more of these barriers. In this chapter, we will discuss the challenges of ocular drug delivery, and the currently used (and also new, investigative) treatments aimed at targeting the pathological factors of dry eye disease, age-related macular degeneration, and uveitis.

1.1 ROUTES OF OCULAR ADMINISTRATION

1.2 ANTERIOR SEGMENT

1.2.1 Topical

A key challenge of ocular drug delivery systems for the treatment of diseases affecting the anterior segment of the eye is to obtain therapeutic levels of drug in the ocular tissues shown in **Figure 1**, while minimizing systemic side effects.^[18] Indeed, even the currently approved therapies for pathologies of the anterior portion of the eye (ex: DED and anterior uveitis), are plagued by short resident time on the ocular surface and poor bioavailability.^[19]

Currently, the standard of care for the treatment of diseases affecting the ocular surface and the anterior segment is the topical administration of ophthalmic medications such as eye drops, suspensions, gels, or ointments as shown in **Figure 2**.^[18] Although topically administered drugs are generally well accepted and tolerated methods of delivering medication by patients, a major limitation is patient compliance, especially for individuals affected by chronic pathologies such as uveitis, and DED.^[19,20] In fact, these pathologies require the self-administration of topical medication several times a day, which can severely decrease patient compliance.^[21] Moreover, this frequent dosing may cause either systemic or local side effects due to the high amounts of total drug administered. Another limitation of topical formulations is their low bioavailability at the site of action.^[22] In particular, it is reported that approximately only 5-10% of the administered drug reaches the target tissue, while the remaining 90-95% is eliminated.^[23] This elimination occurs through natural, precorneal mechanisms of protection from foreign substance such as drainage through the nasolacrimal duct, blinking, tear film, tear turn over, and induced lacrimation as displayed in **Figure 1**.^[24-26] In particular, after the administration of an ophthalmic

medication, the drug is first diluted in the lacrimal fluid, which reduces the effective concentration of the applied drug. Moreover, the precorneal tear drainage washes away topical medication within the first 15-30 seconds after application, reducing the amount of time the drug remains in contact with the ocular surface, and absorption.^[27] Furthermore, another factor reducing the effectiveness of topical eye drops is the anatomic volume of the cul-de-sac, which is approximately 7-10 μL , while the dosing volume of instillation is approximately 20-50 μL .^[25] This difference leads to either the spill of the excess volume on the cheek or to a rapid elimination through the nasolacrimal duct.^[25] Despite these limitations, topical administration of ophthalmic drugs is still the most widely prescribed route of administration as it offers numerous advantages including noninvasiveness, ease of administration, and low absorption into systemic circulation.^[18] Examples of topical ophthalmic drugs are those used for pathologies affecting the surface of the eye, such as DED, in which artificial tears and lubricants are topically administered to relieve symptoms.^[28] However, the development of new methods to enhance drug bioavailability and reduce the frequency of drug administration would greatly improve patient compliance and overall effectiveness of treatment. Thus, in order to improve patient compliance and enhance ocular drug bioavailability new alternative approaches have been developed, which will be discussed in following sections of this chapter.

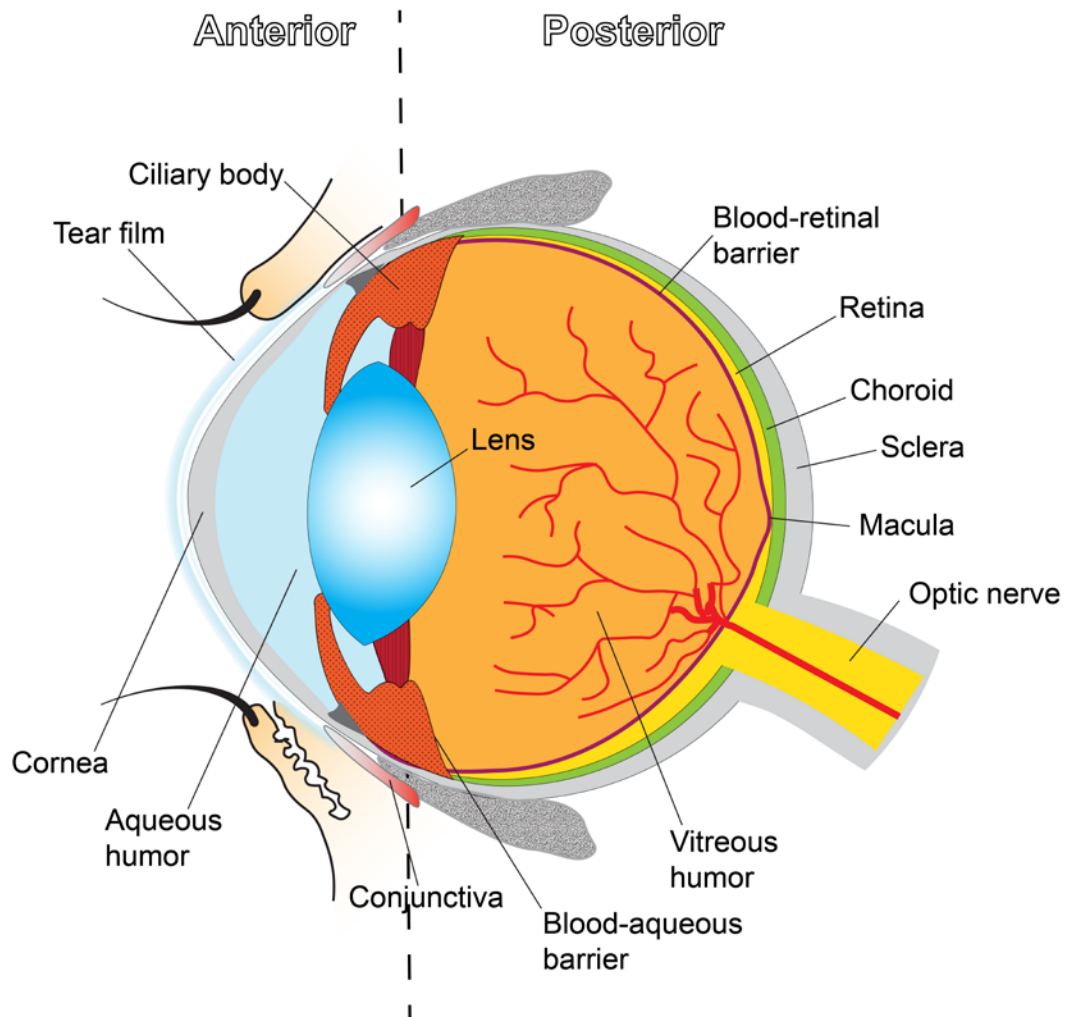


Figure 1. Schematic illustration of the overall structure of the eye.

1.2.2 Contact Lenses

Therapeutic contact lenses as represented in **Figure 2** have been widely studied for controlled and sustained drug delivery in order to overcome the limitations associated with topical eye drops.^[29] Since contact lenses can be worn for a longer length of time, their use for the release of an ophthalmic medication helps to improve patient compliance by reducing the frequency of administration.^[30] Furthermore, in comparison to eye drop formulations, contact lenses allow an increased residence time associated with greater than 50% more bioavailability at the site of action.^[30] Consequently, the administered dosage to obtain therapeutic levels at the desired site can be reduced, limiting systemic absorption and its associated side effects.^[30] Thanks to these advantages, drug loaded contact lenses are under investigation as a possible drug delivery system for pathologies affecting the surface of the eye such as DED. In particular, contact lenses for the release of cyclosporine have been studied in order to provide increased ocular contact time thus enhancing the drug bioavailability, in addition to a controlled and sustained drug release profile.^[31]

The simplest way to obtain drug-loaded contact lenses is by absorption of the drug (soaking the lens into a drug solution), which will be then released on the ocular surface.^[30] The ability to load the drug into the contact lens strongly depends on the water content, thickness, concentration of drug solution, molecular weight of the drug, and soaking time.^[30] Over the years, this technique has been used for loading contact lenses with different ophthalmic medications such as timolol, cyclosporine, and dexamethasone.^[31–35] Despite the simplicity of fabricating a soaked contact lens, it can take a few hours to absorb the drug, and the amount of drug that can be incorporated in the lens matrix is low, especially for hydrophobic drugs.^[36] Moreover, when the drug is incorporated into the lens matrix by soaking, it can quickly diffuse

out of the lens, with release times typically limited to a few hours.^[36] Therefore, contact lenses could be a promising device to achieve sustained delivery of ophthalmic medications. However, their commercialization is still limited because of the need to address some issues that negatively impact lens properties such as transparency, ion and oxygen permeability, water content, and mechanical properties, each of which is coupled to the properties of the drug and the amount of drug that is loaded.^[30] For this reason, alteration of any of these critical properties of contact lenses could result in affected visual ability in patients, presenting significant design challenges for long-term delivery with large amounts of loaded drug.

1.2.3 Punctal Plugs

Punctal plugs as shown in **Figure 2** are a non-invasive therapeutic method and generally well accepted by both patients and physicians, and were originally used for treating DED by blocking tear drainage, thus improving tear film quantity and residual contact time.^[37] Recently, punctal plugs have been proposed for the controlled release of topically administered medications to the ocular surface.^[38,39] For this purpose, punctal plugs are generally coated on all sides (except the head portion) with a material that is impermeable to the tear fluids and the drug. Release is controlled through diffusion of drug following contact of the head of the plug with tear fluid. Common issues associated with the use of punctal plugs are eye irritation, excessive tearing, ocular discomfort, and spontaneous loss of the plug from the punctum.^[19,40,41] However, drug eluting punctal plugs could offer a new approach for the treatment of chronic pathologies, thanks to several potential advantages over topical administration such as dose reduction, controlled release of drugs, reduction in the frequency of administration and potentially better patient compliance with the therapy.^[41]

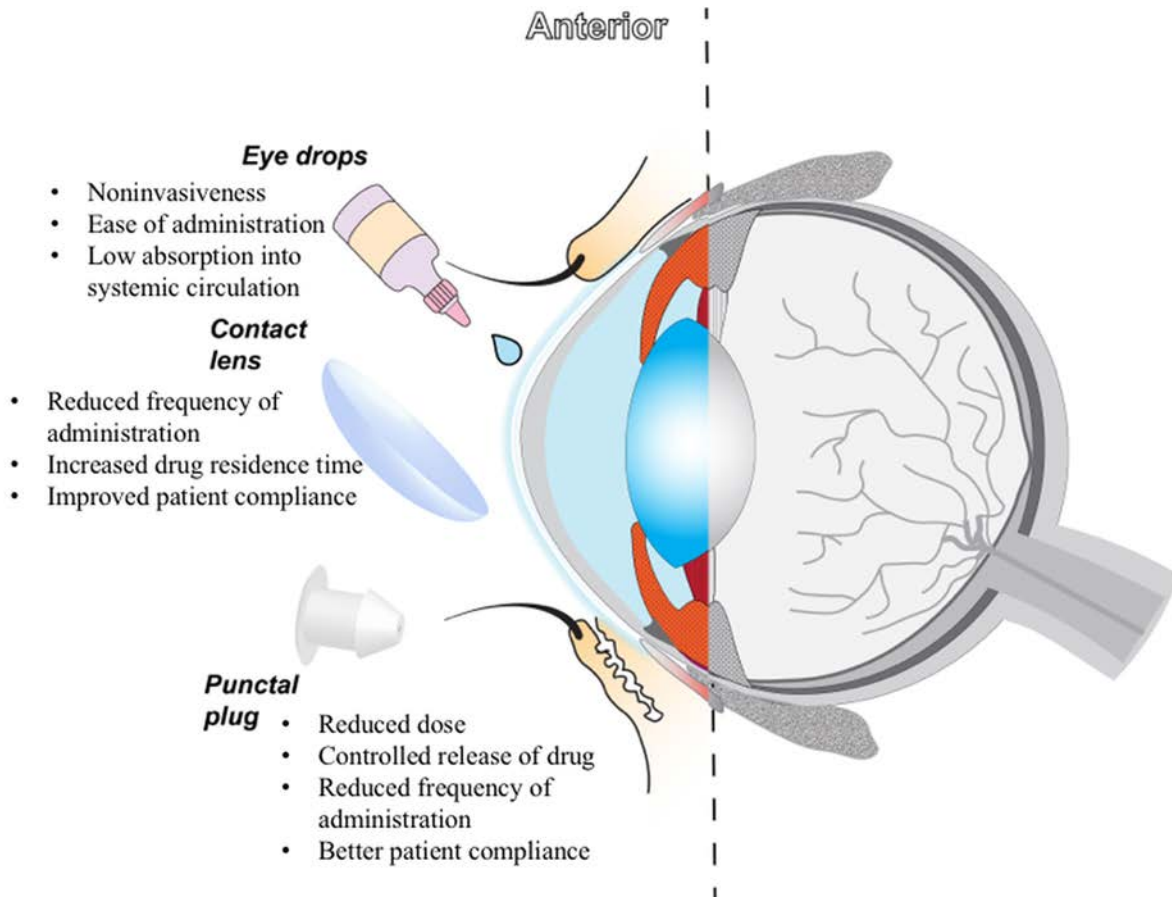


Figure 2. Representative Image of the Anterior Segment of the eye and some examples of different routes of administration.

1.3 POSTERIOR SEGMENT

1.3.1 Topical and Systemic Administration

Treating the less accessible posterior segment of the eye is more challenging for topical delivery than addressing anterior diseases, due to the longer diffusional distance, that the drug has to overcome before reaching the posterior tissues, characterized by additional physical and diffusional barriers.^[42,43] In particular, topical administration is inefficient in delivering medications to the posterior segment because of the rapid drainage through the nasolacrimal ducts, as discussed in section 1.2.1.^[44] To reach the posterior segment of the eye, a topically administered drug must penetrate through the cornea shown in **Figure 1**, which represents a barrier from external agents that naturally serves to hinder the transport of either exogenous substances from the pre-corneal pockets.^[45,46] The cornea allows for only the passage of small, moderately lipophilic molecules, while drug solutions made of macromolecules can often penetrate through the cornea only at very low rates, making it difficult to achieve therapeutic efficacy.^[45] An additional challenge for topically administered drugs to reach the intraocular environment is represented by the blood-aqueous barrier shown in **Figure 1**, consisting of endothelial cells in the uvea and of the non-pigmented layer of the ciliary body epithelium. Specifically, the blood-aqueous barrier forms tight junctions that regulate the exchange of solutes between the anterior and posterior segments, thus impeding nonspecific drug penetration into the inner ocular tissues.^[47,48]

Another possible approach for locating drug molecules to the back of the eye consists in systemic administration (intravenous or oral), however the delivery is limited by blood dilution of the drug, presence of inner and outer blood-retinal barriers shown in **Figure 1**, and in the case

of the oral route, and gastrointestinal barriers.^[49] The presence of these anatomical barriers requires a high drug concentration circulating in the plasma to achieve therapeutic levels in the eye, and such high doses may result in systemic side effects.^[49,50] Consequently, treating disorders that affect the posterior segment of the eye would greatly benefit from specific localized targeting that could be achieved (for instance) by the more invasive intravitreal injections and implants.

1.3.2 Intravitreal Injections

Intravitreal injection as represented in **Figure 3** is a route of administration that intends to target the posterior segment of the eye. This approach consists in a direct delivery of the drug to the vitreous, thereby avoiding passage through the ocular barriers and (in turn) leading to a high availability of the ophthalmic medication in the posterior segment tissues.^[51] Intravitreal injections are currently used for the administration of anti-VEGF drugs for the treatment of AMD and macular edema.^[52,53]

Despite the advantage of delivering medication locally, intravitreal injections are considered an invasive procedure with consequent potential complications, such as raised intraocular pressure (IOP), transient blurry vision, retinal detachment, and cataracts.^[54] Moreover, several injections are often needed to ensure optimal therapeutic drug levels at the site of action due to the short half-life of most ophthalmic drugs, thus increasing the risks of side effects and decreasing overall patient compliance.^[17,55,56] Therefore, alternative methods to deliver ophthalmic formulations to the posterior segment that require less frequent dosing could be extremely beneficial for patients, with the advantage of avoiding the aforementioned complications related to repeated injections, and reducing the risk of rapid clearance.

1.3.3 Intravitreal Implants

Intravitreal implants can be used as controlled/sustained drug delivery systems that can overcome several limitations of topically, systemically, and intravitreal administered medications.^[57] If designed appropriately, implants have the potential to promote the sustained delivery of relatively steady therapeutic levels of drug to the site of action over long periods of time with only one implantation procedure. Moreover, a significantly lower amount of drug is required (due to reduction in clearance and protection of the unreleased dose), thereby reducing the associated potential risks of systemic administration and intravitreal injections.^[57]

Intravitreal implants are classified as either non-biodegradable or biodegradable polymeric devices and are each capable to release drug molecules from a few months to several years depending upon the design.^[21] Typically, non-biodegradable implants can be utilized to achieve a slower rate of release over a longer period of time than biodegradable implants, however, they require surgical removal once the loaded drug is exhausted.^[57] A non-biodegradable implant containing fluocinolone acetonide (Retisert, Bausch & Lomb, Rochester, NY, United States) was the first to be approved by the FDA for the treatment of severe, non-infectious uveitis.^[58] Vitrasert® (Bausch & Lomb, Rochester, NY, United States) is another example of a non-biodegradable implant. Specifically, Vitrasert® is the first implantable ganciclovir delivery system approved for the treatment of cytomegalovirus retinitis. Clinically used in the United States since 1996, Vitrasert® releases the drug over a period of eight months.^[59] Overall, non-biodegradable implants have been demonstrated to be a valid alternative to intravitreal injections to obtain prolonged release of the therapeutic in the posterior segment with only one implantation procedure. However, despite the safety and efficacy demonstrated by non-biodegradable implants, surgical removal can lead to ocular complications.^[57] Hence,

biodegradable implants that ultimately do not need to be removed (and refilled and re-implanted or otherwise replaced when the drug is exhausted) would be a highly desirable alternative. Biodegradable implants are generally composed of biocompatible polymers that either degrade into non-toxic byproducts, or solubilize *in vivo* and can be eliminated safely by the human body, thus avoiding permanent chronic foreign-body reaction.^[60] One of the most commonly utilized biodegradable polymers for controlled release formulations is poly (lactic-co-glycolic) acid (PLGA), which is FDA approved for a number of applications.^[60-62] PLGA degrades into acidic byproducts such as lactic acid and glycolic acid, and although adverse reactions are generally mild to non-detectable, the context will dictate the importance of these effects.^[63,64] Notably, the biocompatibility of PLGA has been investigated in ocular tissues and has shown to possess greater tolerability than when placed in non-ocular tissues, explaining why it is still one of the most widely utilized biodegradable polymers for controlled release today.^[60]

One example of a biodegradable implant is represented by the bioerodible Ozurdex (Allergan Inc., Irvine, CA, United States), approved by the FDA for the treatment of uveitis and macular edema.^[65] It consists in a PLGA matrix that releases dexamethasone for up to four months.^[65] Recently, the use of Ozurdex has been investigated as additional therapy in patients affected by AMD and refractive to ranibizumab.^[66] The results of the study suggest the effectiveness of the dexamethasone-based implant in stabilizing vision, thus encouraging further investigation of the use of Ozurdex as a possible treatment for AMD.^[66] Despite the advantage of requiring only one procedure to be implanted, biodegradable implants (like non-degradable implants) can still move from the original site of injection/implantation in the intraocular environment. Also, if not designed properly, a sudden increase of drug release may occur.^[65] However, recent studies have shown how these matrices degrade, which can be correlated to

initial conditions such as the polymer molecular weight distribution, polymer type, copolymer ratio, size, shape, and type of drug.^[67-69] More so, these properties can be tuned to not only eliminate burst effect, but also to provide a customized release profile for practically any drug.^[67-69] Overall, both non-biodegradable and biodegradable implants represent potential advantages and disadvantages, and represent a potential solution to the many limitations associated with traditional methods of administration of ophthalmic drugs.

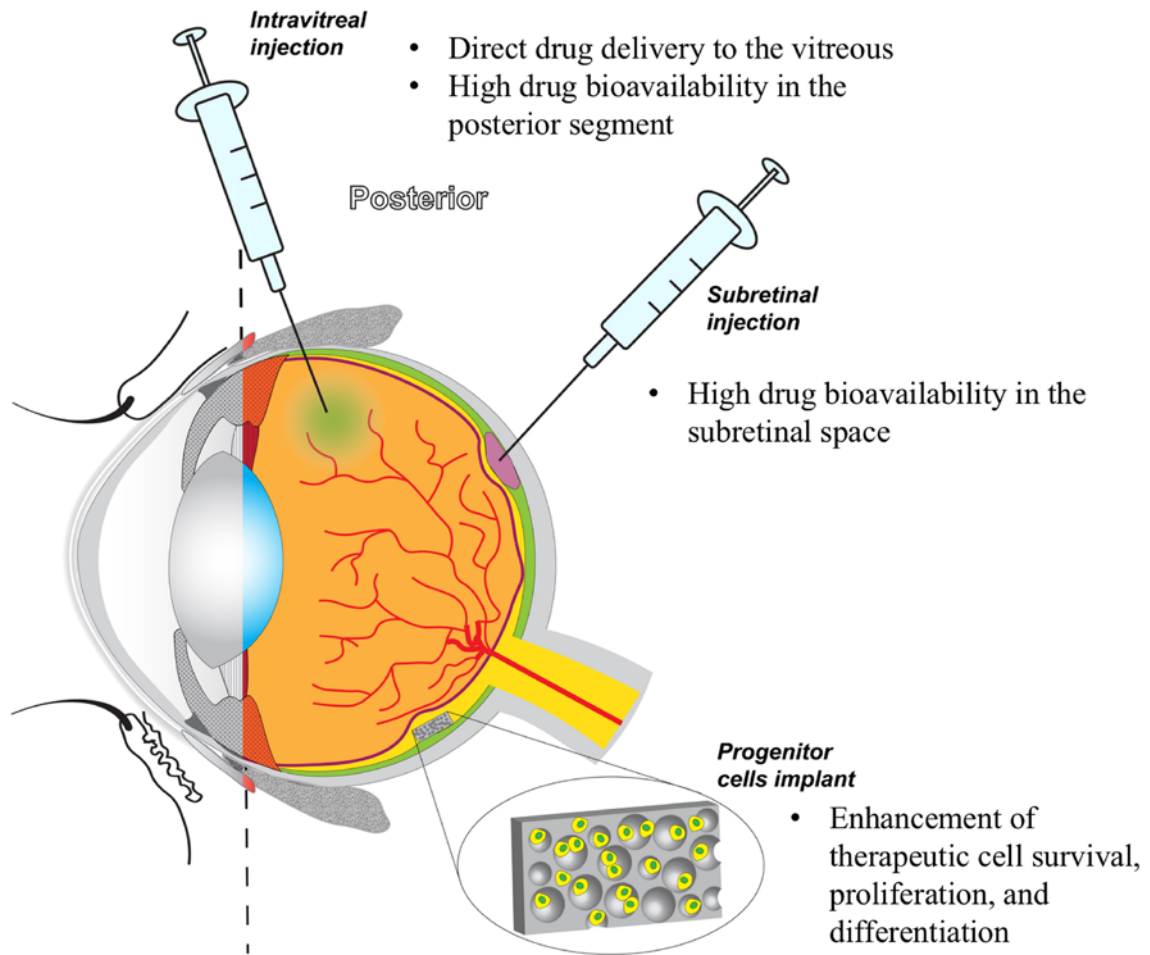


Figure 3. Illustration of the Posterior Segment of the eye and a few examples of some methods of therapeutic administration.

1.4 ENGINEERED DRUG DELIVERY SYSTEMS: MICROPARTICLES AND NANOPARTICLES

New biodegradable polymeric carriers with convenient size/shape, such as microparticles with size in the range of 1-1000 μm and nanoparticles with size of less than 1 μm , represent a promising tool for ocular drug delivery.^[70-74] In particular, micro- and nanoparticles enable the achievement of sustained intraocular therapeutic drug concentrations without requiring the surgical implantation of a drug delivery device (as they can be injected through a needle and syringe), offering a release of drug that can last for weeks or even months.^[57,70,75] Particulates are most often administered intravitreally as a less invasive procedure compared to surgical implantation.^[57] Moreover, these particular drug delivery systems can be engineered to target certain cells type, reducing the risks of systemic side effects.^[57] Micro- and nanoparticles can be classified as “micro- and nanospheres”, and “micro- and nanocapsules”.^[76] In particular, in micro- and nanospheres, the drug and polymer are typically combined, and the drug is dispersed throughout the polymeric matrix.^[76] In such a matrix system, the release of the active molecules is controlled by diffusion through the polymer matrix with simultaneous polymer degradation, which will non-linearly increase the diffusivity over time.^[77] On the other hand, in micro- and nanocapsules, the drug particles or droplets are entrapped in a polymeric membrane.^[76] Active molecules can be encapsulated in micro and nanocapsules via an emulsion-diffusion procedure (for example) while solvent evaporation techniques are used to fabricate drug-loaded micro and nanospheres (for example).^[78,79]

Micro and nanoparticles can be formulated from a variety of polymeric materials. However, the most commonly used synthetic polymers consist in aliphatic polyesters such as polycaprolactone (PCL) polylactic acid (PLA), polyglycolic acid (PGA), and PLGA, due to the

advantages that characterized such polymers, as stated in the previous section.^[80-82] As discussed in the prior section, the desired drug release profile can be engineered through varying the molecular weight of the polymer and copolymer formulation (as well as other formulation variables), allowing the tuning of the duration of release that can range from weeks to months.^[83] One example of PLGA microspheres that are capable of providing one-month of release of an ophthalmic medication following subconjunctival injection has been recently developed.^[84] Specifically, an *in vitro* study suggests that sustained release of the drug can be achieved with an amount of medication that is well above the lower limit of absorption for the entire period of the study.^[84] Moreover, microspheres that were subconjunctivally injected in New Zealand white rabbits led to no observable foreign body response or infection over the course of one month.^[84] Additionally, PLGA-based release systems have been studied as a promising candidate for the treatment of DED and uveitis, and they have been demonstrated a valid candidate for sustained release of therapeutics after a single administration through injection into ocular tissues.^[85,86] In addition, a unique gelling, eye drop-like formulation has been recently reported that is able to comfortably retain the therapeutic drug in the lower fornix (topically) for a period of one month, while simultaneously releasing glaucoma medication over the period of time (without any injection into the ocular tissues).^[87] Although micro- and nanoparticles seem to possess significant potential as ocular drug delivery systems, limitations include encapsulation efficiency of drug (especially in smaller, nanoparticle formulations with high surface area), stability of the molecules during particle fabrication, control of particle size and drug release rate, and large-scale manufacturing of sterile preparations.^[83]

1.5 AGE-RELATED MACULAR DEGENERATION

1.5.1 Background on the Pathology of AMD

Age-Related Macular Degeneration (AMD) is the leading cause of blindness in the elderly population with an average estimated Medicare cost of 724 million dollars in the United States alone.^[88,89] The disease affects the central areas of the macula region of the retina, composed of light sensing cells that enable central vision.^[90] When the central area of the macula is impacted, retinal pigment cells begin to slowly degenerate leading to blurry central vision and metamorphopsia (a type central visual distortion).^[90] Although, most vision loss occurs in the advanced stages of the disease, the early onset can be characterized by the presence of drusens (hard/soft yellow deposits formed from acellular debris under the retina) and/or retinal pigmentary abnormalities as shown in **Figure 4**.^[8,91] As the disease progresses this can lead to a chronic inflammatory response, resulting in the formation of retinal atrophy (also known as “geographic atrophy”), and/or the secretion of angiogenic cytokines (ex: vascular endothelial growth factor-VEGF). Ultimately, these pathological features have been classified into two distinct, advanced clinical classification stages.^[91]

The two advanced stages of the disease are characterized as either dry/non-neovascular AMD or wet/neovascular AMD seen below in **Figure 4**.^[91] Dry/non-neovascular AMD causes slow degradation of vision due to the loss of photoreceptors and development of geographic atrophy.^[91] On the other hand, wet/neovascular AMD is characterized by choroidal neovascularization, leading to sub retinal fluid, retinal pigment epithelium detachment, and formation of fibrotic scars as shown in **Figure 4**.^[8,89] Typically, these clinical signs can be diagnosed during examination using fluorescent angiography (fluorescein highlights leaky

vessels), which is a useful diagnostic tool to identify choroidal neovascularization, and optical coherence tomography (OCT) to detect thinning of the macula tissue.^[91] Upon diagnosis, preventative therapies such as PreserVision (a vitamin and mineral supplement), may be prescribed to abate the risk of advanced stage AMD and the associated vision loss.^[92] However, this therapy may not be useful for all patients. For instance, the use of supplements such as beta-carotene can increase the risk of lung cancer in smokers.^[91] In addition, high doses of vitamin E can increase the risk of heart failure in patients with diabetes and heart disease.^[91]

Due to the potential side effects, studies have examined the pathogenesis of the disease in order to develop new effective therapies.^[93-95] New studies of AMD progression suggest that disease is associated with higher levels of biomarkers that are indicative of inflammation.^[7] It is currently thought that the activation of the innate immune system, upregulation of complement factors, and the secretion of chemokines and cytokines lead to ocular tissue damage in AMD.^[7,11] Although the full pathogenesis has not been elucidated, current (and experimental) treatments have attempted to address the local inflammation in order to decrease the progression of vision loss displayed in **Table 1**.^[11,90,96]

Table 1. Summary of AMD Treatments.

Treatment	Type of Study	Results	Ref.
Rapamycin	Preclinical- Rat	The oral administration of rapamycin was able to lessen abnormalities of the retinal tissue observed in ocular histological sections.	[97]
Doxycycline	Murine	Lower expression levels of M-2 type macrophages markers such as Arg1 and reduced neovascularization were detected with the administration of doxycycline.	[98]
HIF-Antagonist	Murine	The hypoxia-inducible factor (HIF-1) antagonist has shown to reduce levels of pro-angiogenic factors in choroidal neovascularization and may serve as a treatment for wet AMD.	[99]
Anti-VEGF	Clinical	Ranibizumab (Lucentis) and Bevacizumab (Avastin) are both VEGF-A monoclonal antibodies, which have demonstrated clinical efficacy as a therapy for wet AMD. Although, this treatment may lead to hemorrhage and cataract formation.	[52,100]
Gene Therapy	Murine	Preclinical and phase I human trails demonstrated that an adenoviral vector expressing pigment epithelium-derived factor (PEDF) lessened choroidal neovascularization.	[101]
Complement Inhibition		In Phase II clinical trials, Lampalizumab (a humanized monoclonal antibody fragment) has shown to inhibit a component of the complement immune system thereby reducing geographic atrophy observed in AMD.	[93,102]
IL-18	Murine/Primate	Administration of IL-18 reduced choroidal neovascularization in non-human primates.	[103]
Human Embryonic Stem Cells (hESCs)	Rodent/Clinical	Transplanted hESCs in the subretinal space of rodents was able to maintain visual function. In addition, to assess safety of transplanted hESC-derived RPE in humans, a clinical trial was performed. The subjects did not have any adverse effects from the stem cells.	[104,105]
Induced Pluripotent Stem Cells (iPSCs)	Human	An iPSC trial completed in Japan demonstrated that the stem-cells were able to prevent the loss of vision in a woman with AMD. Although, the genetic mutations were observed in the cells of the other trial subject and thus the trial was halted.	[106,107]
Retinal Progenitor Cells (RPCs)	Murine	A scaffold composed of poly (lactic) acid and poly (lactic-co-glycolic) acid seeded with RPCs was able to enhance survival of RPCs. Additionally, a polycaprolactone scaffold was utilized to seed stem cells.	[108–110]

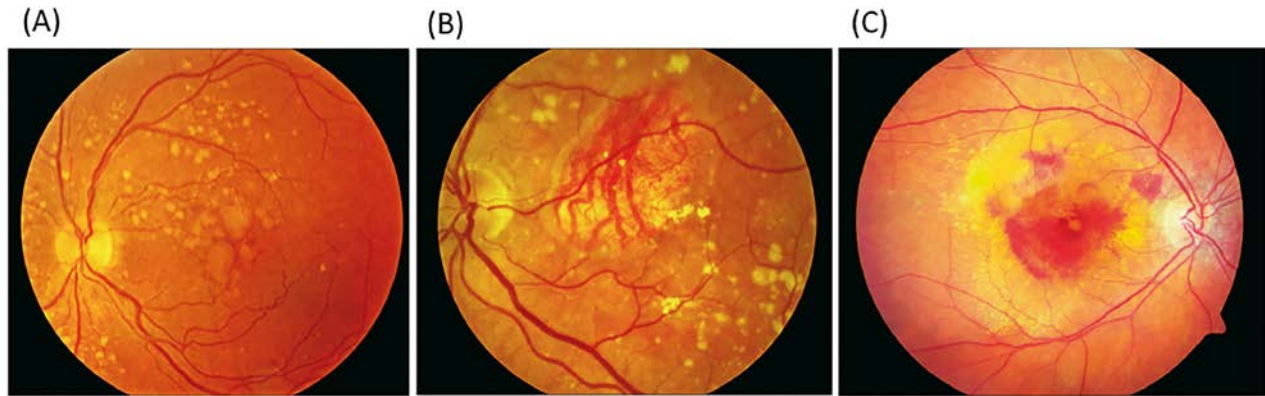


Figure 4. Characteristic features associated with the pathology of Age-Related Macular Degeneration. (A) Intermediate state of AMD with drusen (B) Loss of retinal pigment epithelial cells and choroidal vessels. (C) Neovascular AMD with retinal hemorrhage. Reproduced with permission. ^[160] Copyright 2009, Elsevier, The Lancet

1.5.2 Anti-Inflammatory Therapy Based Treatments for Age-Related Macular Degeneration

1.5.2.1 Immunosuppressive Agent: Rapamycin

Rapamycin (Sirolimus) is an immunosuppressive treatment utilized for a several conditions, such as organ transplantation and ocular inflammatory diseases.^[11,111,112] Rapamycin inhibits a downstream target known as mTOR (mammalian target of rapamycin) that is needed for upregulation of IL-2 production, which sustains T cell activation and proliferation.^[111] The mTOR pathway has also been linked to effects on cellular aging; therefore, mTOR inhibitors,

such as rapamycin, prevent the conversion of quiescence to senescence, which has revealed to slow down aging in mice.^[97] Slowing down the aging process with rapamycin may also be relevant to the progression of age-related diseases such as AMD.^[97] *Kolosova et al.* demonstrated rapamycin could affect retinopathy in senescence-accelerated AMD rat model by reducing histological abnormalities of the ocular retinal tissue.^[97] Overall, pre-clinical evidence suggest rapamycin did not cause any adverse side-effects when administered orally and may have a potential advantage due to its low renal toxicity.^[111]

1.5.2.2 Doxycycline

Doxycycline (as described in section 1.7.2.3) has also exhibited anti-inflammatory and anti-angiogenic properties, making it a potential candidate for the treatment of AMD.^[113] *He et al.* hypothesized that inhibiting the polarization of a subset of pro-angiogenic immune cells, M2 type macrophages, with doxycycline could lead to lower expression levels of pro-angiogenic cytokines and thereby diminish neovascularization.^[114] To test this hypothesis, mice were injected intraperitoneally with doxycycline one day prior to exposing them to laser photocoagulation (to cause choroidal neovascularization injury) and, thereafter, doxycycline was injected daily until the conclusion of the study.^[114] With the administration of doxycycline, there was a significant reduction in the expression of the M2-type macrophage markers such as Arg1 and subsequent neovascularization.^[114] Furthermore, doxycycline can inhibit choroidal neovascularization in other experimental pre-clinical models.^[113] Even though, pre-clinical studies demonstrate doxycycline had a significant effect on neovascularization, there are other types of anti-angiogenic treatments that do not require daily systemic administration.^[52,115]

1.5.3 Anti-Angiogenic Treatments for AMD

1.5.3.1 Sustained Delivery of a HIF-Antagonist

Pro-angiogenic factors can cause disease progression of AMD, and specific promoters for genes encoding these pro-angiogenic factors have been identified.^[99] These promoters possess a hypoxia response element, and they are activated by the hypoxia-inducible factor-1 (HIF-1).^[116] Consequently, a possible strategy to block pro-angiogenic factors is to develop inhibitors of HIF-1, since it is involved in the upregulation of many pro-angiogenic factors.^[99] In particular, doxorubicin (DXR) has been demonstrated to be a potent inhibitor of HIF-1-mediated gene transcription by blocking the binding of HIF-1 on DNA.^[99] For instance, it has been demonstrated that DXR released from polymeric particles was able to significantly reduce the levels of different pro-angiogenic factors (VEGF-A, PDGF-BB, and SDF-1) in an established pre-clinical model of choroidal neovascularization.^[99] Accordingly, these results demonstrate the ability of DXR to suppress HIF-1, representing a promising approach that may be effectively applied as a treatment for AMD.

1.5.3.2 Anti-VEGF Therapy

The pro-angiogenic vascular endothelial growth factor A (VEGF-A) plays a role in disease propagation.^[52] To directly hinder the effects of VEGF-A, new anti-VEGF treatments have been developed, such as Ranibizumab (Lucentis) (a recombinant monoclonal antibody), which promises significant improvement in visual acuity and reduced angiographic lesions after a two-year clinical follow-up of a multicenter clinical trial.^[52,117] Ophthalmologists originally began treating neovascular AMD off-label with bevacizumab (Avastin), another VEGF-A monoclonal antibody originally developed as a treatment for advanced colon or rectal cancer, and costs less

than Ranibizumab.^[100] Although bevacizumab was being used off-label, there was an absence of clinical-trial data supporting its use for AMD. Therefore, the Comparison of Age-Related Macular Degeneration Treatments Trials (CATT) compared the efficacy and safety of bevacizumab to ranibizumab. The results indicated both drugs possessed similar efficacy concerning visual acuity.^[100] Despite the clinical efficacy of anti-VEGF therapies for AMD, these medications can increase the risk of thromboembolic events, and intravitreal injections have been associated with several risks including cataract formation, bacterial endophthalmitis, hemorrhage, and retinal detachment.^[90] In order to avoid these side effects, gene therapies for AMD have been explored as ways to enable effective suppression of the VEGF pathway.^[96,107]

1.5.4 Gene Therapy for AMD

A different therapeutic strategy that could resolve the issue of the short half-life of protein-based treatments may be the use of viral vectors to deliver sustained transgene expression of anti-angiogenic factors.^[118,119] Specifically, approaches using an adenoviral vector expressing pigment epithelium-derived factor (PEDF) to counteract the effects of VEGF have been evaluated in pre-clinical (ex: primate) and phase I human trials.^[101,118] Evidence from these investigations reported lessened choroidal neovascularization and no significant adverse events or dose-limiting toxicities were observed.^[119] In spite of this evidence, there are still concerns surrounding the possible side effects of gene therapy. In particular, viral vectors can induce T-cell responses against the expressed transgene products, and recent evidence has also demonstrated that the usage of viral vectors can result in mutagenesis, ultimately leading to cancer.^[107] Overall, more investigation is warranted for gene-based therapies.

1.5.5 Complement Inhibition

An underlying factor that is linked to the development of AMD is activation (or deregulation) of the complement system.^[7,102] Activation of complement pathways leads to a membrane attack complex (MAC), which can result in cell lysis, the release of chemokines and increase of capillary permeability.^[102] A member of the chymotrypsin family of serine proteases known as complement factor D (CFD) is an enzyme involved in regulating the alternative complement pathway.^[93] Moreover, some of the factors that influence the alternative complement pathway include genetic variations associated with CFD gene single nucleotide polymorphisms (SNP) and AMD.^[93] Due to the association between AMD and genes encoding aspects of the complement system, new AMD therapies have been investigated to block components of the complement system. Specifically, Lampalizumab (Anti-Factor D), a humanized monoclonal antibody fragment administered intravitreally acts to inhibit CFD involved in the amplification of the alternative pathway.^[93] In a Phase II study, there was a reduction of disease progression in patients treated with anti-factor D.^[120] As Phase III clinical trials have begun, evaluations will be required to determine whether the immunogenicity of these types of antibody-based therapeutics can cause any undesirable immunological responses potentially impacting drug efficacy.

1.5.6 IL-18 Therapy

Drusens contribute to the activation of an inflammatory response through NLRP3 inflammasomes.^[95] When stimulated by a damage signal, NLRP3 forms an inflammasome, which leads to the activation and secretion of IL-1 β and IL-18.^[95] Interestingly, studies on IL-1 receptor knockout mice demonstrated that IL-1 did not have a significant effect on the

progression of AMD (choroidal neovascularization). While on the other hand, injecting IL-18–neutralizing antibodies resulted in a significant increase of choroidal neovascularization development. This suggests that IL-18 might prevent the formation of vascularization.^[95] Building upon this evidence, tolerability and efficacy of IL-18 was explored in a mouse and non-human primate model of AMD.^[103] Notably, the images seen below in **Figure 5**, suggest that IL-18 could prevent the choroidal neovascularization in AMD.^[103] Ultimately, the administration of IL-18 reduced the pathology associated with AMD in both murine and non-human primate models, suggesting that this new type of immune-therapy may be able to prevent AMD progression.^[103]

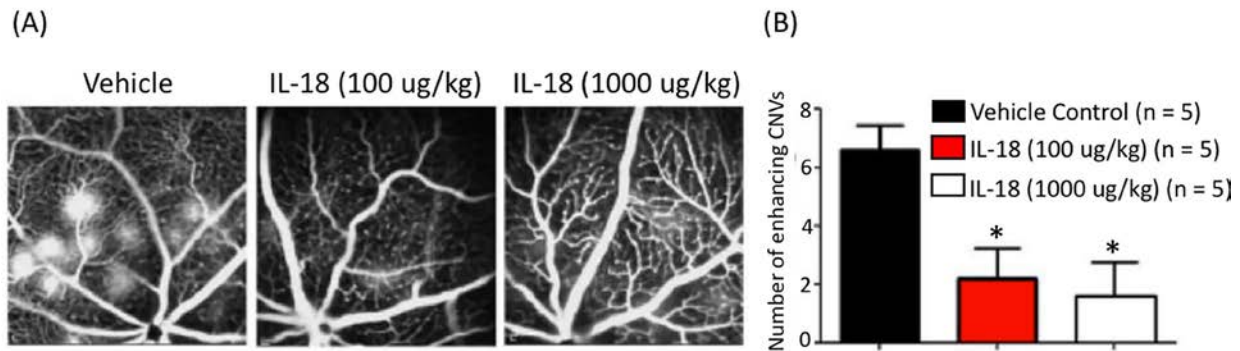


Figure 5. (A) Representative images of fundus fluorescein angiography show a reduction of fluorescein stained lesions in the treatment (IL-18) group (B) The amount of fluorescein lesions were significantly decreased in the IL-18 group suggesting that the immunotherapy, IL-18, can prevent choroidal neovascularization. Modifications/Reproduced with permission^[180] Copyright 2015, Investigative Ophthalmology and Visual Science.

1.5.7 Cellular-Based Therapies

1.5.7.1 Human Embryonic Stem Cells (hESCs)

New stem cell-based treatments are being investigated to regenerate the retinal pigment epithelial cells that are destroyed in AMD.^[121] For example, the use of human embryonic stem cell-derived retinal pigment epithelial cells (hESC-derived RPE) preserved visual function and ensured the health of the photoreceptors in a rodent model.^[121] Moreover, the administration of hESCs did not result in the formation of a teratoma (tumor) in the sub-retinal area of transplantation, and ultimately, the long-term data suggested that hESCs did not result in adverse pathological reactions.^[121]

In addition to a long-term pre-clinical rodent test, two prospective phase I/II clinical studies were designed to examine the medium- and long-term safety of human embryonic stem cells (hESCs) transplanted into patients.^[104] Primary endpoints of safety were assessed concerning the sub-retinal transplantation of hESC-derived RPE in AMD subjects that received three different cell doses and were followed for 22 months.^[104] The evidence collected in this trial indicated that patients did not suffer from any adverse rejection, nor from any systemic effect from the transplanted cells.^[104] However, even though no serious adverse effects were observed, there are still concerns associated with the use of embryonic stem cells, because they have been known to form teratomas in some pre-clinical models.^[105] Furthermore, use of hESC-derived RPE cells is ethically and politically controversial since the stem cells originate from human embryos.^[105]

1.5.7.2 Induced Pluripotent Stem Cells (iPSCs)

Induced pluripotent stem cells (iPSCs) derived from retinal pigment epithelia cells were proposed as an alternative to hESCs as they bypass some of the associated ethical concerns. Although iPSCs have progressed from pre-clinical to clinical trials,^[106,122] there are still concerns about their potential immune rejection.^[122] The promise of iPSC therapy and potential concerns were both highlighted by a recent clinical study carried out in Japan.^[122] In this trial, iPSCs were transplanted into a woman with AMD, and resulted in improved prevention of vision loss.^[122] However, the stem-cell trial was halted after genetic mutations that can potentially carry the risk of cancer, were discovered in the cells of the second trial participant.^[122] Overall, this clinical trial demonstrated that additional investigation is required to examine the potential immunogenicity, possibility of genetic mutations leading to cancer, and likely requirement of immunosuppressive drugs before iPSCs therapy is implemented as a safe clinical treatment.

1.5.7.3 Retinal Progenitor Cells (RPCs)

Retinal progenitor cells possess the ability to differentiate into unique types of retinal cells such as photoreceptors, and may be utilized as a cellular-based therapy for the treatment of AMD.^[109] However, delivering living cells into an unorganized and inflamed ocular microenvironment could affect cell survival. For this reason, new tissue-engineering approaches (such as scaffolds) can potentially provide a unique micro-environmental to enable cells to differentiate and organize into functional layers to repair damaged tissue.^[110] For instance, porous, biodegradable scaffolds composed of a combination of poly (L-lactic acid) and PLGA were fabricated, and subsequently RPCs were seeded on the scaffold and cultured shown in **Figure 6**.^[109] An *in vivo* study was performed on rats using the polymer scaffolds seeded with RPCs, which demonstrated that the implantation of the seeded scaffold enabled enhanced survival of the RPCs.^[109] In addition, another study explored a 3-D thin-film, polycaprolactone-based scaffold seeded with retinal progenitor cells to treat AMD.^[108] The cells were able to stay in close contact with one another, the porosity allowed for diffusion of nutrients, and provided an environment for the cells to adhere.^[108] Overall, three-dimensional polymer-based scaffolds are a new, promising approach to provide an environment that enhances therapeutic cell survival, proliferation, and differentiation.

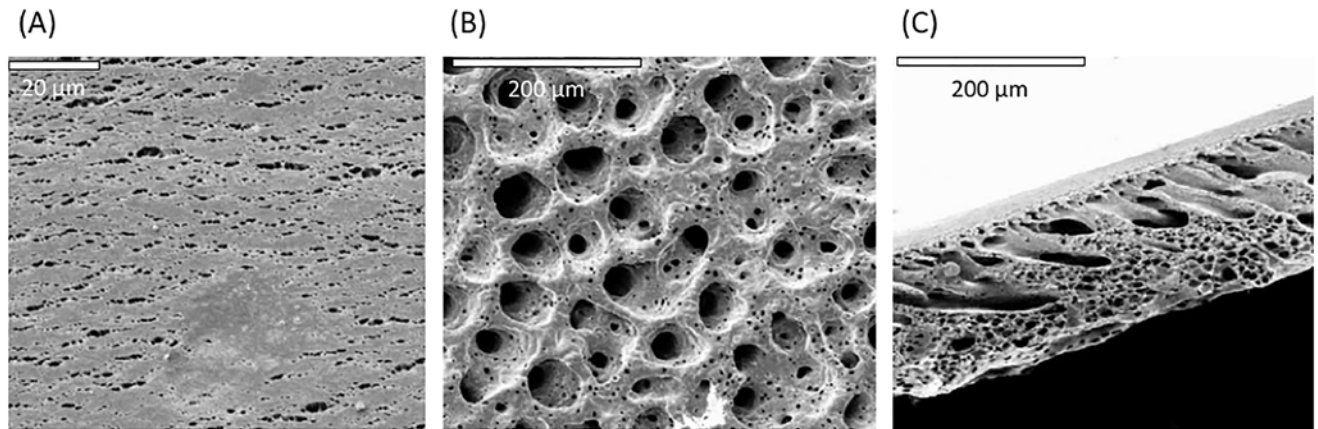


Figure 6. SEM micrographs of PLGA-based scaffolds fabricated using a phase-inversion technique. (A) Representative image of the water-exposed side. (B) Representative image of the glass side. (C) Representative image of the cross section. Reproduced with permission, can prevent choroidal neovascularization. Modifications/Reproduced with permission.^[180] Copyright 2015, Investigative Ophthalmology and Visual Science.

1.6 UVEITIS

1.6.1 Background on the Pathology

Uveitis is a term used to refer to various inflammatory conditions of the eye, and is often associated with irreversible ocular damage, visual impairment or blindness, and with consequent reduction in the quality of life.^[123] Uveitis is estimate to causes 10% of visual loss in the United States each year, and up to 25% of cases in the developing countries.^[124,125] Approximately 70-90% of patients aged between 20-60 years, which represents the age range where individuals are most productive from an economical point of view, are most affected by uveitis. In particular, when vision is lower than 20/40, the ability of a person to accomplish tasks in her/his productive years is impaired.^[126] This leads to a significant encumbrance to the US economy, with cost estimated to be around 242.6 million dollars each year.^[15]

Uveitis typically starts in the uveal tract (ciliary body, iris and choroids), but it can also affect other structures including vitreous humor, retina, vessels and optic nerve.^[127] The disease can be of either infectious or non-infectious nature.^[128] Specifically, infectious uveitis is the most common form, representing approximately 15-20% of all cases in the United States.^[129] It is initiated through an immune response directed against exogenous pathogens such as viruses, fungi, parasites, and bacteria.^[130] Infectious uveitis can affect different parts of the eye, leading to either anterior or posterior uveitis.^[129] However the most devastating cases are those causing posterior involvement such as acute retinal necrosis due to herpes viruses or toxoplasmosis retinochoroiditis.^[129]

Conversely, non-infectious uveitis is often autoimmune-oriented, and is associated with systemic pathologies (for example sarcoidosis, Vogt-Koyanagi-Harada syndrome, Behçet's disease), or local conditions such as punctate inner chorioretinopathy, birdshot chorioretinopathy, multifocal choroiditis, and serpiginous chorioretinopathy.^[131] Non-infectious uveitis is the result of an abnormal response of the immune system to retinal soluble antigens (S-Ag) or interphotoreceptor retinoid-binding protein (IRBP). Such response leads to a non-infectious inflammation of the eye, which is mediated by T-cells and propagated by pro-inflammatory cytokines.^[13,132,133] In particular, during natural development, T-cells migrate from the bone marrow to the thymus, where they differentiate and “learn” how to recognize self-antigens that make up our own tissues. However, thymic education is not always effective, and inadequate elimination from the thymus of effector T-cell precursors that are able to recognize antigens may lead to circulating, non-tolerized T-cells in healthy individuals.^[134] Moreover, when non-tolerized T-cells become activated when exposed to retinal or cross-reactive antigens these cells can differentiate into pathogenic effector T-cells, which can ultimately migrate to the eye. Consequently, this can result in a cascade of inflammatory events initiated by the recognition of ocular antigen by these T-cells, ultimately resulting in the breakdown of the blood-retinal barrier and the recruitment of leukocytes from circulation, which leads to the ocular inflammation observed in uveitis.^[131,134,135] In order to better elucidate the pathophysiology of non-infectious uveitis and develop new therapies, preclinical models of experimental autoimmune uveitis (EAU) have been investigated.^[4,136,137] The most common EAU models utilize mice and rats by actively immunizing them with retinal antigens (S-Ag or IRBP), which are recognized by lymphocytes of uveitis patients.^[138] Some of the characteristics of EAU in animals are retinal vasculitis, photoreceptor damage, retinal and/or choroidal inflammation, and

loss of vision function, thus reproducing the main clinical-pathological features of human uveitis.^[138] Different stages of the EAU model are shown in **Figure 7**. In particular, mice immunized using IRPB are characterized by a decrease in retinal inflammation severity over time, while chronic inflammation persists for more than 120 days post immunization as seen in **Figure 7**.^[139] Moreover, optic disk images have confirmed inflammation characterized by retinal edema and vasculitis in **Figure 7B** with presence of active and old lesions in the chronic stage of EAU observed in **Figure 7E** and **7G**.^[139] Overall, EAU models have been revealed as a valid tool toward a better understanding of uveitis, thus helping the development of current and new therapeutic strategies for managing the associated inflammation described in **Table 2**.

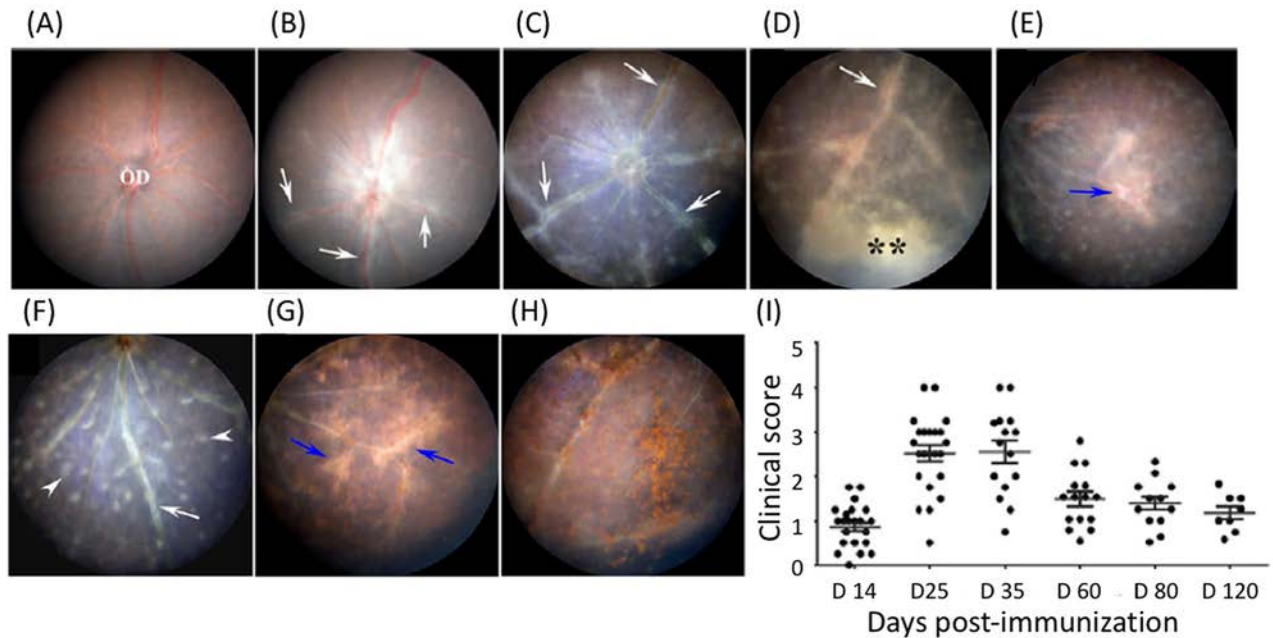


Figure 7. Images showing retinal inflammation characterizing EAU in mice at different time periods after immunization using IRPB. (A) Non-immunized mouse retina. (B) Mouse fundus (25 days post immunization) characterized by severe optic disk inflammation and vasculitis (white arrows). (C) Mouse fundus (60 days post immunization) characterized by retinal atrophy, vascular sheathing (white arrows), and small retinal infiltrates. (D) Mouse fundus (80 days post immunization) characterized by inferior vitreous infiltrates (asterisks) and vascular sheathing. (E) Mouse fundus (80 post immunization) characterized by multiple infiltrates. The blue arrow indicates an area of gliosis or scar. (F) Mouse fundus (90 days post immunization) characterized by vascular sheathing (white arrow) and multiple retinal infiltrates (white arrowheads). (G) Mouse fundus (120 days post immunization) characterized by large scars. (H) Mouse fundus (120 days post immunization) characterized by pigment deposition. (I) The retinal inflammation in the images was quantified with a clinical score and grouped according to the time period after immunization. Reproduced with permission.^[207] Copyright 2012, American Society for Investigative Pathology.

Table 2. Summary of Uveitis Treatments.

Treatment	Type of study	Results	Ref.
Corticosteroids	Human	Topical corticosteroids are effective in controlling inflammation in anterior uveitis. Periocular or intraocular injections or oral administration are required for treating posterior uveitis.	[123,127]
Methotrexate	Human	This folic acid analog has demonstrated to be effective in controlling inflammation.	[140]
Mycophenolate mofetil	Human	This prodrug of mycophenolic acid has shown to control intraocular inflammation, and improve or stabilize visual acuity. Mycophenolate mofetil is well tolerated by patients with low recurrence of uveitis.	[141,142]
Cyclosporine	Human	Cyclosporine is effective in controlling inflammation with sustained effects even after the reduction of corticosteroids. In a retrospective cohort study, cyclosporine has been demonstrated to control inflammation at six months and one year.	[143–145]
Tacrolimus	Human	Tacrolimus is an antibiotic impairing T-cell activity and cytokine production. The drug has demonstrated to possess a more favorable safety profile than cyclosporine.	[146–148]
Anti-TNF- α	Human	Infliximab (Remicade, Janssen biotech Inc., Titusville, NJ) is a monoclonal antibody antagonist of TNF- α . It has been shown to effectively suppress occurrence of uveitis attacks.	[149,150]
Anti-IL-2 - Daclizumab	Human	A phase I/II single armed interventional study has provided preliminary evidence that regular infusions of daclizumab can be administered for years as an alternative to standard immunosuppressive drugs.	[151]
Anti-IL-17A	Human	Secukinumab (Novartis Pharma AG, Basel, Switzerland) is a monoclonal antibody antagonist of IL-17A. Phase III studies have shown secukinumab has beneficial effects for patients with non-infectious uveitis.	[152]
Anti-CD28 - Abatacept	Human	Abatacept (Bristol-Myers Squibb, New York, NY, United States) is a treatment for JIA-related uveitis. Several studies have supported its efficacy in controlling JIA-uveitis in children and young adults.	[153–155]
Retisert	Human	Retisert (Bausch and Lomb, Rochester, NY, United States) is an FDA approved non-biodegradable implant containing fluocinolone acetonide. A double blind, prospective case series has demonstrated an improvement or stabilization of visual acuity, with no recurrence of ocular inflammation.	[156,157]
Cyclosporine-releasing microparticles	Animal model - Rabbits	Cyclosporine-loaded microparticles have shown sustained concentration of cyclosporine in choroid-retina and iris-ciliary body for at least 65 days after intravitreal injection in a rabbit model.	[87]
Gene therapy Ad-IL-10	Animal model - Rats	Systemic administration of Ad-IL-10 in rats has shown to reduce leukocyte infiltration and subsequently decrease inflammation in the anterior chamber.	[158]

1.6.2 Anti-Inflammatory Based Treatments for Uveitis

1.6.2.1 Corticosteroids

Corticosteroids are the primary anti-inflammatory therapy utilized for the treatment of non-infectious uveitis.^[15,159] Corticosteroids have different methods of action to manage the inflammation, as discussed in section 1.7.2.2.^[160] As therapeutic strategy for uveitis, corticosteroids can be administered systemically, such as oral prednisone or intravenous methylprednisolone sodium succinate, or topically in the form of injections.^[15] The choice of the most appropriate route of administration of corticosteroid strongly depends on the site and activity of uveitis. In particular, topical administration of corticosteroids is effective in treating anterior uveitis, but the drug does not typically penetrate adequately to the posterior segment.^[123] For this reason, topical corticosteroids may not be an ideal effective treatment for posterior uveitis, which often requires periocular or intraocular procedures or oral administration of corticosteroids.^[123,127] Accordingly, long-term administration can lead to many side effects including hypertension, diabetes, cataract, and glaucoma.^[161] To reduce corticosteroid dose and associated side effects, immunosuppressive agents such as methotrexate, mycophenolate mofetil, cyclosporine, or tacrolimus are administered as steroid-sparing agents.^[161]

1.6.2.2 Methotrexate

Methotrexate is an analog of folic acid that irreversibly binds and inactivates dihydrofolate reductase, resulting in the inhibition of rapidly dividing cells such as lymphocytes.^[15,161] Methotrexate was first introduced in 1948 as an antineoplastic agent, and subsequently found to have anti-inflammatory effects.^[140] The FDA approved the use of methotrexate as a treatment of rheumatoid arthritis in 1988, becoming the standard antirheumatic drug.^[140,162] Moreover,

methotrexate is a commonly used immunosuppressive agent for the treatment of ocular inflammation, and it can be administered orally, parenterally, or by intraocular injection.^[15,162] In particular, in uveitis patients methotrexate has demonstrated to be effective for controlling inflammation and for achieving corticosteroid-sparing.^[140] Even if several months may be required for therapeutic success, methotrexate is generally well tolerated by most patients, and it seems to have little risks of serious side effects.^[162]

1.6.2.3 Mycophenolate mofetil

Mycophenolate mofetil (MMF) is a pharmacologically inactive drug (prodrug) that, after administration, is metabolized to its active form, the mycophenolic acid.^[163] MMF suppresses the immune system by inhibiting inosine-5-monophosphate dehydrogenase, thus selectively halting T and B lymphocyte replication.^[164] It is currently used as a treatment for organ transplant rejection and for several autoimmune diseases.^[15] The efficacy of MMF therapy has been demonstrated in the treatment of posterior segment intraocular inflammation even when cyclosporine and tacrolimus were not effective. Moreover, MMF inhibits the development of EAU,^[165] and its use in the treatment of uveitis is well documented.^[141,166,167] In particular, MMF is effective both in combination with steroids or another immunomodulatory treatments, and also as monotherapy.^[15] MMF is generally well tolerated by patients, with a low recurrence of the pathology after discontinuation of the therapy, as demonstrated in a retrospective study of 60 uveitis patients.^[141] In addition, MMF can be used as a safe and well tolerated immunosuppressant for the treatment of uveitis in children, with the possibility to decrease the dose of systemic steroids required to control inflammation.^[142]

1.6.2.4 Cyclosporine

Cyclosporine is often topically used for the treatment of immune-mediated ocular pathologies involving activation of T-cells, as mentioned in section 1.7.2.4.^[168] As a treatment for patients with uveitis, cyclosporine is effective in controlling inflammation, and its effects are sustained even after the reduction of corticosteroid dosage.^[144,169] For example, a retrospective cohort study on 373 patients demonstrated clinically acceptable control over inflammation at 6 months and 1 year for 33.4% and 51.9% of patients, respectively.^[145] Despite the efficacy in managing the inflammation, cyclosporine can lead to severe nephrotoxicity,^[170,171] and in addition, some patients can be refractory to treatment.^[172]

1.6.2.5 Tacrolimus

Tacrolimus is an antibiotic that also impairs T-cell activity and cytokine production via inhibition of the calcineurin enzyme.^[146] Tacrolimus was initially approved as a systemic immunosuppressant for liver transplantation, and currently has a broad range of usage.^[146] For instance, tacrolimus is a treatment of choice in uveitis patients refractory to cyclosporine either because of lack of therapeutic effect or undesirable side effects.^[173] Additionally, even though tacrolimus and cyclosporine can have similar efficacy for posterior and intermediate uveitis, tacrolimus therapy has exhibited a more favorable safety profile.^[147] In the treatment of uveitis, tacrolimus has been demonstrated to be effective over time.^[148] Studies have also shown that corticosteroids can be withdrawn in patients treated with tacrolimus.^[174]

1.6.3 Biological Therapeutic Approaches

1.6.3.1 Anti-TNF- α

Anti-TNF- α was identified as a potential candidate for the treatment of patients affected by uveitis, who either did not show an improvement in disease symptoms or did not tolerate traditional immunomodulatory therapies.^[160,175] TNF- α is a pro-inflammatory cytokine, which has been implicated in a number of immune-mediated pathologies, including intraocular tissue damage associated with uveitis.^[176] Specifically, TNF- α recruits leukocyte to the eye in the initial phase of uveitis and favors the adhesion of leukocytes to the vascular endothelium. TNF- α is also a crucial factor in the dendritic cell maturation, macrophages activation, activation of effector function of infiltrating T cells, as well as in the apoptosis of resident ocular cells.^[176] Moreover, it has been indicated that intraocular levels and expression of TNF- α are high during the course of EAU, and systemic neutralization of TNF- α has a suppressive effect on the severity and incidence of EAU.^[176,177] Since TNF- α plays an integral role in the propagation of EAU, the use of biological therapies to block the action of TNF- α has been investigated. One example of such is Infliximab (Remicade, Janssen Biotech Inc., Titusville, NJ), a monoclonal antibody acting against TNF- α .^[149] Its efficacy has been extensively studied as a treatment for many different diseases, including spondiloarthritis, ulcerative colitis, and sarcoidosis, and its use has been also explored for the treatment of uveitis.^[178–180] Intravenous administration of Infliximab results in a half-life of 9.5 days, however the drug is usually given every 4-8 weeks in the maintenance phase of treatment, since the biological effects extend beyond its serum half-life.^[176]

Several studies have reported the efficacy of Infliximab for the treatment of non-infectious uveitis. For example, the effects of infliximab on the occurrence of uveitis attacks and on visual prognosis were investigated in patients affected by uveitis resulting from Behçet's disease. Moreover, patients involved in the trial did not have any therapeutic effect with the combination therapies of azathioprine, corticosteroids, and cyclosporine.^[150] The results from this trial suggest that Infliximab can effectively suppress the occurrence of uveitis attacks. Moreover, Infliximab has a corticosteroid-sparing effect, and positive consequences for the visual prognosis were observed.^[150] However, the beneficial effects of visual acuity are not necessarily preserved over time.^[150] Moreover, in another study, the efficacy of low-dose (<10 mg/kg), moderate-dose (\geq 10-15 mg/kg), and high-dose (\geq 15-20 mg/kg) of Infliximab for the treatment of uveitis was compared.^[181] Although the administration of infliximab had beneficial effects in treating uveitis, an increase in dose up to four times above the approved dosage was often necessary to control the disease. In addition, the study highlighted that doses <10 mg/kg administered every four weeks may not be sufficient.^[181] Overall, the high dose administration of Infliximab has not caused concern of serious side effects, suggesting it is a relatively safe treatment approach for uveitis.

1.6.3.2 Anti-IL-2

IL-2 is a cytokine regulating lymphocyte homeostasis and function. Studies in EAU models suggest that IL-2 is one of the predominant cytokines produced in the early phases of the disease.^[182] One example of anti-IL-2 therapy is represented by daclizumab, a humanized blocking monoclonal antibody acting against an epitope of the alpha subunit of the IL-2 receptor (CD25), which is located on activated T-cells and other immune cells.^[183] Daclizumab has been used in patients experiencing acute reaction episodes following organ transplantation, including

heart, pancreas, liver, and lung. The use of daclizumab for the treatment of intraocular inflammation, including uveitis, has been investigated in a multicenter, non-comparative, interventional case series.^[184–189] In this study, daclizumab was subcutaneously administered to investigate the possibility of whether the drug could safely reduce the need of standard systemic corticosteroids or other immunosuppressive treatments in patients with non-infectious uveitis.^[190] Induction treatment with subcutaneous daclizumab at 2 mg/kg followed by 1 mg/kg maintenance treatments every other week was determined to be safe. In addition, the administration of intravenous daclizumab for the treatment of non-infectious uveitis was explored in a long-term, phase I/II single armed interventional study.^[191] This study provided preliminary evidence that regularly administered infusions of daclizumab can be given as an alternative to standard immunosuppressive therapies for years to treat severe uveitis.

1.6.3.3 Anti-IL-17A

T-helper 17 (Th17) cells are a sub-set of pro-inflammatory T helper cells and one of the main pathogenic effectors in autoimmune uveitis. Specifically, Th17 cells produce the pro-inflammatory cytokine IL-17A and other effector cytokines, including IL-17F and IL-22.^[192] The upregulation of IL-17A in patients with uveitis has led to experimental treatments specific to this target.^[193] For instance, secukinumab (Novartis Pharma AG, Basel, Switzerland) is a selective, high-affinity and fully-human monoclonal antibody that binds to human IL-17A. This binding is thought to inhibit the expression of other pro-inflammatory cytokines and effector proteins, thus preventing the downstream activation of neutrophil granulocytes, macrophages, epithelial cells, and fibroblasts.^[194] Secukinumab blocks inflammation in patients affected by psoriasis, rheumatoid arthritis, and uveitis.^[195] Intravenous dosing of secukinumab has shown greater efficacy than subcutaneous dosing in patients with non-infectious uveitis, suggesting that patients

may not receive a sufficient amount of drug with subcutaneous administration.^[196] Moreover, three multicenter, randomized, double-masked, phase III studies in the United States have examined the efficacy and safety of different doses of Secukinumab in patients with non-infectious uveitis.^[152] Although the study suggested that secukinumab administration resulted in a beneficial effect and allowed for reduction of the use of concomitant immunosuppressive medication, the authors did not discover any dissimilarities in uveitis recurrence between placebo groups and secukinumab treatment groups.^[152] On these bases, further research may be needed to assess the efficacy of secukinumab in managing non-infectious uveitis in patients who are refractory to routine immunosuppressive treatments.

1.6.3.4 Anti-CD28 - Abatacept

Abatacept (Bristol-Myers Squibb, New York, NY, United States) is a fusion protein composed of the Fc region of the immunoglobulin IgG1 and the extracellular domain of cytotoxic T-lymphocyte antigen 4.^[197] T-cell activation involves both the T-cell receptor and a co-stimulatory signal provided through the binding of CD28 on the T-cell to the B7 protein on an antigen-presenting cell such as a dendritic cell. Specifically, abatacept acts by binding to the B7 protein, thus preventing co-stimulatory signaling, and ultimately leading to impedance of T cell activation. Abatacept is currently an approved treatment for juvenile idiopathic arthritis (JIA) - related uveitis and rheumatoid arthritis, and can be administered either as an intravenous infusion or subcutaneous injection.^[153,198] Several studies support the efficacy of abatacept in controlling or improving JIA-uveitis in children and young adults. Particularly, a study carried out on seven patients affected by JIA-related uveitis and refractory or intolerant to immunosuppressive demonstrated an improvement in all patients, although only one patient had complete remission over a follow-up period of 7-11 months.^[199] In addition, the therapy was well tolerated in six of

the seven patients. Another small study performed on two patients showed that the use of abatacept may result in complete remission of uveitis after several months of treatment.^[200] However, both studies involved a small sample size (seven and two respectively), and, for this reason, a larger series of studies and a longer term follow-up may be required to confirm the efficacy and cost effectiveness of this therapy.

1.6.4 Engineering Approaches to Treat Uveitis

1.6.4.1 Fluocinolone acetonide implants – Retisert

Retisert (Bausch & Lomb, Rochester, NY, United States), is a non-biodegradable implant containing a synthetic corticosteroid, fluocinolone acetonide, and designed for a long-term, local release of the therapeutic agent as represented in **Figure 8**. The pharmacokinetics of fluocinolone acetonide was initially tested *in vivo* in 24 rabbits receiving implants of either 0.5 mg or 2 mg.^[156,201] After the first month a constant release of the active principle was observed for a period of 12 months, with minimal systemic absorption as demonstrated by urine and plasma concentration below the detection limits.^[156] Similar results were obtained in another study where the release rate was constant over the one-year testing period.^[201] The effectiveness of the fluocinolone acetonide implant (releasing approximately 2 $\mu\text{g}/\text{day}$) was investigated in a pilot study composed of five patients with severe posterior uveitis.^[202] After a ten month follow-up, visual acuity was either improved or stabilized, and inflammation was under control in all patients treating with the implant.^[202] Successively, in a double-blind study patients were randomized to receive fluocinolone acetonide intravitreal implants of 0.59 mg (0.6 $\mu\text{g}/\text{day}$) or 2.1 mg (2 $\mu\text{g}/\text{day}$) for 58 months.^[157] The outcome of the results of the study showed an improvement in mean visual acuity with no recurrences of ocular inflammation during the first

two years after implantation.^[157] In 2005, Retisert was approved by the FDA for the treatment of chronic, non-infectious, posterior uveitis.^[203,204] Retisert is an ocular the implant composed of a silicone elastomer containing 0.59 mg fluocinolone acetonide, which is surgically implanted in the posterior segment. Over the first month following implantation, the device delivers the medication at a rate of 0.6 $\mu\text{g}/\text{day}$, followed by a continuous delivery of 0.3-0.4 $\mu\text{g}/\text{day}$ for 30 months. The drug delivery rate depends on different factors such as surface area, permeability of polymers, drug solubility, and rate of drug clearance.

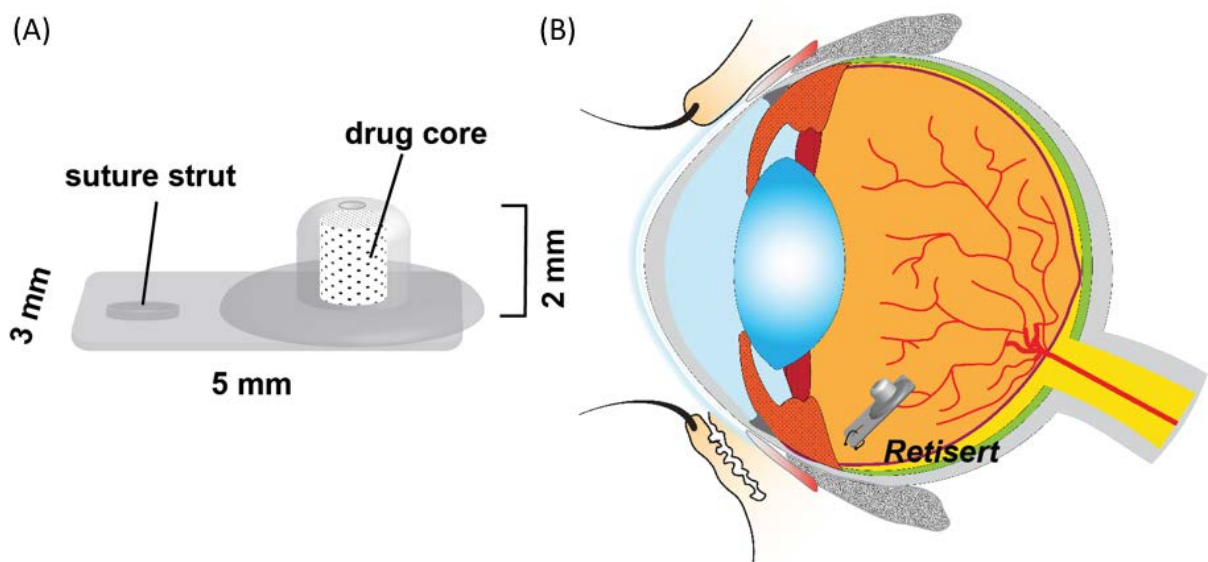


Figure 8. (A) Schematic and (B) site of implantation of Retisert.

1.6.4.2 Cyclosporine-Releasing Microparticles

As discussed previously, cyclosporine has been proven to be effective in controlling inflammation in patients with uveitis. However, there are limitations (low bioavailability and systemic side effects) associated with the commonly used formulations of cyclosporine (topically, systemically administered).^[205,206] To overcome these limitations, microparticles containing cyclosporine have been under investigation as an alternative system for delivering the drug for a prolonged period of time, thus achieving a prolonged drug action with reduced side effects shown in **Figure 9**.^[86,205] In particular, it has been demonstrated that PLGA-based microparticles containing cyclosporine allow for a sustained concentration of the drug in the iris-ciliary body and choroid-retina of healthy rabbits for at least 65 days after injection shown in **Figure 9B**.^[86] Moreover, the mean residence time of the drug loaded in the microparticles was ten times higher than cyclosporine solution.^[86] Similar results have been obtained using cyclosporine-loaded lipid microspheres, capable of a prolonged release of the medication with cyclosporine concentration much higher than in the traditional ocular emulsion.^[207] These results suggest that patients affected by uveitis could potentially benefit from the use of sustained-release drug formulations, representing a way to localized and deliver the drug more efficiently than topical or systemic administration.

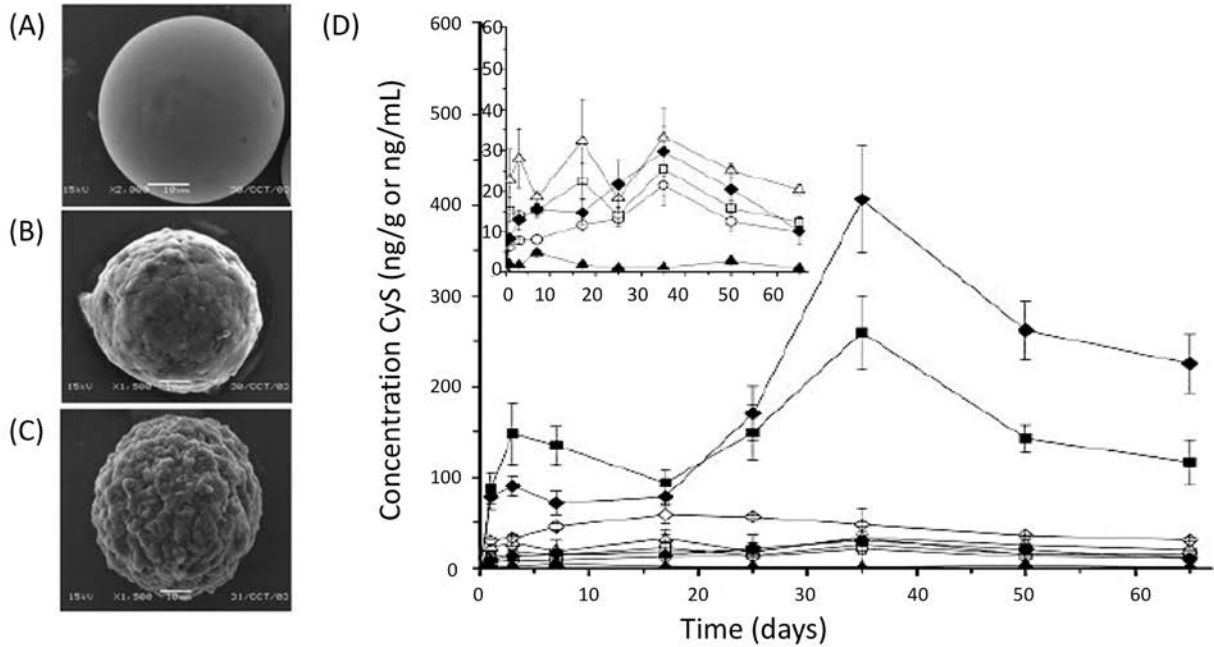


Figure 9. Scanning electron microscopy images (SEM) of PLGA microparticles loaded with cyclosporine (A) SEM image of microparticles before the in vitro release assay (B) SEM image after two weeks of in vitro release (C) SEM image taken after two months of *in vitro* release (10 μ m scale bar). (D) Diagram showing the concentration of cyclosporine released overtime in different ocular tissues and blood subsequently after the cyclosporine microparticles are intravitreally injected for the treatment of uveitis. (□) Iris-ciliary body; (□) cornea; (Δ) conjunctiva; (O) aqueous humor; (□) blood; (□) vitreous body; (●) choroid-retina; (•) sclera; (▲) lens. Reproduced with permission.^[86] Copyright 2006, Association for Research in Vision and Ophthalmology.

1.6.5 Gene Therapy for Uveitis

Although gene therapy of retinal degeneration has been under investigation in diseases such as AMD, it is also a new approach for uveitis, and only few studies on animal models have been attempted.^[160] For example, an adenoviral-mediated transfer of the interleukin (IL)-10 gene for the inhibition of autoimmune anterior uveitis was investigated using a rat model.^[158] Specifically, the adenoviral construct expressing IL-10 (Ad-IL-10) or carrying no cytokine transgene was systemically administered to the rats. The results from the study suggested that rats receiving one or two divided administrations of Ad-IL-10 had a reduction of leukocyte infiltration in the anterior chamber of the eye. In another experimental study, a lentiviral vector was developed for the delivery of genes encoding murine IL-1Ra (mIL-1Ra) and murine IL-10 to the anterior chamber, in order to determine whether it could affect the inflammatory response.^[208] A significant reduction in the severity of experimental uveitis was demonstrated, suggesting that the utilization of lentiviral-mediated expression of immunomodulatory could be promising as a potential, future treatment for the anterior chamber of the eye.

1.7 DRY EYE DISEASE

1.7.1 Background on the Pathology

Dry eye disease affects the tears and ocular surface, afflicting more than 10 million individuals in the United States alone.^[209–213] Epidemiological studies suggest that aging and female sex are two of the most common risks factors for DED.^[5] Several other risk factors for this particular ocular condition include autoimmune diseases (rheumatoid arthritis, Sjögren’s Syndrome), thyroid disease, hormonal changes, and refractive laser surgery.^[2] Typically, patients with one or more of these risks factors will also experience symptoms such as ocular irritation, dryness, tear hyperosmolarity, and foreign body sensation.^[214,215] In severe cases, DED can lead to the risk of developing infections and corneal ulcerations resulting in blindness.^[6] Moreover, these symptoms can have a significant effect on the patients’ quality of life by affecting their visual ability to complete daily tasks (ex: reading or driving), which may lead to psychological side effects such as anxiety and depression.^[215] Given the surprisingly serious nature of these side effects, a variety of methods has been explored in an attempt to mitigate these symptoms.

One common therapeutic strategy to help minimize the symptoms of dry eye is tear plugs (as described in section 1.2.3), which preserve the health of the ocular surface by conserving tears.^[216] Plugs as shown in **Figure 2** are classified by the location of insertion, which can include either the puncta or canaliculi (nasolacrimal drainage ducts) and plugs can be either permanently or temporarily inserted.^[217] A factor that contributes to the intended duration of usage is the composition of the tear plug, which could be made of degradable collagen, gelatin, as well as non-degradable materials such as silicone, Teflon, and hydromethylacrylate.^[216] Even though tear plugs are considered safe and have shown to be effective for maintaining ocular

lubrication, some individuals experience complications associated with plug retention rates and infection.^[216] It also has been demonstrated that closing the puncta exposes the ocular surface to high levels of pro-inflammatory cytokines in the tears, which can lead to exacerbated symptoms of DED.^[217]

A common alternative to help lubricate the ocular surface for individuals with dry eye symptoms is the use of artificial tears.^[218] As administered in eye-drop format, artificial tears can help to reduce the friction between the ocular surface and eyelids, providing relief for some (but not all) patients.^[215] However, preservatives that are included in the formulation can result in hyperosmolarity of the tear film, leading to ocular surface inflammation.^[215] One type of preservative known as benzalkonium chloride (BAK) has been speculated to cause hyperosmolarity of the tears, induce ocular irritation, lower cell viability, and induce oxidative stress on conjunctival epithelial cells in long-term treated dry eye patients.^[219] Due to these potential side effects, new formulations have been developed that contain electrolyte-based artificial tear substitutes with a buffering component to help decrease the hyperosmolarity of the tears and aid to preserve the ocular surface.^[220]

Ultimately, although artificial tears and punctal plugs have proven to lessen various symptoms of DED in some patients (such as ocular irritation and discomfort), they are not designed to address the underlying cause of the condition.^[5] More recently, the inflammatory response has been identified to play a prominent role in the development and propagation of DED.^[12,14,221–223] Specifically, inflammation leads to hyperosmolarity of the tear film and, ultimately, tissue destruction.^[215] One of the primary mediators of ocular inflammation and tissue destruction are pathogenic effector T lymphocytes.^[6] Generally, these lymphocytes are associated with chronic inflammation.^[224] Adoptive transfer of pathogenic CD4⁺ T lymphocytes

from mice that have induced DED into a nude mice develops DED in cell recipients.^[225] Also, ocular inflammation is associated with increased expression of CCR5, which, in turn, results in the recruitment and infiltration of pathogenic effector T cells to the ocular tissue.^[6,225–227] Building upon this evidence, current and new investigative therapeutic approaches have been developed to reduce ocular inflammation in order to restore the ocular microenvironment in DED as shown in **Table 3**.^[112,228,229]

Table 3. Summary of Dry Eye Disease Treatments.

Treatment	Type of Study	Results	Ref.
Lipids	Murine	Topical administration of omega-3 fatty acids reduced corneal fluorescein staining and altered pro-inflammatory cytokine milieu in the ocular tissue.	[111]
LipiFlow	Clinical	Approved in 20011 by the FDA, LipiFlow is a medical device that uses vectored thermal pulsation to stimulate the release of meibum.	[113] [114] [115] [116] [117]
Corticosteroids	Murine	This class of steroid hormones can suppress molecular stress responses through reducing inflammation and resolving signs of DED.	[121] [122]
Doxycycline	Murine	PLGA-based microspheres loaded with doxycycline were able to modulate the effects (ex: corneal fluorescein staining) of DED.	[108]
Cyclosporine A (CsA)	Clinical	Restasis®; Allergan Inc, Irvine, California is a cyclosporine A ophthalmic emulsion used to treat patients with chronic DED.	[109] [124]
Contact Lenses	Rabbit	In order to overcome the low bioavailability of topically administered drugs to the ocular surface, contact lens (ex: silicone based and hyaluronic acid-laden ring implants) have been utilized to enhance drug residence time.	[28] [136]
CCR2	Murine	Biological immune antagonists have shown to decrease mRNA expression levels of cytokines and reduce the infiltration of antigen-presenting cells to the ocular surface.	[125]
Lifitegrast	Murine and Clinical	An FDA approved integrin antagonist of LFA-1 demonstrated the ability to reduce ocular surface inflammation in a desiccating stress murine model and significantly improved ocular irritation in clinical trials.	[107] [139] [141]
Regulatory T cells	Murine	The <i>ex vivo</i> expansion of Tregs into a mouse with DED was able to resolve signs of inflammation.	[154]
Synthetic Approaches to Recruit Tregs	Murine	PLGA-based microspheres loaded with a chemokine, CCL22, was able to resolve signs of DED and shift the ratio of Tregs to effector T cells in the lacrimal gland tissue.	[85]

1.7.2 Anti-Inflammatory Based Treatments for Dry eye Disease

1.7.2.1 Lipids and LipiFlow

One therapeutic strategy for DED is the administration of fatty acids such as omega-3s, which are known to reduce inflammation through the downstream effects on the NF- κ B pathway.^[230] Topical administration of omega-3 was explored in attempt to mitigate DED symptoms such as corneal fluorescein staining,^[231] as an increase in corneal staining is an indicator of corneal disease severity.^[232] Specifically, the fluorescein dye stains dead squamous epithelial cells and can diffuse into areas where cellular tight junctions have been compromised.^[232] The results of the sample scoring suggest that the fluorescein staining was decreased in animals treated with fatty acids.^[231] In addition to a reduction of corneal fluorescein staining, mRNA levels of pro-inflammatory cytokines in the cornea and conjunctiva (e.g. IL-1 and TNF- α) were lower in treated animals, suggesting that omega-3 fatty acids can alter the pro-inflammatory milieu and lessen the signs of dry eye.^[212,214,223,233]

Other types of lipid-based treatment approaches have also been developed to mitigate the symptoms associated with the disease including a device known as LipiFlow represented in **Figure 10**.^[234] This particular medical device uses a 12-minute vectored thermal pulsation (VTP) treatment that applies heat to the eyelid while also applying pressure to the outer eyelids to enable the release of meibum (oil like substance found in the tears).^[233,235] A clinical trial revealed that LipiFlow was able to improve symptoms of ocular irritation, and subsequently in 2011, the FDA approved LipiFlow as a medical device.^[236,237] Although the treatment is an effective therapy for some patients, it is still not widely available due to its high cost.^[237] Hence, additional numerous topical cost-effective pharmaceutical agents are being screened as a potential therapy for DED.^[238]

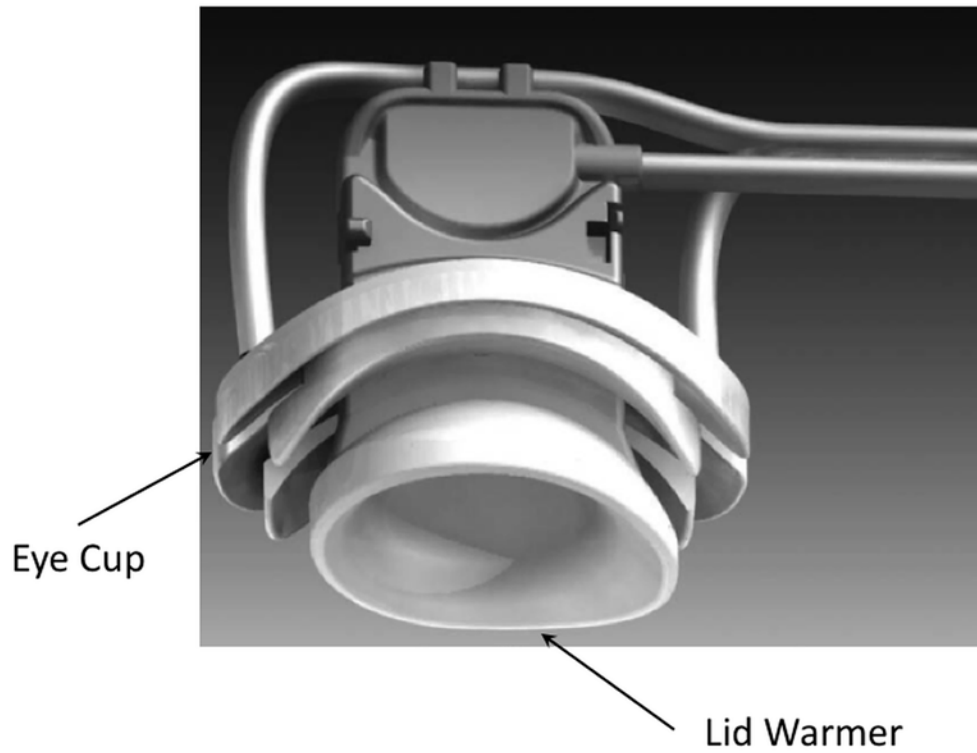


Figure 10. Representation of the LipiFlow Disposable. Black arrows show the Eye Cup and Lid Warmer. Reproduced with permission.^[114] Copyright 2012, Lippincott Williams & Wilkins.

1.7.2.2 Corticosteroids

Corticosteroids (glucocorticosteroids) are a class of steroid hormones widely exploited for a range of inflammatory and immune-based diseases.^[239] A few inflammatory conditions treated with the administration of corticosteroids include: asthma, chronic obstructive pulmonary disease (COPD), uveitis, and age-related macular degeneration.^[58,91,239] Corticosteroids have multiple methods of action to abate inflammation.^[239] Classically, one prominent method of action is through the glucocorticoid receptor mediated pathways, which act to inhibit the synthesis of multiple inflammatory proteins thereby suppressing pro-inflammatory genes and lymphocyte activation.^[239] Since inflammation and lymphocyte activation are recognized in diseases such as dry eye, others have examined whether glucocorticosteroids can resolve DED symptoms.^[240,241] Several murine studies have suggested that the administration of corticosteroids can suppress molecular stress responses through lowering the levels of pro-inflammatory cytokines, and improving clinical signs of disease such as corneal fluorescein staining.^[240,241] However, even though corticosteroids have exhibited to be efficacious for DED in short-term studies, there are many potential deleterious side effects associated with their long-term usage including cataracts, high blood pressure, increased risk of infection, and corticosteroid-induced glaucoma resulting from an increase of intraocular pressure (IOP).^[242] Thus, in order to circumvent the potential long-term side effects associated with corticosteroid usage, other types of treatments have been examined as a therapy for patients with symptoms of dry eye.^[243–245]

1.7.2.3 Doxycycline

Doxycycline is antibiotic classified as a tetracycline derivative used for a variety of conditions ranging from rosacea to cancer.^[229,246] Mechanistically, doxycycline acts as a matrix metalloproteinase (MMP-proteolytic enzymes) inhibitor and ^[247] can suppress the expression of

pro-inflammatory cytokines.^[248] In DED, it has been observed that the upregulation of several MMPs can result in the breakdown of tight junction protein degradation and an increase of epithelial desquamation to the ocular surface.^[229] Due to the effects of MMPs in DED, doxycycline was subconjunctivally administered in order to modulate the effects of these proteolytic enzymes.^[229] Specifically, doxycycline-loaded polymer microspheres (made from PLGA), that controllably release the doxycycline over time, abated the effects of desiccating stress induced DED in a murine model.^[229] Ultimately, this investigation suggests that doxycycline PLGA-based microspheres resolved corneal barrier disruption in mice as compared to the unloaded (no drug) microspheres.^[229]

1.7.2.4 Cyclosporine A

Cyclosporine A (CsA) is an immunosuppressive agent utilized for several inflammatory conditions such as organ transplantation, rheumatoid arthritis, and uveitis.^[111,143,169,249] CsA inhibits calcineurin, (a serine/threonine phosphatase), decreasing the expression of specific genes that are involved in T-cell activation and the production of interleukins (IL-2), which acts as a lymphocyte mitogen.^[250] A recent clinical trial evaluated the use of topical CsA ophthalmic emulsion 0.05%, for the treatment of DED (Restasis®; Allergan Inc, Irvine, California).^[112] One-hundred and fifty-eight subjects ranging in severity from mild, moderate and chronic DED were monitored for a period of 3-16 months, and by the end of the study, the administration of CsA appeared to be responsible for significant reduction in clinical symptoms of DED.^[112] Notably, however, it can take several months for CsA to have a therapeutic effect in some patients.^[251] Therefore, new treatments continue to be developed with the goal of achieving a more rapid onset of action and sustained delivery while simultaneously addressing the underlying inflammation mediating DED.^[244,251]

1.7.3 Contact Lenses

As an approach to overcome the low bioavailability of topically administered cyclosporine A, a silicone-based contact lens was investigated.^[31] Specifically, the incorporation of vitamin E and cyclosporine A into a silicone-based contact lens appeared to enhance the release duration of the drug to more than 1-month with only utilizing 10% of vitamin E added into the lens.^[31] However, the incorporation of vitamin E into the contact lens induced a minor alteration in the refractive index of the contact lens.^[31] In an attempt to evade this issue, others have attempted to achieve sustained ophthalmic drug delivery without altering the optical properties of the contact lens with a new hyaluronic acid-laden ring-implant contact lens shown in **Figure 11**. The combination of the ring/implant (separation of drug to the outer rim of the lens leaving the central portion over the pupil unloaded) enabled the sustained delivery of the drug while maintaining ideal optical properties over the pupil for vision.^[252] This delivery system showed hyaluronic acid (HA) was released in the therapeutic range for up to nine days, and the ocular healing was considerably faster in the rabbits treated with HA implanted contact lenses as compared to the untreated group.^[252] The extended release of hyaluronic acid was accomplished through optimizing the amount of cross linker and the thickness of the implant.

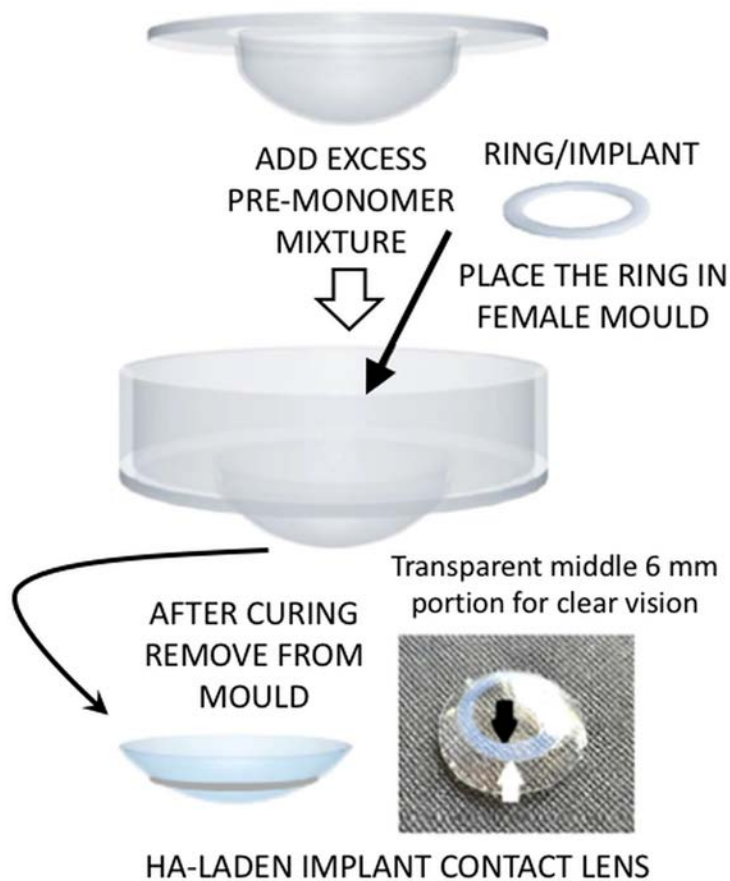


Figure 11. Image of a hyaluronic acid-laden implant contact lens fabricated to enable the sustained delivery of hyaluronic acid while maintaining ideal optical properties over the pupil for accurate vision. Reproduced with permission.^[26] Copyright 2017, Elsevier

1.7.4 Biological/Small Molecule Antagonist Therapies

1.7.4.1 CCR2

Immune antagonists/agonists (ex: chemokine, interleukin, and ICAM-1) are a biologically-oriented approach to halt effector T lymphocytes that can generate destructive inflammation.^[228,244,253] One specific type of immune antagonist that has been analyzed as a potential treatment for DED is the chemokine receptor, CCR2 antagonist.^[244] Topical administration of CCR2 antagonist can reduce mRNA expression levels of interleukins, IL-1 α , IL-1 β , and TNF- α in the cornea and conjunctiva, thereby affecting the pro-inflammatory microenvironment in the ocular tissue.^[244] Furthermore, the CCR2 antagonist decreased the number of CD11b⁺ monocytes (type of antigen-presenting cell on the ocular surface) in the conjunctiva and cornea, which is important because antigen-presenting cells located in the cornea can significantly affect corneal disease pathogenesis.^[209,244] Importantly, the lower levels of pro-inflammatory cytokine expression and cellular infiltrates in the ocular tissue contributed to a reduction of disease severity.^[244] Despite these promising results, the administration of immunological antagonists may require additional investigation given the associated, serious side effects.^[254] For example, treatment with anti-TNF- α therapy increases the patients' chances of developing infections, congestive heart failure, and their overall rate of mortality.^[254] Given this evidence, studies are needed to determine the side effects of administering a topical antagonist to chemokine receptors in order to determine whether this type of treatment has severe side effects similar to anti-TNF- α therapy.

1.7.4.2 Lifitegrast

Lifitegrast is an integrin antagonist (small molecule-“tetrahydroisoquinoline”) therapy that acts to block the binding of two cell surface proteins known as lymphocyte function-associated antigen (LFA-1) and intercellular adhesion molecule 1 (ICAM-1).^[228] This interaction is essential to a number of T-cell interactions such as T-cell activation by antigen-presenting cells and strong adhesion to the endothelial cells during extravasation.^[228,255] Due to the role of LFA-1 in T-cell function, an antagonist of LFA-1 was investigated for the treatment of DED.^[255] In a desiccating stress murine model, a reduction of ocular surface inflammation was observed.^[256] Furthermore, the drug was assessed in a clinical trial of 588 masked, randomized subjects who either were given a placebo (control) or received topically administered Lifitegrast (5.0%) (Twice a day) for a period of 84 days.^[257] The subjects were evaluated at days 14, 42, and 84, and the primary measurement of efficacy was to observe a mean change from baseline inferior corneal staining score (ICSS).^[257] The data revealed that Lifitegrast markedly reduced corneal fluorescein, and improved symptoms of ocular discomfort when compared to the placebo control group.^[257] Lifitegrast ophthalmic solution is currently approved by the FDA and is commercially marketed as Xiidra® (Shire Pharmaceuticals, Lexington, MA, USA).^[255]

1.7.5 Cell-Based Therapy

1.7.5.1 Regulatory T cells

As an alternative to blocking or suppressing T-cell mediated inflammation, it may be possible to take advantage of a natural mechanism the body uses to regulate inflammation.^[258] In the healthy steady state, our bodies regulate inflammation through directing the migration of lymphocytes to areas of inflammation in order to resolve tissue damage and ultimately promote immune

regulation.^[259] Within the classification of lymphocytes is a subset population of immunosuppressive lymphocytes known as regulatory T cells (Tregs), which are utilized by the body to control pathogenic effector T cells, regulating the destructive inflammation that can lead to tissue damage.^[260–264] Disruption in the function, development or number of Tregs can lead to autoimmune and inflammatory diseases.^[265,266] Moreover, it is now understood that an immunological balance of effector T cells and Tregs between the two populations is critical to maintain a healthy microenvironment.^[265] Overall, Tregs are naturally tuned to regulate the proliferation of pathogenic effector T cells, and maintain immunological homeostasis in the ocular tissue.^[267]

Accordingly, Treg-based cell therapies have been explored (the *ex vivo* differentiation/expansion and re-implantation of live cells) for the treatment of diseases such as DED.^[268,269] It also has been suggested that regulatory T cells (Tregs) could be harvested from peripheral blood, expanded *ex vivo* and injected back into the patient in order to boost circulating Treg numbers thereby reducing/resolving the destructive inflammation.^[268] Such would represent a biologically oriented “drug” that is multi-modal, dynamic, and responsive in the local environment and capable of communicating to the immunological milieu. *Siemasko et al.* demonstrated that the *ex vivo* expansion of Tregs injected into a mouse with DED were able to suppress ocular surface inflammation.^[270] Although adoptive transfer of Treg represents tremendous promise (with potential to be more effective than any “drug” while eliminating severe side effects), there are still several issues with the clinical translation of *ex vivo* expanded Tregs.^[268] For instance, expanding sufficient numbers of Tregs can be challenging, and current good manufacturing practices and FDA criteria need to be maintained during *ex vivo* culture to ensure that contamination does not occur.^[268] Likewise, the plasticity of Tregs causes regulatory

concerns, given that some Tregs may differentiate into effector T cells *in situ*.^[268] Also, differentiation into effector T cells *in situ* can lead to an increase of abnormally high levels of IL-2, which can result in vascular leakage syndrome, a life threatening condition.^[268,271] Collectively, there are still many hurdles to ensure safety and efficacy before being implemented as a clinical therapy.^[268]

1.8 CONCLUSION

Ophthalmic drug delivery has undergone substantial transformation, with treatment strategies now being created that specifically address the underlying disease mechanisms. Prior to their application to ophthalmic pathologies, antibiotics (ex: doxycycline) and immunosuppressant agents (ex: rapamycin) were employed for a variety of conditions ranging from rosacea to organ transplantation. These drugs have now been repurposed for additional types of diseases that involve inflammation, which include DED, AMD and Uveitis. Newer approaches include targeted biologics, drug delivery systems, and gene therapies. A key element of each of these new methods is local delivery to the ocular tissue to halt the subsequent effects of inflammation. Although, these modern drug delivery systems may benefit patients that do not respond well to current conventional therapies, the existing regulatory guidelines make it extremely difficult to facilitate clinical translational of these complex therapeutic modalities. While the regulations concerning traditional pharmaceuticals are well established and require straightforward approaches that measure purity and bioactivity, new modern drug delivery therapies (ex: gene therapies) are far more complex from a regulatory perspective, requiring evaluation of multiple factors with unpredictable downstream effects. Yet new technology is consistently being

developed that is more specific, leading to better safety and efficacy. For example, a new targeted gene-editing technology is CRISPR-Cas9 (gene-based technology), which could be a powerful future treatment for ocular diseases since it has demonstrated promise in a preclinical wet AMD model.^[272] In addition, modern ophthalmic therapeutic approaches are becoming more interdisciplinary, combining biologicals/small molecules/cells with engineered polymeric materials in order to create drug delivery systems that even attempt to mimic the body's natural functions. As the understanding of these disease mechanisms has evolved, the body's natural process of restoring homeostasis may serve as an important inspiration for the development of safer, targeted ocular drug delivery therapies.

2.0 CONTROLLED RELEASE OF TREG-RECRUITING MICROSPHERES FOR THE PREVENTION OF DRY EYE DISEASE

This chapter is adapted from Michelle L. Ratay, Andrew J. Glowacki, Stephen C. Balmert, Abhinav P. Acharya, Julia Polat, Lawrence P. Andrews, Morgan V. Fedorchak, Joel S. Schuman, Dario A. A. Vignali, Steven R. Little.(2017) Treg-recruiting microspheres prevent inflammation in a murine model of dry eye disease. *Journal of Controlled Release*. <https://doi.org/10.1016/j.jconrel.2017.05.007>

Specific Aim 1: To examine *in situ* recruitment of endogenous Tregs in a murine model of DED.

2.1 INTRODUCTION

Current/investigative modern therapeutics have been developed (ex: cells, proteins, genes etc.) for the treatment of inflammatory ocular diseases such as DED. However, most of these treatments tend to merely block inflammation rather than address the underlying immunological imbalance observed in DED. Specifically, the maintenance of a healthy ocular immune microenvironment is dependent upon an immunological balance between pro-inflammatory and anti-inflammatory cells.^[273] Moreover, this involves the prevention of pro-inflammatory lymphocytes (ex: effector T cells: Th1) from infiltrating into the ocular tissue and secreting pro-inflammatory cytokines that can directly hinder the ability of anti-inflammatory lymphocytes

(regulatory T cells: Tregs) to resolve the inflammation. Thus, being able to restore the immunological balance between pro-inflammatory and anti-inflammatory cells in the ocular microenvironment would represent a departure from traditional drug-based treatments. One potential approach to manipulate the local immunological milieu may be through enhancing the ratio of Tregs to effector T cells. Therefore, our efforts have been focused on increasing the ratio of Tregs to effector T cells, through recruiting the body's own repertoire of Tregs to model how the body itself regulates inflammation and tissue destruction, and thereby ultimately preventing DED.^[274]

The inspiration from this approach was in fact, from a natural immunological process found in the body. Specifically, one particular type of protein referred to as the macrophage-derived C-C motif chemokine ligand 22 (CCL22) is known to promote chemotactic migration of cells that express the corresponding chemokine receptor CCR4.^[275-277] Notably, since Tregs express higher levels of CCR4 than other cells,^[278] CCL22 can be used for preferential recruitment of endogenous Tregs.^[279,280] Originally, Curiel *et al.* demonstrated that ovarian tumors can suppress anti-tumor immune responses, in part, by secreting CCL22 to recruit tumor-protective Tregs.^[281] Subsequent studies demonstrated that cells/tissues that are attacked by the immune system (e.g. islet allografts or skin melanocytes in patients with vitiligo) can be protected by gene therapy to attract suppressive Tregs by producing CCL22.^[282,283] Additionally, our group previously demonstrated that an alternative method to gene therapy such as the sustained release of CCL22 from biodegradable polymeric poly (lactic-co-glycolic acid) (PLGA) microspheres (Treg-recruiting microspheres) can mimic cellular secretion and establishment of a gradient of CCL22 synthetically *in vivo*.^[279,280] This leads to recruitment of Treg *in situ* and a marked reduction of symptoms in models of a disease of local, destructive inflammation

(periodontal disease).^[279,280] Given that DED is also characterized as a disorder of local, destructive inflammation, we hypothesized that this approach could recruit Tregs in order to reduce inflammation associated with DED.

Herein, we provide evidence that Treg recruitment, through local release of CCL22 in the lacrimal gland, effectively reduces inflammation in a model of DED. The findings from this study illustrate that the controlled release of CCL22 can influence endogenous Treg and, in turn, prevent destruction of ocular surface tissue.

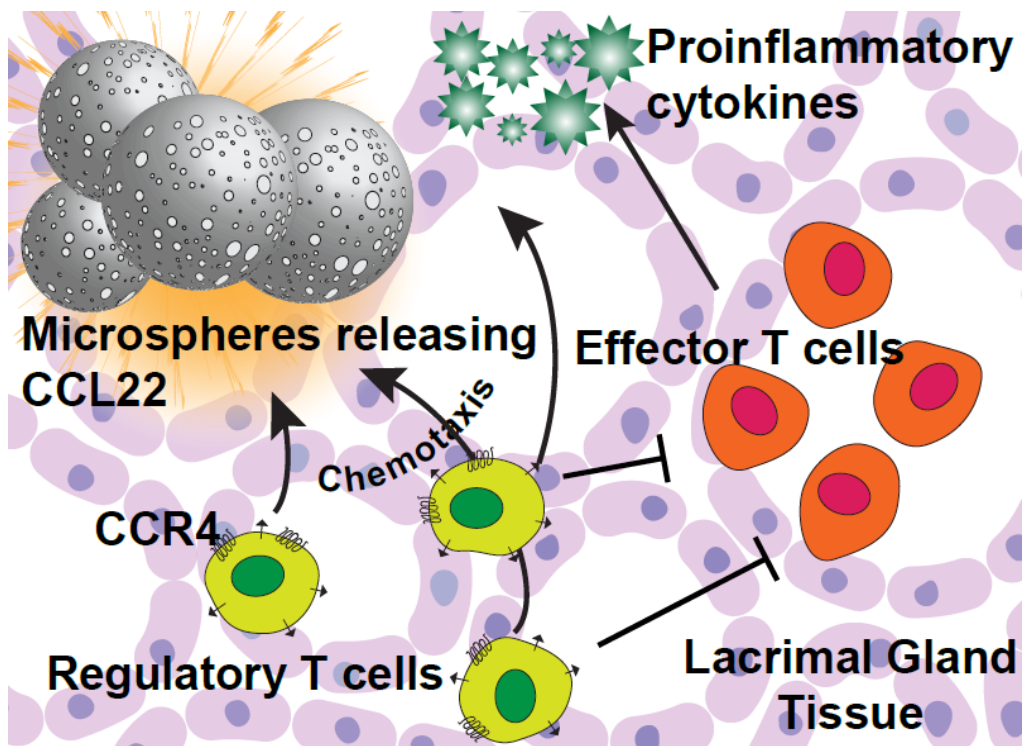


Figure 12. Synthesis strategy to recruit Tregs and shift T effectors and Treg balance for the prevention of dry eye disease.

2.2 MATERIALS AND METHODS

In the following experiments, we aimed to assess the efficacy of Treg-recruiting microspheres for the prevention of pathological signs of DED. Moreover, we also aimed to determine whether the Treg-recruiting microspheres were able to shift the immunological ocular microenvironment.

2.2.1 Fabrication of Microspheres

Poly (lactic-co-glycolic) acid (PLGA) microspheres encapsulating recombinant mouse CCL22 (R&D Systems, Minneapolis MN) were formulated utilizing a water-oil-water double emulsion technique. Briefly, 200 mg of Poly (D, L-lactide-co-glycolide) PLGA polymer (acid terminated, 50:50 lactide:glycolide, molecular weight 7,000-17,000) (viscosity: 0.16-0.24 dL/g, 0.1 % (w/v) in chloroform) (Sigma Aldrich, St. Louis, MO) was dissolved in 4ml of dichloromethane and mixed via vortexing. Then 200 μ L of an aqueous solution containing 5 μ g of recombinant mouse CCL22 (R&D Systems, Minneapolis, MN) and 2 mg of BSA (Sigma Aldrich, St. Louis, MO) with 15 mmol NaCl was pipetted into the mixture of polymer and dichloromethane (Sigma Aldrich, MO). The first water-in-oil emulsion was prepared by sonicating the polymer with CCL22 solution at 25% amplitude for a period of 10 seconds. Then the second water-oil emulsion was created by homogenizing (L4RT-A, Silverson) the first water-oil emulsion with 60 mL 2% (wt. /vol) polyvinyl alcohol (molecular weight \sim 25,000 g/mol, 98 mole % hydrolyzed; PolySciences) for a period of 60 seconds at 3,000 rpms. The homogenized solution was then mixed with 1% polyvinyl alcohol and placed onto a stir plate for 3 hours in order for the dichloromethane to evaporate. The microspheres were then collected and washed four times via

centrifuge with deionized water in order to remove any remaining residual polyvinyl alcohol. Lastly, the microspheres were placed in 5 mL of deionized water, frozen in liquid nitrogen, and lyophilized for 72 hours (VirTis BenchTop K freeze dryer). The microspheres were then stored at -20 °C until use. The overall fabrication process of the microspheres are shown below in **Figure 13**.

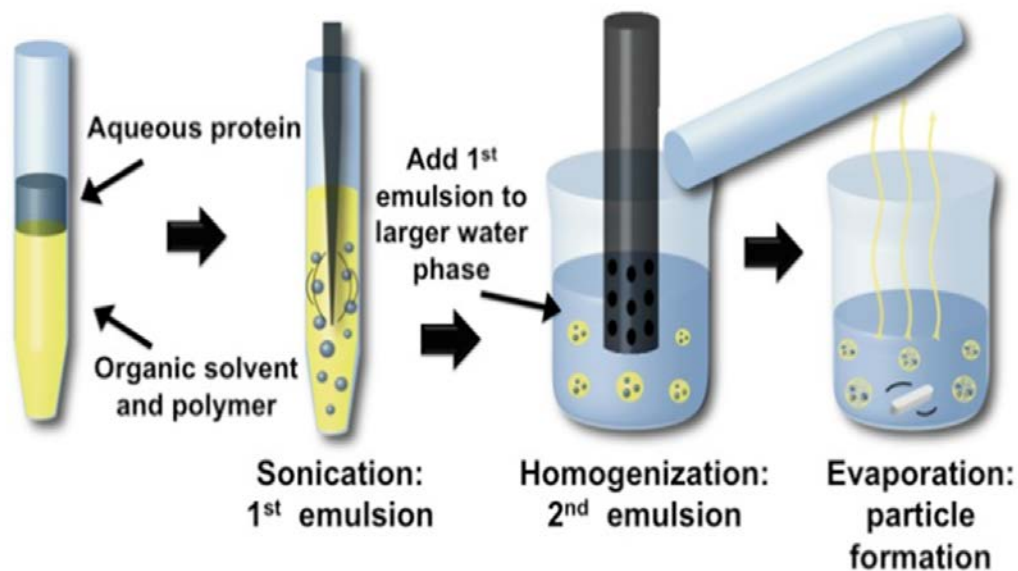


Figure 13. Schematic of the Double Emulsion Fabrication Process of PLGA Microspheres for the encapsulation of an aqueous protein.

2.2.2 Characterization of Microspheres

The morphology of the Treg-recruiting microspheres was characterized using scanning electron microscopy (JEOL, JSM-6330F, Peabody, MA) and volume impedance measurements were performed on a Beckman Coulter Counter (Multisizer-3, Beckman Coulter, Fullerton, CA). In vitro release was determined by incubating 10 mg of Treg-recruiting microspheres in 1ml of phosphate buffered saline (PBS) with 1% BSA, placed on a rotator at 37°C. Release media (supernatant) was sampled periodically. Specifically, triplicates of each release sample were centrifuged at 3,500 rpm at 4°C. After centrifuging 800µl of the supernatant was removed and placed into an Eppendorf tube and then replaced by 800µl of new PBS with 1% BSA. (Leaving the remaining 200µl for a total volume of 1ml). The CCL22 concentrations were quantified using an enzyme-linked immunosorbent assay (ELISA) (R&D Systems, Minneapolis, MN). The encapsulation efficiency was completed by dissolving 10 mg of microspheres in 200µl of dichloromethane (DCM) (Sigma Aldrich, MI). Subsequently, 200µl of PBS was added to the dissolved microspheres and centrifuged. The remaining aqueous supernatant was isolated and the concentration of protein was quantified using an enzyme-linked immunosorbent assay (ELISA) (R&D Systems, Minneapolis, MN).

2.2.3 Experimental DED Model and Treatments

Female Balb/c mice aged 6-8 weeks were used in this study. (8 mice per group) (Charles Rivers Laboratories, Wilmington, MA). All animal experiments were approved by the Institutional Animal Care and Use Committee, University of Pittsburgh. To induce DED, mice were anesthetized, and 10mg/ml of Concanavalin A (ConA) (Sigma Aldrich, St. Louis, MO) of saline

was injected (30 μ l) into each lacrimal gland with a 28.5 gauge needle under a dissecting microscope (Olympus SZX10, Waltham, MA). DED treatments included Blank (empty) or Treg-recruiting microspheres (25 mg/ml), which were mixed with ConA or saline and injected into the lacrimal glands. Soluble CCL22 was injected with ConA at a concentration of (62.5ng /1ml) (volume of 30 μ l injected). For controls intended to probe the necessity of Treg action, Treg function was inhibited in vivo using anti-GITR (DTA-1) (BioXCell, Lebanon, NH), which was injected intraperitoneally (500 μ g per mouse) five days prior to the injection of ConA and Treg-recruiting microspheres.

2.2.4 Measurement of Tear Production

Tear production was measured with phenol red cotton threads (Oasis Medical, San Dimas, CA). Thread was placed in the lateral canthus of the eye for a period of 60 seconds, and wetting was measured in millimeters using a dissecting microscope (Olympus SZX10, Waltham, MA).

2.2.5 Corneal Permeability

To evaluate the corneal epithelial layer, fluorescein stain (1 μ L of 1% solution) was applied to the conjunctival sac and 5 μ l of saline was used to wash off any excess dye. The surface of the cornea was evaluated using a dissecting microscope with a fluorescent excitation lamp (Olympus SZX10, Waltham, MA). Eyes were evaluated in a masked fashion by an independent ophthalmologist, and scored 0 for no staining, score 1 for a quarter of staining, score of 2 for less than a half, score of 3 for half, and 4 for more than half of the eye.

2.2.6 Histopathology

At the end of the study, eyeballs were exenterated then harvested and fixed in formalin for 24 hours. Eyes were sectioned 5µm thick and stained with Periodic Acid Schiff (PAS) to identify goblet cells in the conjunctiva. The histology section images were scanned using a Zeiss Axio Scan Z1 (Thornwood, NY). Numbers of goblet cells were quantified using Pannoramic Viewer software (3D HISTECH Ltd.) of Zeiss Axio Scanned slides at 20x.

2.2.7 Immunophenotyping Analysis by Flow Cytometry

Lacrimal glands, regional draining cervical lymph nodes (CLN) were harvested from the experimental murine groups at the end of the study, and single cell suspensions were prepared. In order to increase total cell counts multiple tissue samples were combined. Cells were stained with the following fluorescent conjugated antibodies: anti-CD4 eFluor450 (RM4-5), anti-CD25 APC-Cy7 (PC61), anti-FoxP3 PE (FJK-16s) (eBioscience, San Diego, CA and BD Bioscience, San Jose, CA). For intracellular cytokine staining, the cells were placed in a 96-well plate overnight in cell culture media with Cell Stimulation Cocktail (plus protein transport inhibitor, eBioscience) and stained with anti-IFN-γ FITC (XMG 1.2) (eBioscience, San Diego, CA). Absolute counting beads were used for the lacrimal gland (ThermoFisher Scientific, Waltham, MA). Stained cells were analyzed using FlowJO (Ashland, OR).

2.2.8 Statistical Analysis

Data are expressed as mean \pm standard deviation. Comparisons between multiple treatment groups were performed using one-way ANOVA, followed by Bonferroni multiple comparisons, and $p \leq 0.05$ was considered statistically significant. Statistical tests were performed using GraphPad Prism Software 6.0, San Diego, CA.

2.3 RESULTS

2.3.1 Characterization of Treg-recruiting Microspheres

We first sought to engineer a Treg-recruiting MS formulation that sustained the release of the chemokine, CCL22 in a relatively linear fashion such that they could potentially be used to produce a biological gradient *in vivo*. A double emulsion-evaporation technique was used to encapsulate CCL22 (hydrophilic protein with high water solubility) into poly (lactic-co-glycolic) acid (PLGA-polymer, which is hydrophobic with a low water solubility and high solubility in dichloromethane) to produce microspheres.^[279,280] Treg-recruiting MS were then characterized to determine size, surface morphology, and release kinetics as shown in **Figure 14**. Specifically, a Coulter Counter was used to determine the average size of the microspheres, which were approximately 16 μ m displayed in **Figure 14C**. The Coulter Counter software guided the selection of an optimal concentration range for the sample in order to obtain a size distribution. Moreover, this microsphere size was designed to avoid cellular uptake by macrophages and other phagocytes.^[284] The microspheres were also designed to contain surface pores, which ensured

minimal burst release of CCL22 from the system.^[279] This can be accomplished through adjustment of the osmolality difference between the inner and outer aqueous phases as described previously by Jhunjhunwala et al.^[279] Surface porosity was confirmed using scanning electron microscopy (SEM) seen in **Figure 14A** and **14B**.^[279] Additionally, an enzyme linked immunosorbent assay (ELISA) was performed to determine protein loading and measure release from the microspheres over time represented in **Figure 14D**. Lastly, in order to determine the encapsulation efficiency an ELISA was completed, and the total amount of CCL22 encapsulated in the microspheres was approximately $4.6 \text{ ng} \pm 0.5$ (18.64% encapsulation efficiency).

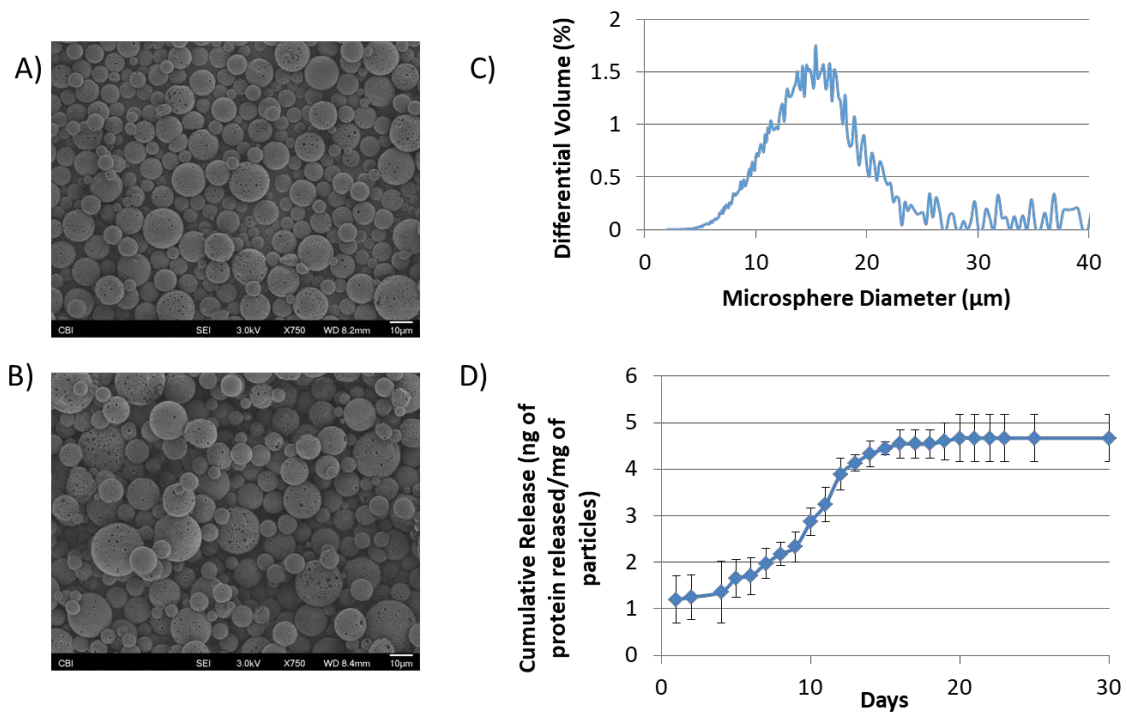


Figure 14. Characterization of engineered porous microspheres loaded with the chemokine CCL22 and blank microspheres. (A) Representative SEM image of porous blank microspheres (1000x) (B) Representative SEM image of porous microspheres with CCL22 encapsulated (1000x) (C) A representative particle size distribution obtained using a Coulter Counter shows the Treg-recruiting microspheres. (D) Release Kinetics of CCL22 (Treg-recruiting microspheres) from porous microspheres is shown (n=3).

2.3.2 Treg-recruiting microspheres Prevent Decrease in Tear Production, Corneal Staining, and Goblet Cell Depletion

To assess whether Treg-recruiting microspheres could prevent clinical evaluations associated with DED, tear production, corneal fluorescein staining, and goblet cell density were used individually as outcomes.^[285] Concanavalin A (ConA-T cell mitogen) served to establish DED, which causes T cell proliferation resulting in the clinical signs associated with DED^[286]. Saline administration (in place of ConA) served as a negative control.^[286] As expected, ConA-treated mice (diseased) exhibited significantly reduced tear secretion, relative to saline (non-diseased). In treatment groups (“treatment” here is referred to application of the formulation at the same time as the establishment of the disease), microspheres (0.5mg/30 μ l) were injected locally into the lacrimal gland as outlined in **Figure 15**. The treatment group significantly prevented tear production loss as compared to the diseased mice. Specifically, the wetting of thread (measured in millimeters) for the treatment group was 4 ± 0.3 mm. Moreover, the thread wetting for the diseased-with-blank-microsphere group was 3 ± 0.5 mm and the diseased was 3 ± 0.3 mm. Overall, blank microspheres did not worsen the signs of DED compared to the untreated, disease group as shown in **Figure 16**.

Experimental Timeline

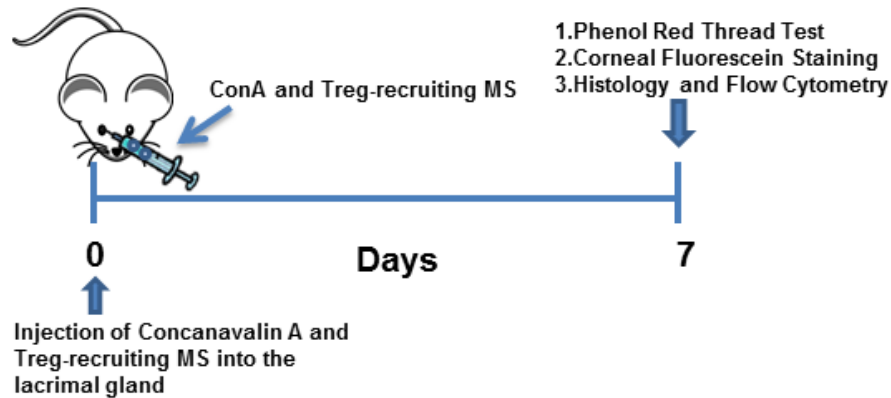


Figure 15. Treg-recruiting MS for preventing Dry eye Disease (DED) in mice. At Day 0, ConA and Treg-recruiting microspheres (MS) were injected into the lacrimal glands.

The integrity of the corneal epithelial barrier via fluorescein staining was also examined as an indicator of disease severity. As seen in **Figure 16**, Treg-recruiting microsphere administration appears to maintain the integrity of the corneal epithelium. Consistent with an intact/undamaged cornea, no staining was observed on the corneas of the treatment group and non-diseased mice after instillation of fluorescein as represented in **Figures 16B** and **16C**. The corneal fluorescein scoring for the diseased was 1 ± 1.3 as compared to the saline, which had an average staining score of 0.5 ± 0.6 and saline with blank microspheres of 0.4 ± 0.5 corneal fluorescein staining score. In contrast, corneal permeability is known to cause a decrease in the rate of fluorescein elimination in DED patients compared to healthy individuals ^[287]. Upon examination, central punctate fluorescein staining was observed on corneas of the diseased, diseased with blank MP treatment, and diseased with soluble CCL22 groups shown in **Figure 16C**.

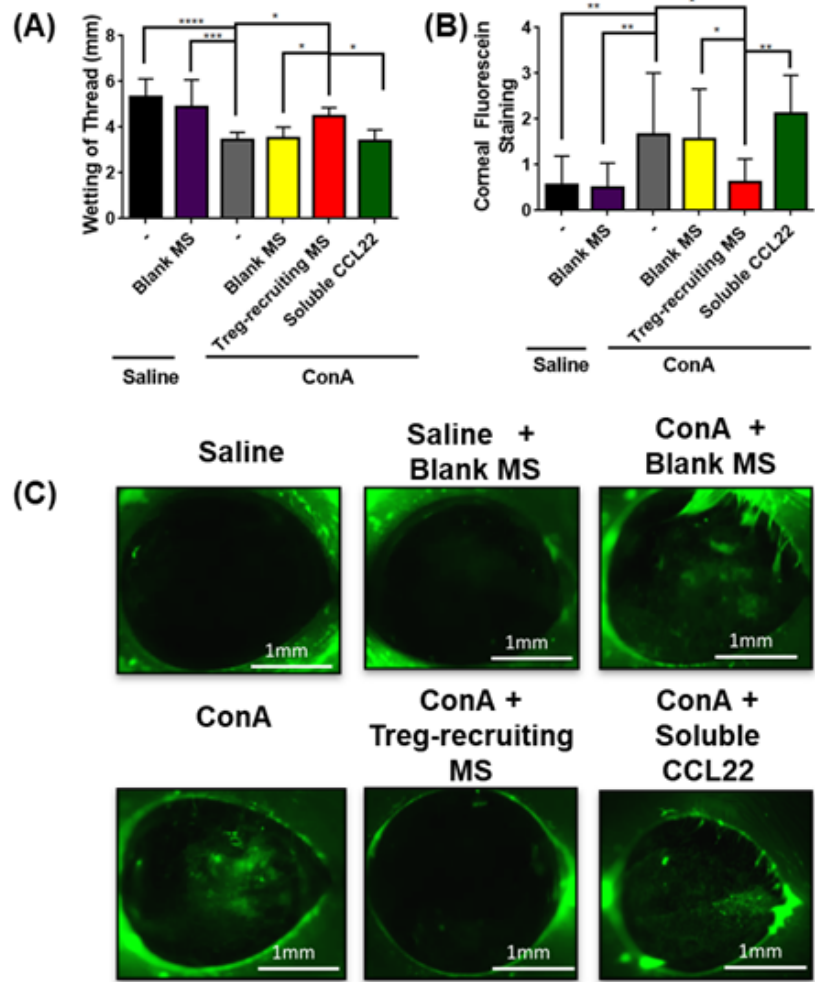


Figure 16. Treg-recruiting MS prevent DED symptoms in mice. (A) Phenol red thread wetting measured in millimeters for aqueous tear production (n = 8) shown as mean \pm S.D. (B) A clinical score of the ocular surface staining scored on a scale of (0-4) (n = 8) show the integrity of the epithelial layer of the cornea. Green staining on the cornea is a positive indication of disease (n=8). * $p \leq 0.05$; ** $p \leq 0.01$; *** $p \leq 0.001$, **** $p \leq 0.0001$.

Histological sections of the ocular tissue were also observed to make record of any differences in treated vs. untreated groups in our model of DED. After one week, eyes were exenterated, and the conjunctiva was stained with Periodic Acid Schiff (PAS) to identify goblet cells (appearing as bright purple/pink cells) interspersed throughout the stratified squamous cells of the conjunctiva. As a loss of goblet cell density occurs, tear film composition changes correlating to severity of conjunctival disease such as DED.^[288] The diseased mice, with or without administration of blank microspheres and diseased with soluble CCL22 exhibited a significant decrease in goblet cell density compared to the non-diseased control group (saline and saline with blank microspheres). Specifically, the soluble CCL22 (bolus) was approximately 45 ± 8 goblet cells while the diseased with blank microspheres was 41 ± 11 , and diseased 36 ± 5 total numbers of goblet cells counted in the conjunctiva. Administration of Treg-recruiting microspheres diminished goblet cell depletion to levels comparable of those observed in non-diseased mice represented in **Figure 17**.

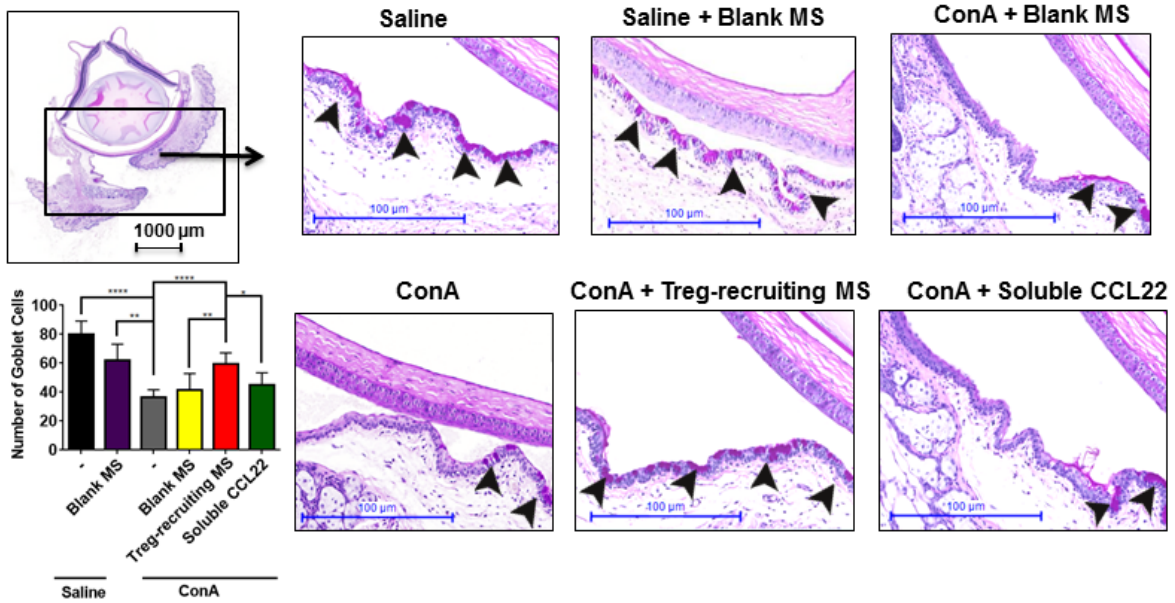


Figure 17. Treg-recruiting MS prevent reduction of goblet cell density in the conjunctiva. Representative images of histological sections of the eyes (20X) were examined to identify differences in the Treg-recruiting MS group compared to the diseased groups (100μm scale bar). Goblet cells shown are the pink/purple cells located in the conjunctiva labeled with arrows and the groups are shown as mean ± S.D. * $p \leq 0.05$; ** $p \leq 0.01$; *** $p \leq 0.001$, **** $p \leq 0.0001$.

2.3.3 Treatment with Treg-recruiting microspheres decreases the frequency of CD4⁺ T Cells in Regional Draining Lymph Nodes

To determine whether attenuation of DED symptoms by Treg-recruiting microspheres was due to local cellular changes in the regional lymphoid tissue, a phenotypic analysis was performed of T-cell populations in the cervical lymph nodes (CLN). CLN from diseased mice exhibited a significantly greater percentage of CD4⁺ T cells compared with non-diseased mice, both with and without administration of blank microspheres shown in **Figure 18A**. In order to further assess phenotypic expression of CD4⁺ T cell population expression of the intracellular cytokine, IFN- γ was investigated. Accordingly, our results suggest that there is a significant difference between the diseased-with-blank microspheres, non-diseased, soluble CCL22 and the treatment group as shown in **Figure 18B**. Interestingly, there was also a decrease in the percentage of Tregs for the treatment group (as compared to diseased-with-blank microspheres), but no significant difference in activated T effectors and Tregs with the soluble CCL22 in the draining lymph nodes as compared to the treatment group shown in **Figures 18C** and **18D**. Additionally, the diseased mice exhibited significantly higher levels of CD4⁺CD25⁺Foxp3⁻ in the CLN compared with non-diseased mice as represented in **Figure 18C**; this was reduced in Treg-recruiting microsphere groups as compared to diseased mice treated with blank microspheres.

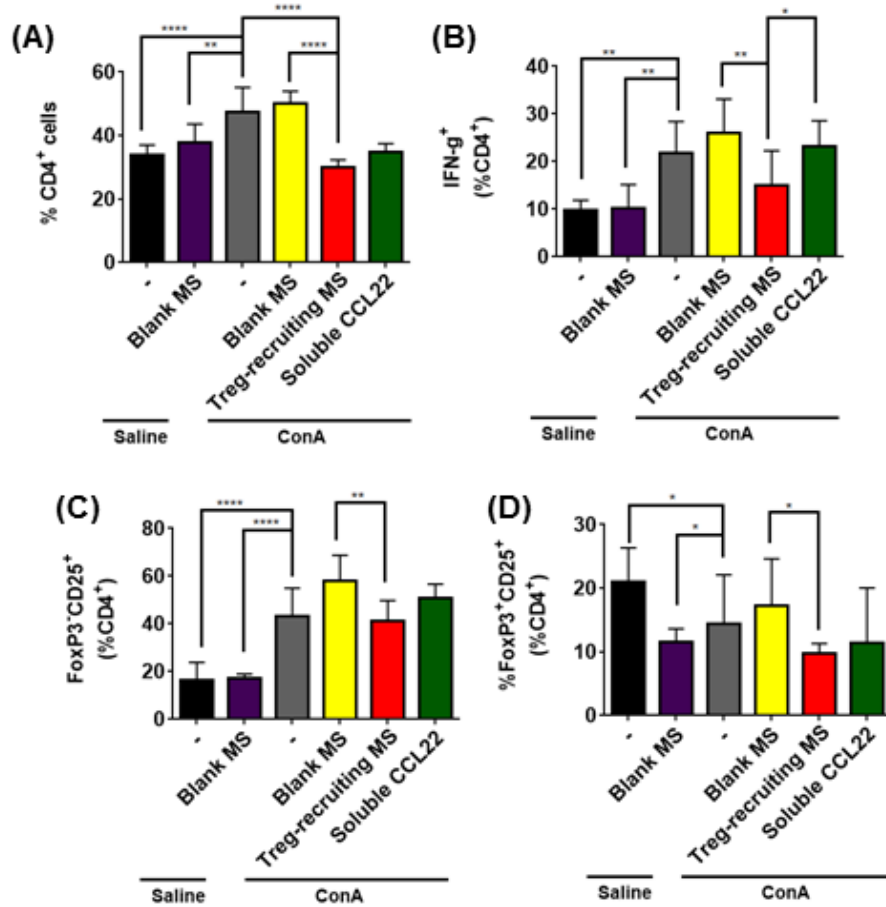


Figure 18. Treg-recruiting MS suppress T effector cells in the regional draining lymph nodes. (A) Data from flow cytometry performed on the regional draining lymph nodes in order to examine overall CD4⁺ T cell percentages (n=8) shown as mean \pm S.D. (B) IFN- γ cytokine expression was examined in the regional draining lymph nodes (n = 8) shown as mean \pm S.D. (C) Activated T effector percentages were analyzed using flow cytometry (n = 8) shown as mean \pm S.D. (D) FoxP3⁺ Tregs analysis on the regional draining lymph nodes using flow cytometry (n = 8) shown as mean \pm S.D. * p \leq 0.05; ** p \leq 0.01; *** p \leq 0.001, **** p \leq 0.0001.

2.3.4 Treatment with Treg-recruiting microspheres Reduces Infiltration of CD4⁺ IFN- γ ⁺ T cells in the Lacrimal Gland

To determine whether Treg-recruiting microspheres alter T-cell populations in the lacrimal gland, lacrimal glands were harvested and flow cytometry was performed to analyze T-cell populations. Specifically, frequencies of pro-inflammatory CD4⁺ IFN- γ ⁺ (Th1) T cells and CD4⁺ FoxP3⁺ Tregs were examined in the gland. We observed significantly greater proportions of IFN- γ -producing CD4⁺ T cells shown in **Figure 19A** and significantly lower proportions of FoxP3⁺ Tregs as shown in **Figure 19B** in the lacrimal glands of diseased mice, diseased-with-blank microspheres, and soluble CCL22 as compared to the treatment group (Treg recruiting microspheres). Notably, the treatment group exhibited a significant reduction in the frequency of IFN- γ ⁺ cells with a concomitant increase in the frequency of FoxP3⁺ Tregs represented in **Figure 19A** and **19B**, relative to untreated diseased mice. The CD4⁺ IFN- γ ⁺ (Th1) T cells and CD4⁺ FoxP3⁺ Tregs in the treatment group were similar to the saline and saline-with- blank microspheres as shown in **Figure 19A** and **19B**. Ultimately, shifts in the pro-inflammatory cytokine, IFN- γ ⁺, and anti-inflammatory Treg populations contributed to a two-fold increase in the Treg/Th1-type ratio in the lacrimal gland of the treatment group relative to diseased, and was significantly higher for the soluble CCL22 and blank microspheres displayed in **Figure 19C**.

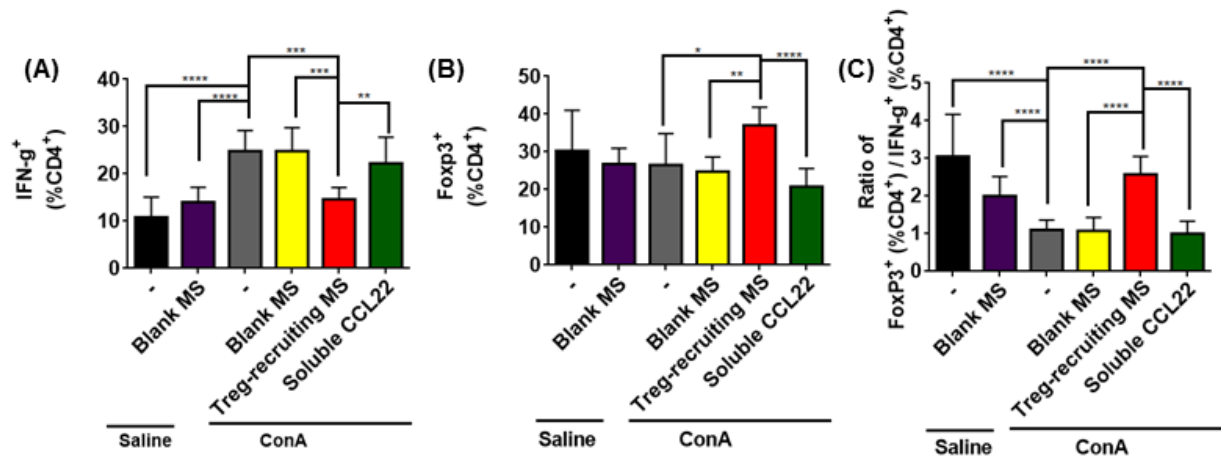


Figure 19. Treg-recruiting MS enhance anti-inflammatory responses in the lacrimal gland. (A) IFN- γ cytokine expression was analyzed in the lacrimal gland (n=8) shown as mean \pm S.D. (B) Analysis of intracellular staining for Tregs (n = 8) shown as mean \pm S.D. (C) The ratio of CD4⁺ FoxP3⁺/CD4⁺IFN- γ ⁺ cells in the lacrimal gland (n=8) shown as mean \pm S.D. * p \leq 0.05; ** p \leq 0.01; *** p \leq 0.001; **** p \leq 0.0001.

2.3.5 Administration of anti-GITR Reverses the Effect of Regulatory T-cell Recruiting Formulations

To confirm that the observed suppressive effects were due to Tregs, a glucocorticoid-induced tumor necrosis factor receptor (GITR) agonistic antibody (Anti-GITR) was administered five days before injection of treatment. Anti-GITR is thought to inhibit the ability of Tregs to suppress other T cells (non-Tregs).^[289] We compared the two groups ConA and Treg-recruiting microspheres with the anti-GITR. As expected, anti-GITR injected before treatment completely eliminated the symptom-reducing effects of Treg-recruiting microspheres, with tear production and punctate staining of the cornea comparable to (or a lower degree than) that of the diseased mice as shown in **Figure 20A, 20B, 20C, and 20D**. There was also a significant decrease of the number of goblet cells in the anti-GITR + Treg-recruiting MS as compared to the treatment group shown in **Figures 20D and 20E**. Additionally, mice treated with anti-GITR before treatment did display a significantly greater percentage of total CD4⁺ T cells as compared to the treatment group shown in **Figure 20F**. In addition, there was no significant difference of activated effector T cells and comparable numbers of IFN- γ ⁺ Th1-type cells in the CLN of the anti-GITR + Treg-recruiting MS, relative to the diseased mice displayed in **Figure 20F**. Moreover, the lacrimal gland tissue of mice treated with anti-GITR exhibited similar frequencies of CD4⁺ IFN- γ ⁺ T cells, as compared to diseased mice and a significantly lower percentage of CD4⁺ FoxP3⁺ as compared to the Treg-recruiting MS group as shown in **Figure 20G**. Overall, the administration of anti-GITR worsened signs of disease and significantly increased Th1 cells in the lacrimal gland.

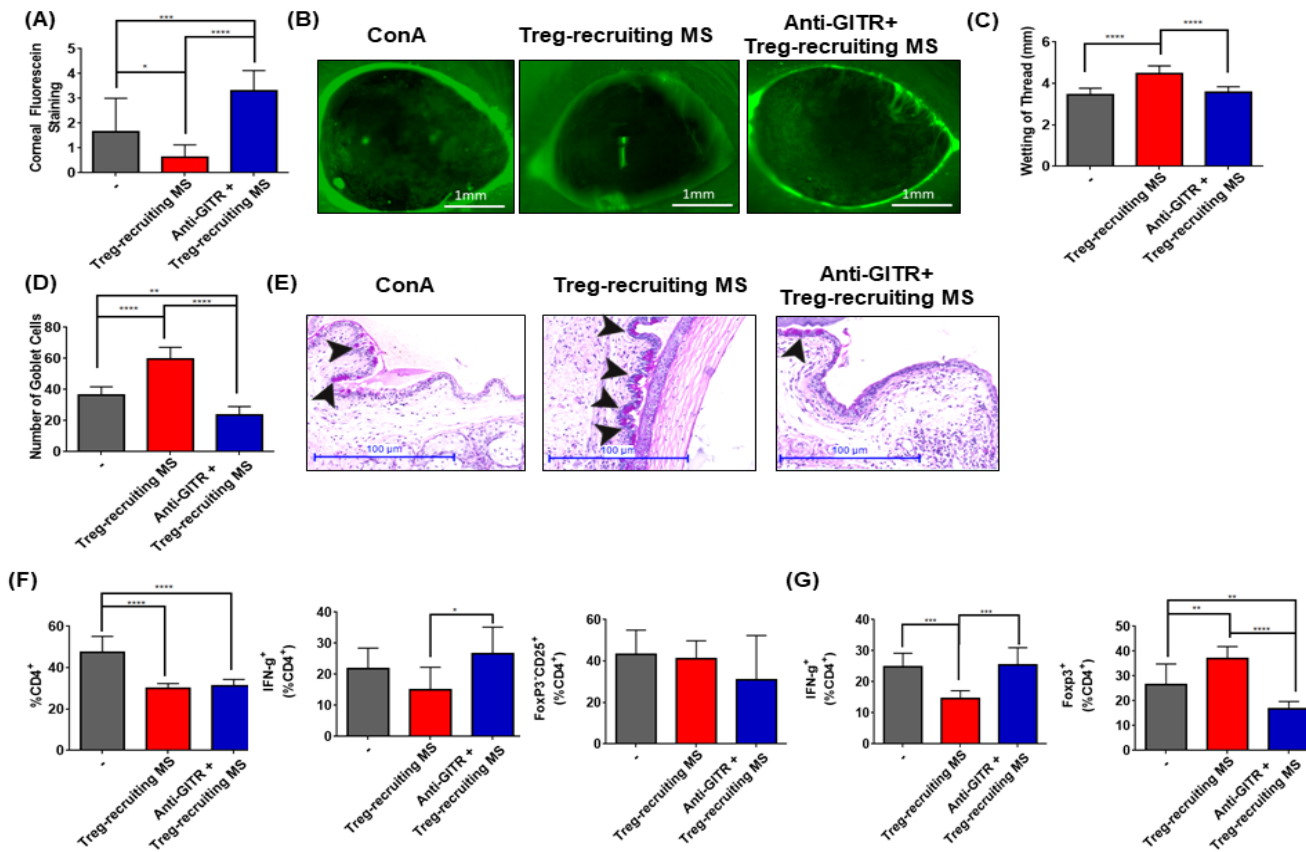


Figure 20. Administration of anti-GITR reverses the prevention signs associated with DED by Treg-recruiting MS. (A) Quantification of corneal fluorescein staining shown as mean \pm S.D. (B) Representative images of corneal fluorescein staining shown as mean \pm S.D. (C) Aqueous tear production was quantified using phenol red threads (D) Goblet cells located in the conjunctiva were counted and data is shown as mean \pm S.D. (E) Representative histology images (20X) indicates arrows pointing to the pink/purple goblet cells (F) Data from flow cytometry was performed on the regional draining lymph nodes shown as mean \pm S.D. (G) Cytokine expression and Treg percentages were analyzed in the lacrimal gland shown as mean \pm S.D. * $p \leq 0.05$; ** $p \leq 0.01$; *** $p \leq 0.001$, **** $p \leq 0.0001$.

2.4 DISCUSSION

The objective of this experimental study was to utilize a sustained release formulation designed to balance destructive inflammation through the local chemotactic recruitment of Tregs and ultimately thereby prevent clinical signs of DED. In order to cause the chemotactic recruitment of Tregs, a sustained gradient of CCL22 (a molecule that binds to the T cell surface receptor, CCR4 inducing directional migration of Tregs) was required to promote cellular migration.^[290–292] The intended chemotactic gradient will ultimately be sensitive to the amount of concentration released, with higher amounts of release having the downside of saturating directional receptor binding and decreasing chemotaxis of leukocytes thus the gradient of the microspheres is critical for migration.^[291] As Tregs migrate to a local area of inflammation, the immunological homeostatic balance is altered, resulting in the reduction of inflammation. The importance of maintaining this gradient for the recruitment of Tregs was demonstrated in the study, when a bolus injection of soluble CCL22 administered into the lacrimal gland did not prevent clinical signs associated with ConA-induced DED as shown in **Figures 16** and **17**. This may be the result of the rapid diffusion of the soluble CCL22 from the lacrimal gland.^[290–292] Interestingly, however, we did observe a significant decrease in overall CD4⁺ T cells in the cervical lymph nodes (CLN) represented in **Figure 18**. Since soluble CCL22 injected into the lacrimal gland could drain to the CLN, this result may be attributed to a transient gradient-independent effects of CCL22 on T-cell activation in the CLN.^[293] The lack of therapeutic efficacy with soluble CCL22, however, supports previous studies that suggest that a sustained gradient of chemokine (here CCL22 originating from the lacrimal gland) is required for recruitment of lymphocytes due

to the short *in vivo* half-lives of proteins and chemokines (in some cases on the order of 30 minutes) (here Tregs).^[276,290–292,294–297] As further confirmation, we observed Treg-recruiting microspheres at one week remaining in the lacrimal gland when cells were counted for flow cytometry (data not shown), which suggests that the microspheres remain in the lacrimal gland and maintain a sustained gradient of CCL22 to attract Tregs to the tissue.

In regard to the clinical signs of DED, we first investigated if the Treg-recruiting microspheres could preserve the health of ocular surface. Inflammation seen in DED can affect the integrity of the cornea, which can lead to ocular irritation and an increase risk of infections^[298]. Therefore, in this study we examined the integrity of the cornea.^[299] Our data suggest that there was a significant reduction of punctate staining on the corneal surface of the treatment group suggesting that the treatment led to maintenance of ocular surface homeostasis shown in **Figures 16B** and **16C**.^[300,301] By contrast, a disruption of the ocular surface can be due to an unstable tear film, which can contribute to inflammation of the ocular surface environment as seen in the diseased, diseased with blank microspheres and soluble CCL22 group in **Figures 15B** and **15C**.^[302] Notably, administration of Treg recruiting microspheres maintained significantly higher levels of tear production as compared to the diseased groups shown in **Figure 15**. This is consistent with a previous finding that suggested that a reduction of tear production can result in corneal epithelial defects, potentially linking these two results.^[293] Overall, the data suggest that Treg-recruiting microspheres aid in preserving corneal health, and preventing the loss of tear production.

Since goblet cells are involved in the production of mucin (a component of tear fluid)^[303] we also investigated goblet cell density in our study. Histological sections revealed that the treatment was able to markedly decrease the attenuation of goblet cells displayed in **Figure 16**.

This maintenance of goblet cells may be associated with lower levels of the Th1 cytokine (IFN- γ) secreted by effector T cells, which were lower in Treg recruiting microsphere treated mice as shown in **Figure 18**.^[288,300,303] Notably, it has been suggested that altered ratios IFN- γ / IL-13 cytokines are associated with goblet cell loss in the gut mucosa, which could be related to loss of goblet cells in the conjunctiva.

Since previous reports have suggested a correlation to the frequency of CD4⁺ IFN- γ ⁺ cells and goblet cell density, the phenotypic expression of T cells were examined to identify the percentage of cells in the regional draining lymph nodes.^[288,300,303] To the best of our knowledge, previous reports utilizing this particular model have not investigated the phenotypic expression of T cells in the regional draining lymph nodes, which serve as critical sites for the induction of ocular surface immune responses.^[293,304,305] Our data suggest that the administration of ConA possessed a significantly greater percentage of CD4⁺ T cell populations in the cervical lymph nodes (CLN), which might be due to ConA increasing the proliferation of CD4⁺ T cells.^[306] Interestingly, populations of pro-inflammatory Th1 cells in the CLN of diseased mice and soluble CCL22 were observed to be significantly higher than the saline and saline-with-blank-microsphere control groups as shown in **Figure 18**. This is not unexpected, since mice challenged with ConA have been previously reported to possess an increased IFN- γ production^[286]. Interestingly, treatment with Treg-recruiting microspheres is associated with a significant decrease of Th1-type cells when compared to administration of blank microspheres and soluble CCL22 as shown in **Figure 18B**. This is consistent with previous findings by our group and others that report how sustained local concentrations of CCL22 can decrease IFN- γ levels.^[280,283] Moreover, Saban et al. demonstrated that the Th-1 type immune response can be induced in the regional lymph nodes causing ocular surface inflammation in DED.^[307] Therefore, we

hypothesize that the recruitment of Tregs may decrease the CD4⁺ IFN- γ response in the CLN ultimately leading to the prevention of ocular surface inflammation.

To further examine the effects of Tregs, resident T-cell populations were examined in the lacrimal gland.^[308] Specifically, as immune cells migrate from the lymph nodes to the lacrimal gland, these cells secrete pro-inflammatory cytokines, perpetuating inflammation and negatively affecting function of the gland in DED.^[309] Notably, the data suggest that the treatment with Treg recruiting MS decreases the percentage of CD4⁺ IFN- γ ⁺ T cells and increases CD4⁺ FoxP3⁺ Treg populations (Foxp3 can be transiently expressed in effector T cells; however, steady Foxp3 expression is needed for the development of a functionally suppressive Treg phenotype),^[310] which may prevent inflammation mediated tissue destruction. This is consistent with other reports suggesting that Tregs can mediate a tissue-protective function by suppressing effector T-cells as shown in **Figure 19**.^[311–313] Overall, the data suggests that Treg-recruiting microspheres generate a favorable increase in the ratio of Tregs to pro-inflammatory IFN- γ ⁺ Th1 cells, which suggests an explanation for the observations of suppressed ocular inflammation, goblet cell maintenance, and restored tear film production.

Finally, in order to demonstrate that the effect observed with Treg-recruiting microspheres was due to Tregs suppressing ocular inflammation, an agonistic monoclonal antibody against GITR was utilized to inhibit the suppressive effects of Tregs on effector T cells.^[314] Anti-GITR is thought to modulate Tregs through directly abrogating their suppressive function while co-stimulating other conventional T cells.^[289,315] In humans, it has been suggested that the intensity of GITR expression on Tregs directly corresponds to the suppressive ability of regulatory T-cells.^[316] The ability of anti-GITR to suppress Treg function and worsen evaluations of DED here is consistent with recent work suggesting that the upregulation of GITR

ligand expressed on retinal pigment epithelial cells in the eye via pro-inflammatory cytokines plays an integral role in ocular immunity health.^[316] Consistent with the diseased, diseased-with-blank microspheres, and soluble CCL22 treated mice, there were also increased percentages of CD4⁺ IFN- γ ⁺ cells, and decreases in the percentages of Tregs in the lacrimal gland of mice treated with the Treg-recruiting microspheres and anti-GITR. Overall, the data suggests that anti-GITR reversed the beneficial effects of preventing clinical signs and inflammation associated with DED, likely by affecting the suppressive function of Tregs as shown in **Figure 20**.^[302]

Even though the data suggest that the Treg-recruiting microspheres were able to prevent signs and reduce inflammation in DED, there are several limitations of this particular study of note. For instance, the double-emulsion fabrication technique utilized can result in protein denaturation in the water/oil interface, which may explain the low encapsulation efficiency and potential protein damage that was not able to be detected using an ELISA.^[317] Although, the double emulsion technique is well established and has been utilized in many reports to encapsulate proteins, other techniques have shown to increase encapsulation efficiency and protein activity.^[318] Future work could include fabricating the microspheres with an alternative process by Reinhold et al. that does not result in some protein damage and can enhance the encapsulation efficiency of the protein.^[319] Additionally, we may need to examine residual polymer accumulation by examining histological sections of the tissue in order to identify whether the biodegradation of PLGA over time could potentially cause granulation of tissue development.^[284] Future work should be geared toward examining this potential polymer accumulation and confirm that the recruitment of Tregs to the lacrimal gland can overcome pre-established inflammation. We hypothesize that, if optimized, Treg-recruiting formulations could be effective as a potential therapeutic since it has been previously demonstrated that Tregs

indeed play an integral role in resolving established inflammation associated with DED.^[320] One particular point of focus could be the ability of recruited Tregs to overcome any pre-existing ocular surface tissue destruction, which may serve to catalyze inflammation and disease.^[321,322] However, and notably, our previous data using Treg-recruiting microspheres in a murine model of periodontitis started a pronounced reversal of the characteristic destructive tissue microenvironment towards expression of markers that would best characterize a regenerative microenvironment.^[280] Ultimately, however, further studies would be required to determine if the same shift in expression in the ocular microenvironment would result from treatment with Treg-recruiting formulations. It is also important to consider the method of administration for any potential therapeutic strategy. Although, injections (such as the ones into the lacrimal glands used herein) could be applicable given that injections in the eye and lacrimal gland have become more common in clinical studies and treatments ^[323–326], less invasive strategies (which are still effective) would (all things being equal) be more attractive.^[327,328]

In summary, in this chapter, our study collectively suggests that the administration of Treg-recruiting microspheres effectively prevents destructive inflammation in an experimental murine model of DED. Specifically, the sustained release of the chemokine CCL22 in the lacrimal gland prevented a loss of tear production, corneal fluorescein staining and goblet cell depletion, which resulted in the decrease of signs associated with DED. This resolution of inflammation and signs of DED is likely due to the increase of Tregs and decrease of Th1 cells in the lacrimal gland. Future studies will focus upon extending this proof-in-principle toward exploration of therapeutics that recruit the body's own endogenous Tregs to resolve inflammation in DED.

3.0 TRI MICROSOPHERES PREVENT KEY SIGNS OF DRY EYE DISEASE IN A MURINE, INFLAMMATORY MODEL

This chapter is adapted from: Michelle L. Ratay, Stephen C. Balmert, Abhinav P. Acharya, Ashlee C. Greene, Thiagarajan Meyyappan, and Steven R. Little. (2017). (Submitted to *Scientific Reports*)

Specific Aim 2: To explore induction of Tregs as an alternative treatment for DED.

3.1 INTRODUCTION

In the previous chapter, we discussed a biomimetic approach to locally recruit Tregs to the lacrimal gland utilizing the controlled release of CCL22 (chemokine) to restore immunological homeostasis and ultimately prevent clinical signs of DED.^[329] Notably, however, Tregs can represent low total numbers of T-cells in the periphery, which could possibly make it non-trivial to achieve enough functional Treg to shift the homeostatic balance.^[330] For this reason, we hypothesized that inducing (differentiating) Tregs from a more prevalent, naïve CD4⁺ population could also be a viable strategy that was worth exploring. Specifically, prevalent, naïve CD4⁺ T cell populations in the periphery are capable of differentiating into functional Tregs under the direction of a subset of antigen presenting cells known as tolerogenic dendritic cells (tDCs).⁵³

tDCs induce differentiation of naïve CD4⁺ T cells into Tregs (in part) through the secretion of a combination of IL-2 and TGF-β cytokines.^[331,332] However, the maintenance of Tregs is somewhat more complex and depends on a local microenvironment that is not only favorable to differentiation of Tregs, but also unfavorable to differentiation into other effector T cells.^[333] One method of creating such a local microenvironment is through administration of the small molecule, rapamycin. Rapamycin (Rapa) is an mTOR inhibitor that can suppress the generation and proliferation of effector T cells.^[334] We have previously demonstrated that sustaining the presence of TGF-β, Rapamycin and IL-2 using degradable microspheres was able to induce/differentiate naïve CD4⁺ T cells into FoxP3⁺ Tregs *in vitro* with high efficiency as represented in **Figure 21**.^[334]

Here we describe the *in vivo* application of T-Reg Inducing (TRI) microspheres (MS) in a model of murine dry eye disease. Data suggests that this drug-delivery strategy can influence local Treg numbers and, in turn, prevent key signs of DED. Application of this new strategy could provide a potential avenue for new types of immune based treatments for DED that influence the body's own cells to address destructive inflammation.^[335,336]

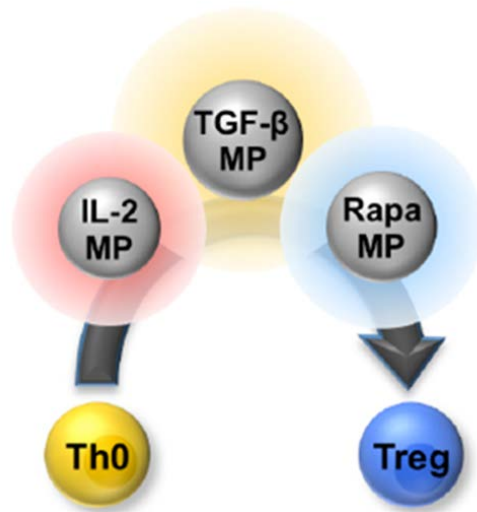


Figure 21. Microspheres that release a combination of recombinant proteins and a synthetic drug in order to promote Treg differentiation.

3.2 MATERIALS AND METHODS

TRI microspheres were fabricated as a controlled release system to promote the induction of naïve CD4⁺ T cells found in the periphery into Tregs. Subsequently, we investigated whether this preventative therapeutic method could shift of the pro-inflammatory microenvironment of the lacrimal gland and ultimately prevent clinical signs of DED.

3.2.1 Fabrication of Microspheres

TGF- β and IL-2 microspheres were fabricated using a double emulsion- evaporation technique. For the TGF- β microspheres, Poly (lactic-co-glycolic) acid (PLGA-50:50 lactide:glycolide, acid terminated) (MW:7,000-17,000) (viscosity: 0.16-0.24 dL/g, 0.1 % (w/v) in chloroform) (Sigma Aldrich, MO) and PEG-PLGA (PolySciTech, IN) was used to encapsulate rh-TGF- β (PeproTech, NJ). Specifically, 170 mg of PLGA and 30 mg of PEG-PLGA was dissolved in 4ml of DCM (Sigma Aldrich, MO). Then 200 μ l of aqueous solution containing 10 μ g of rh-TGF- β was added to the polymer DCM mixture. The mixture was sonicated using a sonicator (Vibra-Cell, Newton, CT) for 10 sec. at 25% amplitude. Next, this emulsion was then mixed with 60 ml of 2% polyvinyl-alcohol (PVA, MW ~25,000, 98% hydrolyzed; PolySciences) and homogenized (L4RT-A, Silverson, procured through Fisher Scientific) at 3,000 rpm for 1 min. The homogenized mixtures were then added to 80 ml of 1% PVA on stir plate and left for 3 hours in order for the DCM to evaporate. After three hours, the microparticles were centrifuged (200 g, 5 min, 4 °C), washed five times with deionized water, and lyophilized for 48 hours (Virtis Benchtop K freeze dryer, Gardiner, NY).

For the IL-2 microspheres, 200 mg of PLGA (PLGA-50:50 lactide:glycolide, acid terminated) (MW:7,000-17,000) (viscosity: 0.16-0.24 dL/g, 0.1 % (w/v) in chloroform) (Sigma, Aldrich, MI) was dissolved in 4ml of DCM. Subsequently, 5 μ g of IL-2 and 150 μ l (R&D Systems, Minneapolis MN) of deionized water was added to the organic phase. Next, the two phases were emulsified using a sonicator probe (Vibra-Cell, Newton, CT) at 25% amplitude for a period of 25 seconds. Then this emulsion was mixed with 60 ml of 2% polyvinyl-alcohol (PVA, MW ~25,000, 98% hydrolyzed; Polysciences) with 51.66 millimoles of NaCl and homogenized (L4RT-A, Silverson, procured through Fisher Scientific) at 3,000 rpm for 1 min. This secondary

emulsion was then then added to 80 ml of 1% PVA on stir plate and stirred for 3 hours. After finishing stirring, the microparticles were centrifuged (200 g, 5 min, 4 °C), washed 5 times with deionized water, and lyophilized for 48 hours (Virtis Benchtop K freeze dryer, Gardiner, NY).

The rapamycin (rapa) microspheres were fabricated using a single emulsion-evaporation technique due to the hydrophobic nature. Rapamycin (Sigma Aldrich, MO) was dissolved in DMSO (Sigma, Aldrich, MO) at 10mg/ml. Then 200 mg of PLGA (Sigma Aldrich, MI) was dissolved in 4 ml of DCM. Next, 100 μ l of rapamycin (10mg/ml) was added to the polymer/DCM mixture. The solution was then homogenized with 60 ml of 2% PVA at 3,000 rpm for 1 min. After homogenizing, the emulsion was then added to 80 ml of 1% PVA and stirred for 3 hours. At the end of stirring, microspheres were washed 5 times with deionized water and lyophilized for 48 hours.

3.2.2 Characterization of Microspheres

The morphology of the microspheres were characterized using scanning electron microscopy (JEOL, JSM-6330F, Peabody, MA) and volume impedance measurements were performed on a Beckman Coulter Counter (Multisizer-3, Beckman Coulter, Fullerton, CA). The release assay of the IL-2, TGF- β , and rapamycin was completed by incubating 10 mg of microspheres in 1ml of phosphate buffered saline (PBS) and 1% BSA, which was placed onto a rotator at 37°C. The supernant was sampled at different time intervals and the TGF- β and IL-2 release profiles were quantified using an enzyme-linked immunosorbent assay (ELISA) (R&D Systems, Minneapolis, MN). The release profile of rapamycin microspheres was determined using UV-vis spectroscopy, and the release media contained 0.2% Tween-80 in PBS (absorbance at 278 nm).

3.2.3 Mice

Female Balb/c mice aged 6-8 weeks were used in this experimental study. (Charles Rivers Laboratories, Wilmington, MA). The Institutional Animal Care and Use Committee, University of Pittsburgh approved all murine experiments. All methods were performed in accordance with the relevant guidelines and regulations.

3.2.4 Murine DED Model and Treatment

Dry eye disease was induced using 10 mg/ml of Concanavalin A (ConA) (Sigma Aldrich, St. Louis, MO) in phosphate buffered saline solution (PBS) was injected into the lacrimal glands with a 28.5 gauge needle using a dissecting microscope.^[222,337] The controls for examining the effects of the TRI MS included Blank (unloaded) or TRI MS (25 mg/ml), which were combined with a PBS solution of ConA (10mg/ml). (Olympus SZX10, Waltham, MA).

3.2.5 Suppression of Tregs via the Administration of Anti-GITR

In order to identify the role of Tregs with the administration of our preventative treatment, the function of Tregs were inhibited using anti-GITR (DTA-1) (BioXCell, Lebanon, NH) via an intraperitoneal injection of (500 µg per mouse) 1 day after injecting the ConA and TRI MS.^[280]

3.2.6 Tear Production

Phenol red cotton threads were utilized to measure tear production. (Oasis Medical, San Dimas, CA). The thread was placed in the lateral canthus of the eye for a period of 60 seconds, and the amount of wetting on the thread was measured using a dissecting microscope (Olympus SZX10, Waltham, MA).^[222]

3.2.7 Corneal Fluorescein Staining

Fluorescein stain (1% solution) was applied to the conjunctival sac. The surface of the cornea was examined using a dissecting microscope (Olympus SZX10, Waltham, MA). The scoring of staining was completed by a masked ophthalmologist, and scored 0 for no staining, score 1 for a quarter of staining, score of 2 for less than a half, score of 3 for half, and 4 for more than half of the eye.

3.2.8 Ocular Histology

At the conclusion of the study, the eyes were exenterated and fixed in 10% neutral buffered formalin. Sections were prepared at approximately 5 μ m and stained with Periodic Acid Schiff (PAS) in order to examine goblet cell density. Histological sections were scanned and quantified using a Zeiss Axio Scan. Z1 (Thornwood, NY) and Pannoramic Viewer software (3D HISTECH Ltd.).

3.2.9 qRT-PCR

Total RNA was extracted from excised lacrimal glands using TRI-reagent (Molecular Research Center, Cincinnati, OH), and quantified using a NanoDrop 2000 (Thermo Scientific). For the reverse transcriptase assay, 2 µg RNA was converted to cDNA using a QuantiTect Reverse Transcription Kit (Qiagen, Valencia, CA). Quantitative real-time PCR was then performed using VeriQuest Probe qPCR Mastermix (Affymetrix, Santa Clara, CA), (Thermo Scientific) specific for (IFN- γ :Mm01168134_m1, FAM-MGB dye), (IL-2:Mm00434256_m1, FAM-MGB dye), (IL-6:Mm00446190_ml, FAM-MGB dye), and (Gusb: Mm01197698_m1, VIC-MGB PL dye, endogenous control). Duplex reactions (target gene + GUSB) were run and analyzed on a StepOnePlus Real-Time PCR System (Applied Biosystems, Carlsbad, CA). Relative fold changes of IFN- γ , IL-6 and IL-2 expression were calculated and normalized based upon the $2^{-\Delta\Delta C_t}$ method, with the Saline group as the untreated control.

3.2.10 Immunofluorescence of the Lacrimal Gland

At the end of the study, lacrimal glands were excised from the mice. Lacrimal glands were fixed with 4% PFA overnight, followed by cryoprotection through incubation in 30% sucrose overnight, and lastly embedded in O.C.T. medium. The cryosections were obtained at 7µm thick and stained with fluorescent antibodies. Specifically, 7µm sections were blocked with 5% normal donkey serum and 1% Tween20 in PBS. Blocked sections were incubated overnight at 4°C with rat anti-FoxP3 (FJK-16s; eBio) and rabbit anti-CD3 (SP7, monoclonal rabbit IgG; Abcam, Cambridge, MA). The sections were then incubated with a secondary antibody, Alexa Fluor 594 donkey anti-rat IgG (ThermoFisher Scientific Waltham, MA) and Alexa Fluor 647 donkey anti-

rabbit IgG (Jackson ImmunoResearch Laboratories, West Grove, PA) for 1 hour at room temperature and then mounted using Fluoroshield mounting medium with DAPI (Abcam, Cambridge, MA). The images were captured using a Zeiss Axio Scanner Z.1. Only positively stained cells overlapping DAPI (nuclei) were quantified.

3.2.11 Statistical Analysis

Data expressed as mean \pm S.D. Comparisons between multiple treatment groups were performed using one-way ANOVA, followed by Bonferroni multiple comparisons, and $p \leq 0.05$ was considered statistically significant. The PCR data expressed as mean \pm SEM was analyzed utilizing a t-test with Welch correction, and $p \leq 0.05$ was considered statistically significant. Statistical tests were performed using GraphPad Prism Software 6.0 (GraphPad Prism, San Diego, CA).

3.3 RESULTS

3.3.1 Characterization of TRI MS: IL-2, TGF- β 1 and Rapamycin

TGF- β microspheres (MS) were reformulated to eliminate the 20-day initial lag phase of release in the prior formulation. The new formulation of TGF- β MS contains a PEG-PLGA diblock copolymer (4 wt%, $M_n \sim 5$ kDa), which accelerated release by increasing matrix swelling, and

the ester-terminated PLGA helped to minimize the electrostatic interactions between the PLGA polymer and the positively charged protein.^[338] After measuring the release of TGF- β , the surface morphology of the microspheres was characterized using scanning electron microscopy (SEM). The representative SEM images indicate that the rapamycin and IL-2 MS possessed similar surface morphology and release behavior as previously reported and shown in **Figure 22**.^[334] SEM images reveal spherical non-porous PLGA-based rapamycin microspheres represented in **Figure 22**. IL-2 MS exhibit surface porosity and a high initial burst followed by a slow continuous release for the length of the experimental study, as previously described and shown in **Figure 22**.^[334] The newly fabricated TGF- β microspheres contained an uneven surface morphology, similar to a previous report utilizing PEG and PLGA microcapsules.^[339] The average size of TRI MS was 12 μm (rapamycin), 19 μm (IL-2), and 17 μm (TGF- β) as determined by Coulter Counter (volume impedance method).

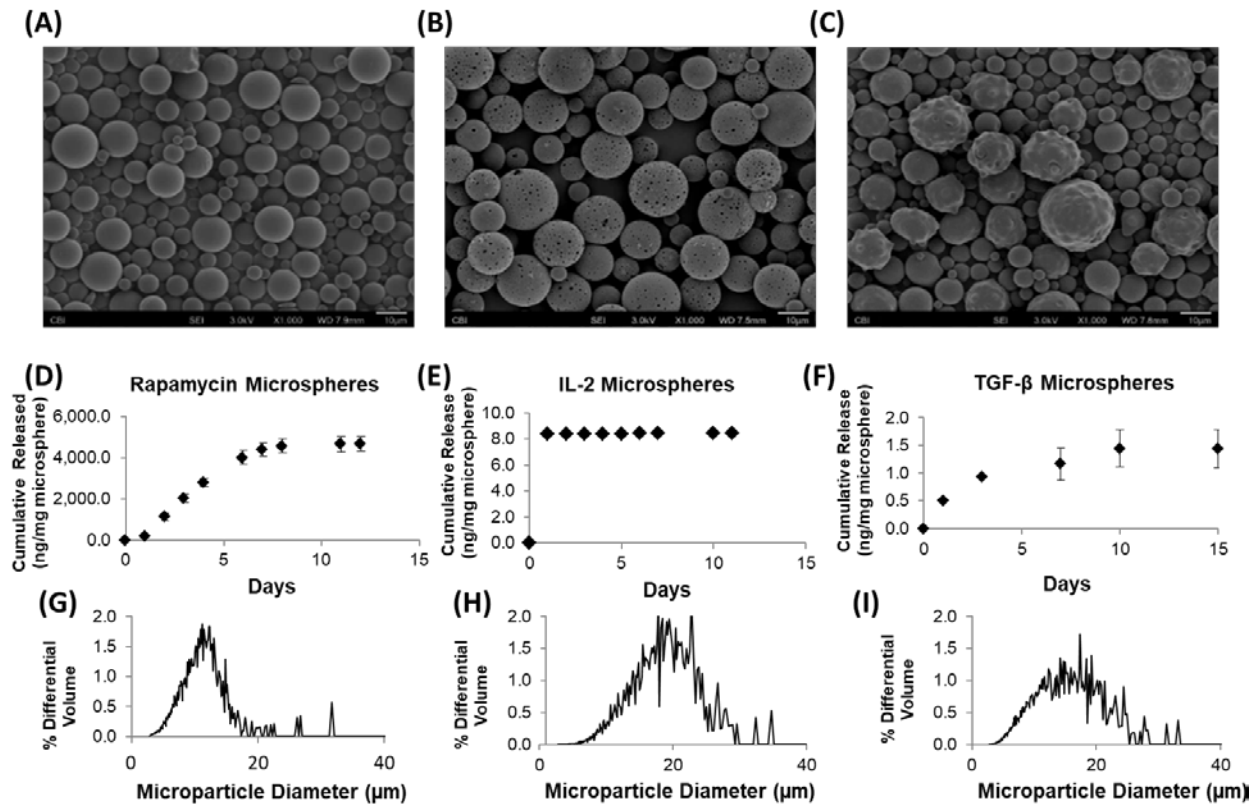


Figure 22. Characterization of Treg-inducing Microspheres. (A) Representative Scanning electron microscopy (SEM) image of Rapamycin microspheres (1000x) (B) Representative SEM image of IL-2 Microspheres (1000x) (C) Representative image of TGF- β Microspheres. (D) Release Kinetics of Rapamycin Microspheres is shown (n=3) (E) Release Kinetics of porous IL-2 Microspheres (n=3) (F) Release Kinetics of TGF- β Microspheres (n=3). (G)Size distribution of Rapamycin Microspheres (H) Size distribution of IL-2 Microspheres (I) Size Distribution of TGF- β Microspheres

3.3.2 TRI MS Prevent Loss of Aqueous Tear Production

To investigate whether TRI MS were capable of preventing key signs of dry eye disease, we first examined aqueous tear secretion.^[222] Concanavalin A (ConA) was injected into the lacrimal gland to induce DED, and for TRI MS or Blank MS treatment groups, MS were incorporated in ConA injections as shown below in **Figure 23**. One week following the administration of ConA with either Blank MS or TRI MS, phenol red thread testing was performed to evaluate tear secretion. The administration of ConA alone (diseased) significantly reduced tear production as compared to an injection of Saline (non-diseased) as shown in **Figure 24A**. Notably, tear secretion was restored to non-diseased levels in DED mice treated with TRI MS, while administration of ConA + Blank MS (unloaded) had no noticeable effect on tear production in mice **Figure 24A**. In order to identify whether all three factors (TRI MS) were required to prevent loss of aqueous tear production, mice were treated with individual microsphere formulations alone (Rapa, TGF- β , or IL-2) or combinations of two microsphere formulations (Rapa + TGF- β ; Rapa + IL-2; TGF- β + IL-2). Notably, the individual microspheres alone and the combinations of two microsphere formulations were unable to restore tear production inhibited by ConA as shown in **Figure 27**, suggesting that therapeutic efficacy required the delivery of the TRI MS to prevent the loss of tear production.

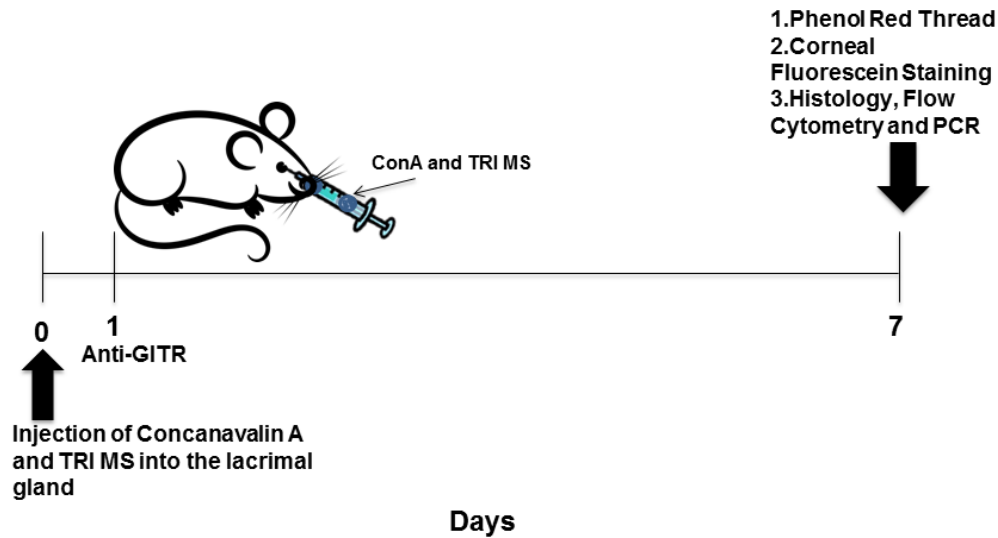


Figure 23. TRI microspheres for the prevention of inflammation associated with Dry eye Disease (DED) in mice. A timeline for the experimental murine model of inflammation induce via Concanavalin A.

3.3.3 Goblet Cell Density Maintained with the Administration of TRI MS

Mucin is a key component associated with a healthy tear film, which is produced by goblet cells located in the conjunctiva.^[303,340] As the density of goblet cells are diminished this can contribute to an unstable tear film and lead to ocular surface destruction.^[340] Upon examination of ocular tissue histology, we observed a significant decrease in the density of Periodic Acid Schiff (PAS)-stained goblet cells (pink/purple cells in conjunctiva epithelium layer) in the ConA group as compared to the Saline group as shown below in **Figure 24B** and **24C**.^[222,301,303,337,341] Treatment with TRI MS led to maintenance of goblet cell density, unlike mice with ConA-induced DED displayed in **Figure 24B**. Overall, histological sections revealed that TRI MS treatment markedly inhibited ConA-induced attenuation of goblet cells **Figure 24** and **25**.

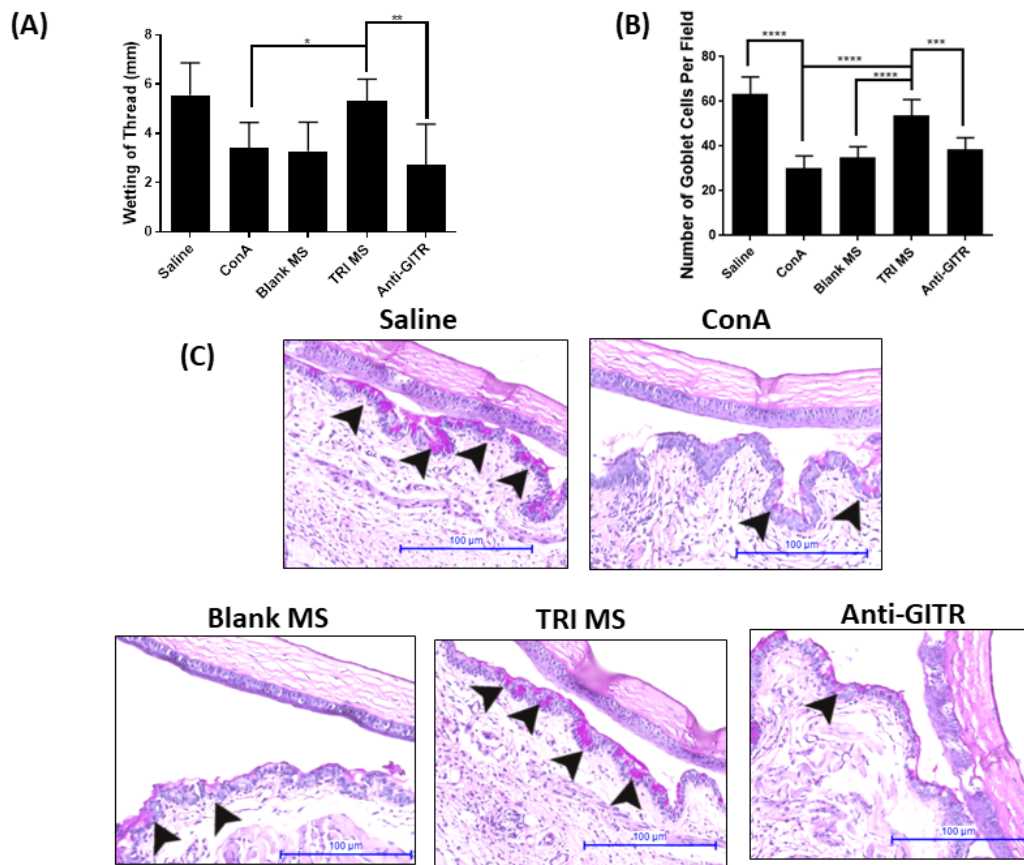


Figure 24. TRI MS prevent clinical signs of inflammation associated with DED. (A) Wetting of phenol red threads were measured in millimeters using a dissecting microscope (n=6) shown as mean \pm S.D. (B) Representative images of histological sections of the eyes (20X) were quantified to identify differences in the TRI MS group compared to the diseased groups and non-diseased group (100 μ m scale bar). (C) Goblet cells shown are the pink/purple (Periodic Acid Schiff stained) cells located in the conjunctiva labeled with arrows and the groups are shown as mean \pm S.D. * $p \leq .5$; ** $p \leq .1$; * $p \leq .1$, **** $p \leq .1$.**

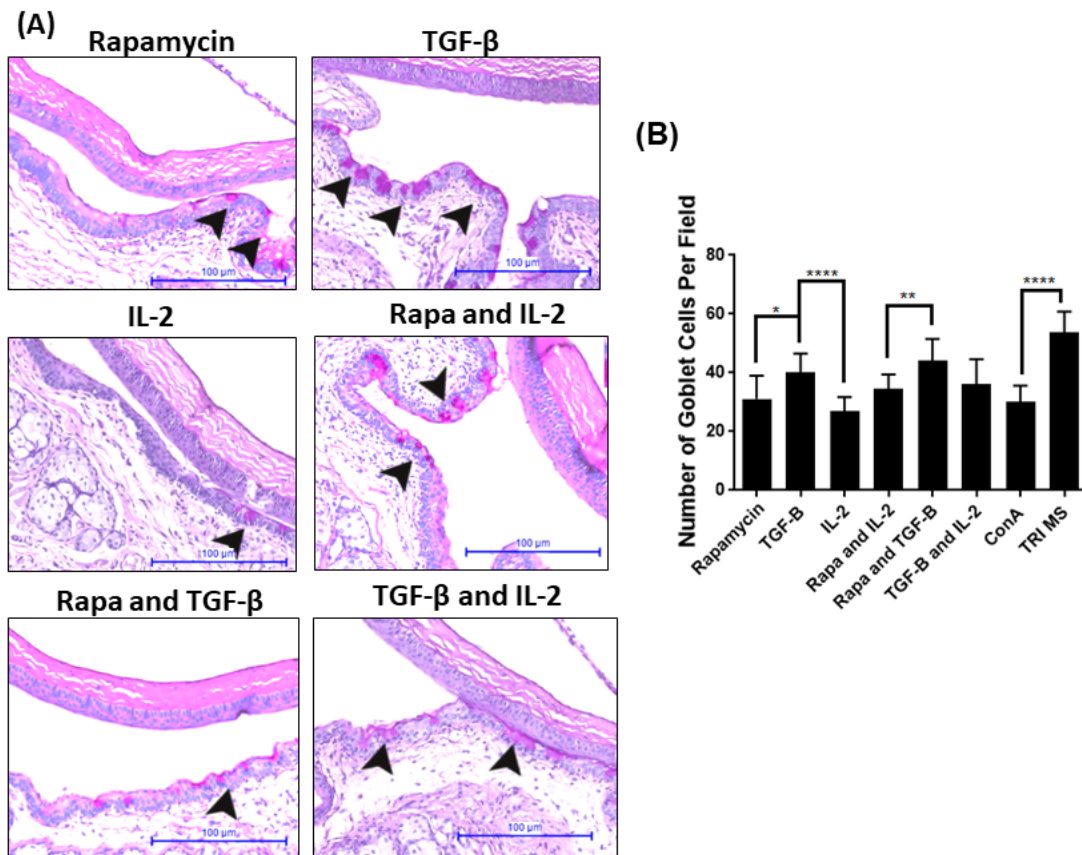


Figure 25. Single factors (Rapamycin; IL-2; TGF- β) and combinations of two factors (Rapa + TGF- β ; Rapa + IL-2; TGF- β + IL-2) were utilized to examine goblet cell density in the conjunctiva. (A) Representative images of single and combination factors of PAS stained goblet cells in the conjunctiva (B) Quantification of goblet cell numbers from the histology of the conjunctiva

3.3.4 Corneal Fluorescein Staining Reduced with TRI MS

To determine the health of the ocular surface, corneal fluorescein staining was performed, with the degree of punctate staining as an indicator of disease severity.^[342] Fluorescent images of the ocular surface were captured and scored by a masked ophthalmologist on a scale of 0 to 4, with 0 corresponding to no staining, and 4 corresponding to staining on more than 50% of the cornea, as seen in **Figure 26A**. The ocular staining score was significantly lower for the Saline and TRI MS groups as compared to the ConA + Blank MS group as shown below in **Figure 26B**. We also examined eyes from mice treated with ConA plus individual microsphere formulations alone or combinations of two microspheres. Neither individual microspheres alone and combinations of two microsphere formulations, were able to reduce corneal fluorescein staining to the same extent as the TRI MS treatment as shown in **Figure 27**, suggesting that local administration of TRI MS is necessary to restore ocular surface health that is impaired by ConA.

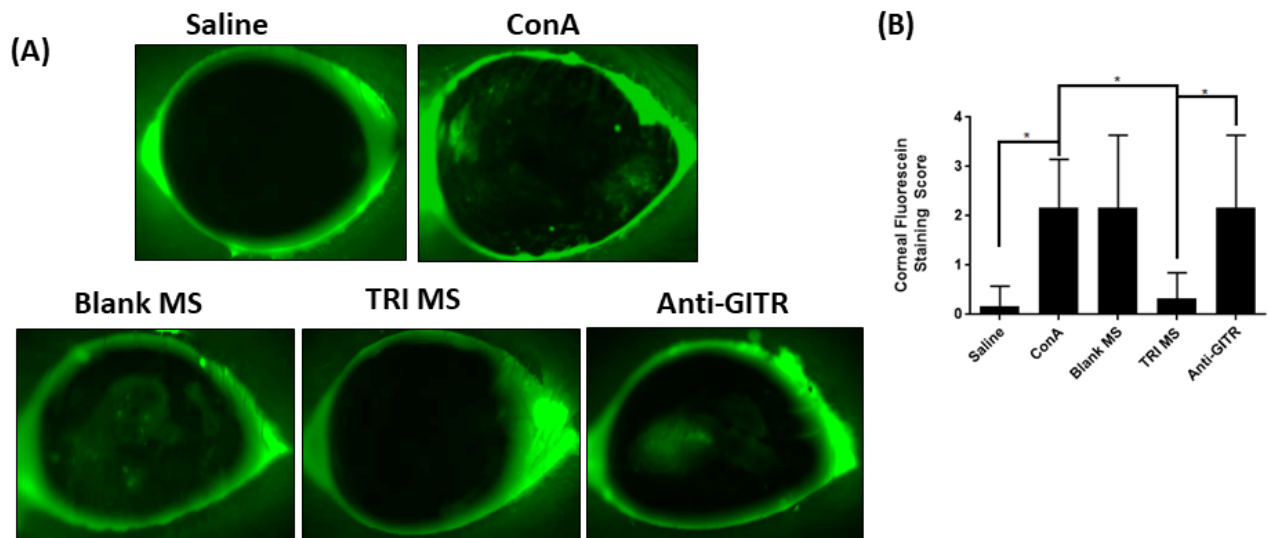


Figure 26. TRI MS reduce ocular surface staining. (A) Representative images of corneal fluorescein staining. (B) Clinical corneal fluorescein staining scores of the ocular surface on a scale of (0-4) (n = 6) shown as mean \pm S.D. * $p \leq 5$

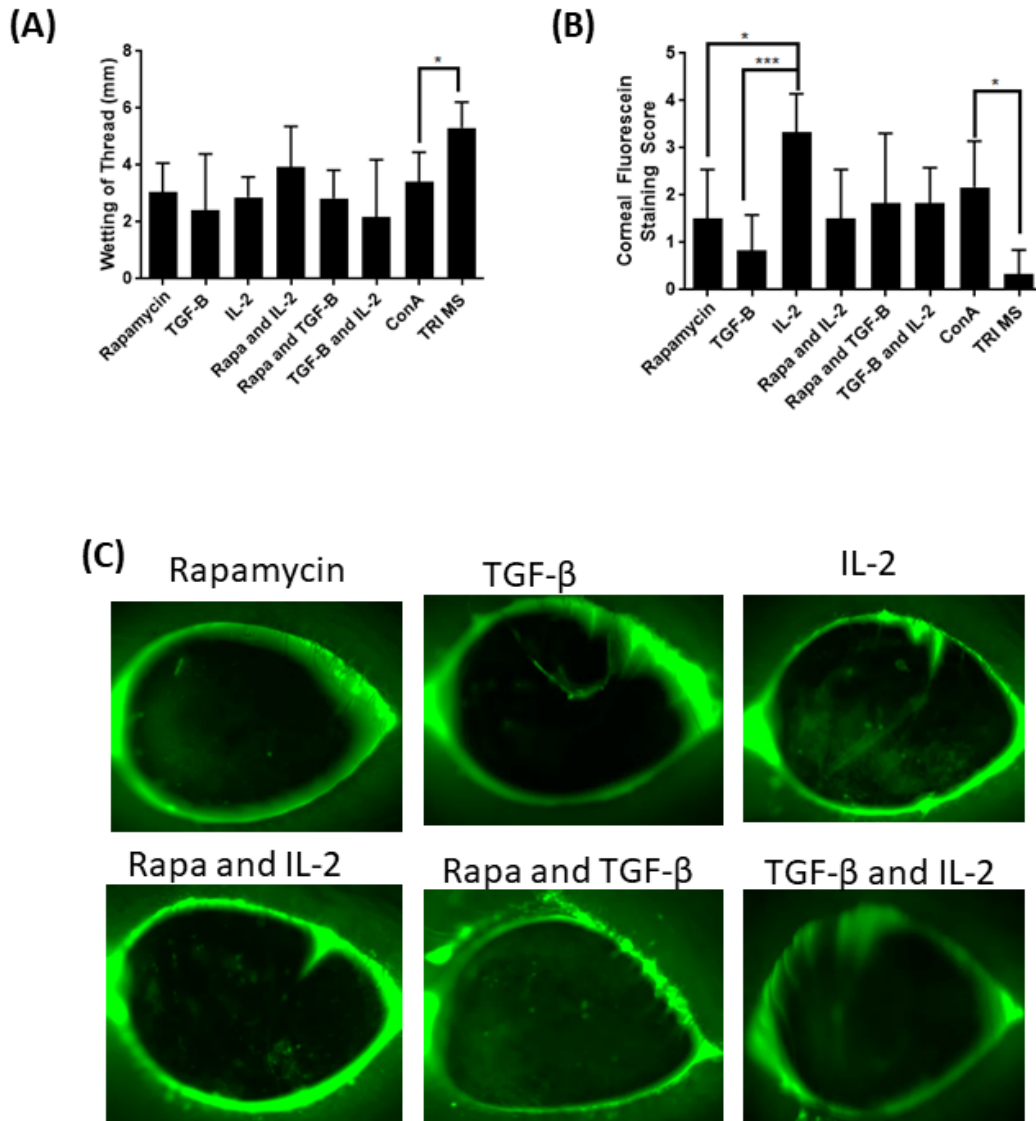


Figure 27. (A) Phenol Red Thread testing for the single factor (Rapamycin; IL-2; TGF-β) and combination of two factors (Rapa + TGF-β; Rapa + IL-2; TGF-β + IL-2) experimental groups. (n=6) (B) Ocular Surface Staining score (n=6) (C) Representative images of corneal fluorescein staining

3.3.5 TRI MS Decrease Pro-Inflammatory Cytokines

Several cytokines in the local milieu of the lacrimal glands were examined following treatment. Notably, while ConA induced expression of pro-inflammatory IFN- γ , IL-6, and IL-2 in the lacrimal gland as shown in **Figure 28**, TRI MS treatment significantly reduced expression of each of these cytokines, compared to the administration of ConA alone as shown below in **Figure 28**.^[222,337] The relative expression of pro-inflammatory cytokines in the lacrimal glands can be correlated with infiltration of CD3⁺ T cells, which was increased in the ConA + Blank MS group and reduced with TRI MS treatment shown in **Figure 29**.^[286] Together these data indicate that the TRI MS treatment was able to reduce the ConA-induced expression of pro-inflammatory cytokines in the lacrimal gland tissue.

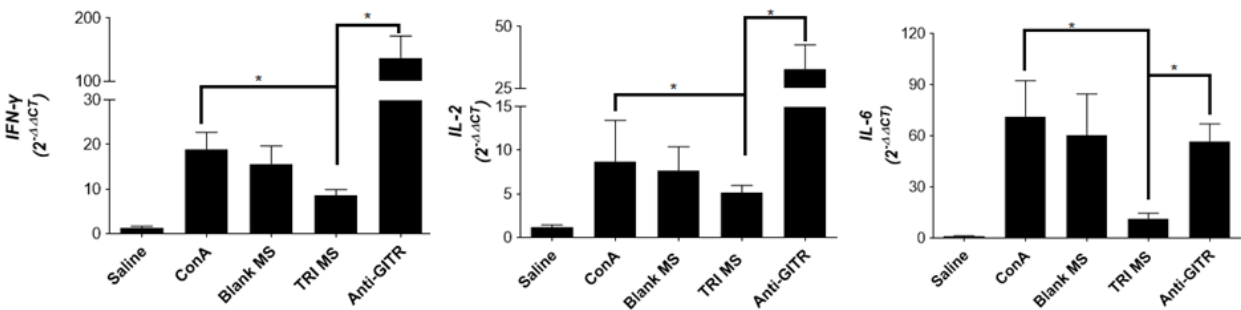


Figure 28. Administration of TRI MS reduces levels of cytokines in the lacrimal gland shown as mean \pm SEM * $p \leq 0.05$

3.3.6 TRI MS Increase the Percentage of FoxP3⁺ Tregs of overall CD3⁺ T cells in the Lacrimal Gland

In order to examine the local immune environment of T-cells in the lacrimal gland, we performed immunofluorescence staining of lacrimal gland sections with anti-CD3 and anti-FoxP3 monoclonal antibodies. While there were fewer total numbers of infiltrating CD3⁺ T cells with TRI MS treatment, there was a larger ratio of those FoxP3⁺ Tregs of overall CD3⁺ T cells, compared to the ConA alone and ConA + Blank MS groups as represented in **Figure 29**. Collectively, this data suggest that the sustained delivery of TRI MS is capable of locally enriching Treg populations as compared to effector T cells in the lacrimal gland tissue.

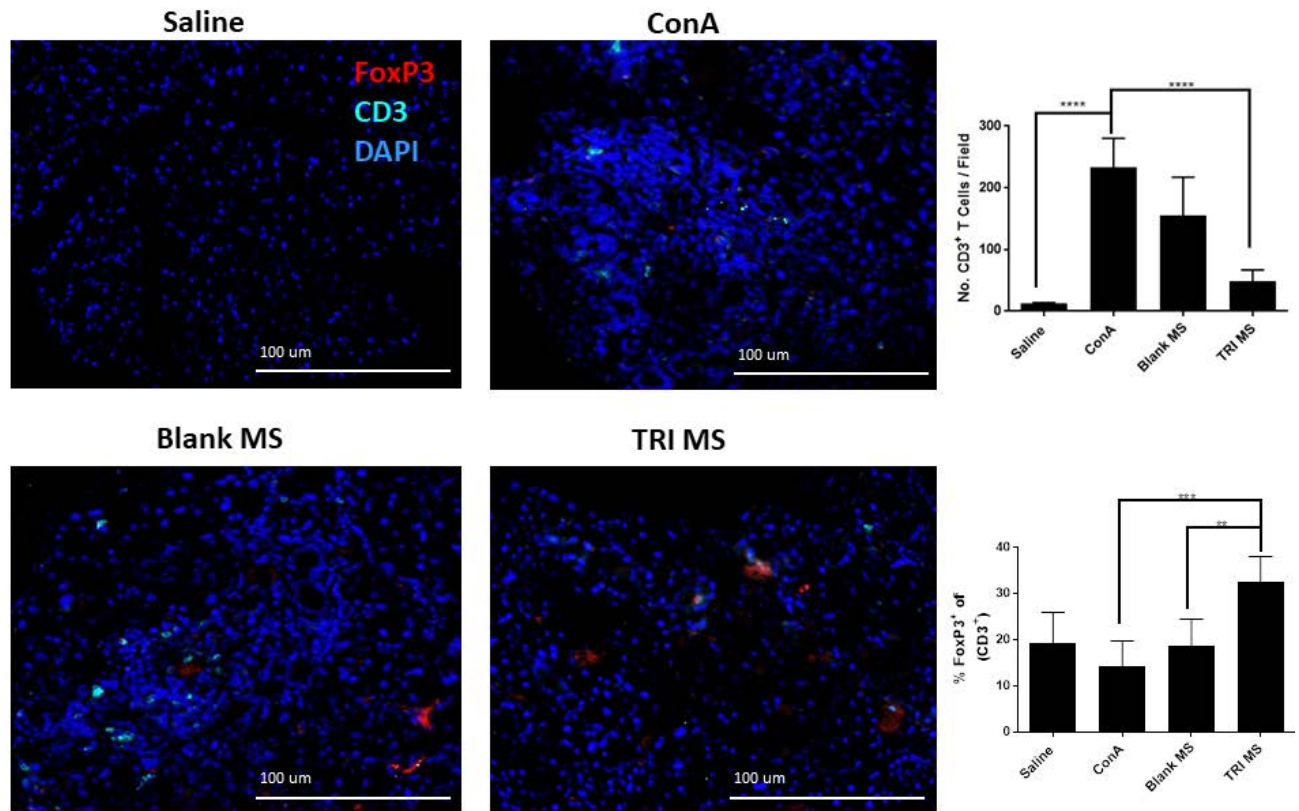


Figure 29. Representative lacrimal gland fixed frozen cryosections (10X magnification) stained for T-cells (CD3+ T cells-Cyan), Regulatory T-cells (FoxP3+ T cells - Red), and nuclei (DAPI-blue). Scale bars are 100µm. Quantification of lacrimal gland T cells per imaged field and % Treg, based on IHC images with FoxP3 staining (n=5). * $p \leq 0.05$; ** $p \leq 0.01$; *** $p \leq 0.001$

3.3.7 Suppression of Tregs via Administration of Anti-GITR

An agonistic antibody (DTA-1) specific for GITR (glucocorticoid tumor necrosis factor) was administered 1 day after the injection of the ConA and TRI MS to determine whether the prevention of dry eye symptoms are mediated by the expanded Treg population.^[314] Monoclonal antibody anti-GITR (DTA-1) acts to systemically attenuate the suppressive function of Tregs by inhibiting the ability of conventional T cells to be suppressed by Tregs.^[289,315,343] Mice were administered anti-GITR, one day after ConA and TRI MS. The anti-GITR group (with TRI MP administration) exhibited restored pathological features of DED as indicated by the decrease of aqueous tear secretion as shown in **Figure 21A**, reduction of goblet cells in the conjunctiva as shown above in **Figure 21B** and **21E**, an increase of fluorescein staining as shown in **Figure 22C** and **22D** as compared to the TRI MS group without anti-GITR. Moreover, with the administration of anti-GITR, expression of pro-inflammatory cytokines were significantly increased in the lacrimal gland as compared to the TRI MS with no anti-GITR as shown in **Figure 28**.

3.4 DISCUSSION

A number of investigations have demonstrated that DED is thought to be mediated by CD4⁺ T cells.^[298,304,344–346] Moreover, hallmarks of CD4⁺ T cell-mediated inflammation associated with DED include epithelial apoptosis, abnormal tear film composition and an increase of pro-inflammatory cytokines within the ocular tissue.^[305,347] Typically, one the first features DED patients recognize as a symptoms is ocular dryness due to a reduction in tears (abnormal tear film composition), which can lead to a decrease of visual acuity.^[340,348] Within the tears there are three main components that support the ocular surface; water, mucin, and lipid.^[349] All of these three components play an integral role in lubricating the ocular surface and maintaining health.^[350] As ocular dryness ensues, a lack of lubrication and epithelial surface protection can result.^[351] Due to the integral role tears play in maintaining a healthy ocular surface, tear secretion was evaluated to determine whether the preventative treatment (TRI MS) decreased tear loss thereby subsequently preserving ocular lubrication. Our data suggest there was a significant reduction of tears in the ConA alone as compared to the Saline as shown in **Figure 24**, as expected.^[222,329,337] Notably, the TRI MS significantly prevented the reduction of tears as compared to the ConA alone group shown above in **Figure 24**. However, when either the individual microsphere formulations alone (Rapa, TGF- β , IL-2) or the combination of two microsphere formulations (Rapa + TGF- β ; Rapa + IL-2; TGF- β + IL-2) were administered, there was no significant restoration of tear production observed as shown in **Figure 27**. These data suggest the combination of all three factors (TRI MS) are required to achieve prevention of tear loss.

In addition to tear production, we also investigated the effects of the treatment on goblet cells, which produce the tear film (mucin);^[285] a key component that provides a protective and stabilizing function for the ocular surface.^[352] The histological sections of the eye tissue were examined to identify if goblet cells were preserved with the administration of TRI MS. Notably, there was a significant preservation of goblet cells in the TRI MS group as compared to the ConA alone and ConA + Blank MS groups as shown in **Figure 21**. This may be due to reduced expression of IFN- γ in lacrimal glands of mice treated with TRI MS, compared to the ConA alone treated mice as shown in **Figure 28**. Specifically, an increase expression of IFN- γ has been attributed to the sustained proliferation of CD4⁺ effector T cells (Th1 cells).^[305,344] For example, mice with DED exhibit increased frequencies of the pro-inflammatory Th1 cytokine IFN- γ , which can infiltrate the conjunctiva, causing a reduction of goblet cells.^[353] Notably, previously published data suggest that the overall number of goblet cells were not affected in IFN- γ knock out mice with DED, demonstrating the potential specific involvement of IFN- γ in DED pathogenesis.^[288] Indeed, the protective effects of TRI MS may be a result of reduced infiltrating Th1 cells in general, or a reduction in IFN- γ specifically as shown in **Figure 28**.^[347]

As goblet cells undergo apoptosis, potentially due to IFN- γ , the composition of the tear film can become abnormal, which may lead to a disruption of the corneal epithelial tissue.^[351] For this reason, an ocular staining test was performed to determine if the reductions in tear secretion and goblet cell density corresponded to an increase of corneal fluorescein staining.^[354] Specifically, the increase in corneal staining may be due to the fluorescein dye remaining in areas left by desquamated epithelial cells.^[354] As expected, corneas from the ConA alone and ConA + Blank MS groups showed a significant increase of corneal fluorescein staining compared to the Saline and TRI MS groups as shown in **Figure 26**.

Previous reports have shown that a potential explanation for the reduction of fluorescein staining may be reduced levels of pro-inflammatory cytokines.^[298,355] To investigate whether the reduction in corneal epithelial destruction in our studies corresponded with a decrease in pro-inflammatory cytokines, qRT-PCR was performed on the lacrimal gland tissue to detect changes in expression of IL-2, IL-6 and IFN- γ . In addition to the better-known inflammatory function of IL-2 and IFN- γ , there has been observed increases of the pro-inflammatory cytokine IL-6 in dry eye patients.^[298] As expected, IL-2 and IFN- γ levels were significantly decreased in the TRI MS as compared to the ConA alone and ConA + Blank MS groups, which may be due to TRI MS mitigating the effects of ConA causing inflammation.^[337,356] A decrease of IL-6 expression levels was also detected in the TRI MS as compared to ConA alone group. Overall, there was a significant difference between the ConA alone and ConA + Blank MS and TRI MS groups levels of pro-inflammatory cytokines within the lacrimal gland. These results likely correlate to the observed decrease of CD3⁺ T cells in the TRI MS as compared to the ConA alone group as shown in **Figure 29**.

If the shift in the pro-inflammatory milieu of the ocular tissue was a result of the TRI MS expanding the expression of FoxP3⁺, then it would be expected that there would be a greater number of Tregs (or at least an increase in the ratio of Treg-to-effector T-cells) in the lacrimal gland tissue. Accordingly, immunofluorescent staining of total CD3⁺ T cells and FoxP3⁺ Tregs was performed on the lacrimal gland tissue. We indeed observed a significant increase in total numbers of CD3⁺ T cells in the lacrimal glands of ConA alone and ConA + Blank MS groups, as compared to the Saline and TRI MS groups as shown in **Figure 29**. We also observed a significant increase in the ratio of Treg-to-effector T-cells in the TRI MS as compared to the ConA alone and ConA + Blank MS groups as shown in **Figure 29**, supporting the hypothesis

that TRI MS are expanding the percentage of Tregs to overall CD3⁺ T cells. To further test whether TRI MS were preventing signs of DED through the expansion of Tregs, anti-GITR was administered to impair Treg function.^[289] We observed that anti-GITR reversed the beneficial effects of the TRI MS as shown above in **Figures 21A, 21B, 21C, and 22B** potentially indicating that Tregs are needed to mediate the therapeutic effects of TRI MS treatment. Although, the current study demonstrates prevention of DED in an experimental murine model, future studies will need to evaluate this drug-delivery system as a treatment for pre-existing DED, and test TRI MS efficacy in a pre-clinical larger animal model such as rabbits.

In conclusion, the present study suggests TRI MS were able to reduce the local pro-inflammatory milieu of the lacrimal gland tissue. TRI MS prevented tear loss, preserved goblet cell density and reduced corneal fluorescein staining, which indicate that the therapy prevented signs of DED. Importantly, TRI MS were able to decrease the total number of CD3⁺ T cells infiltrating the lacrimal gland tissue and enhance the frequency of FoxP3⁺ T cells among infiltrating T cells. Ultimately, this experimental murine study provides one potential strategy for future anti-inflammatory therapies to focus on harnessing Tregs to restore the local immunological homeostasis within the ocular tissue.

4.0 CONTROLLED RELEASE OF AN HDAC INHIBITOR FOR REDUCTION OF INFLAMMATION IN DRY EYE DISEASE

This chapter is adapted from: Michelle L. Ratay, Stephen C. Balmert, Abhinav P. Acharya, Ashlee C. Greene, Thiagarajan Meyyappan, and Steven R. Little. (2017). (Submitted to *Molecular Pharmaceutics*)

Specific Aim 3: To develop and evaluate local controlled release of an HDACi for the induction of Tregs.

4.1 INTRODUCTION

Several different acellular methods were explored to either recruit/induce Tregs in order to shift the ocular immunological microenvironment to promote homeostasis and subsequently prevent clinical features of DED. Although, these acellular approaches to recruit/bolster the overall pool of Tregs demonstrated promising results, there are several hurdles concerning the clinical translation of biologics like recombinant proteins (ex: CCL22, IL-2, TGF- β) (or even combinations of proteins/small molecule such as IL-2, TGF- β , and Rapamycin) as discussed in Chapters 2 and 3. Therefore, the development of formulations that can induce endogenous Tregs *in vivo* using one small molecule would drastically diminish concerns of clinical safety and

regulations. One particular potential class of drugs that could serve to simplify clinical translation is a class of small molecules known as histone deacetylase inhibitors (HDACi). Specifically, this particular class of small molecule drugs are known to induce differentiation and cell cycle arrest in cancer, and in particular an HDACi known as, SAHA(N-hydroxy-N'-phenyl-octanediamide, Suberoylanilide hydroxamic acid), has been approved by the FDA for cutaneous T cell lymphoma (Commercially referred to as Zolinza®; Merck & Co., Inc., Whitehouse Station, NJ).^[357] In addition to its usage as an anti-cancer therapeutic, this small molecule drug has been attracting interest as a potential anti-inflammatory therapeutic.^[358] Moreover, HDACi have recently shown to enrich/enhance the local population of Tregs.^[359] Specifically, the HDACi, SAHA, promotes Foxp3 acetylation, thereby increasing the binding of Foxp3 to DNA and enhancing suppressive functions of natural Tregs (nTregs) as shown in **Figure 30**.^[360,361] Moreover, SAHA can also induce the generation of tolerogenic APCs via acetylation and activation of STAT-3, which can then lead to differentiation of induced Tregs (iTregs) as shown in **Figure 30**.^[362]

Given that HDACi can both expand Tregs and enhance their immunosuppressive function, we hypothesized that using an HDACi (ex: SAHA) will effectively cause local induction of Tregs and prevent clinical symptoms associated with DED. In order to test this hypothesis, SAHA was formulated into degradable microspheres made from a polymer with an excellent track record of prior FDA approval (poly (lactic-co-glycolic) acid). These microspheres are capable of sustainably releasing SAHA for several days. Local release of SAHA from these formulations in the lacrimal gland of mice prevent damage to the ocular tissue, enhance FoxP3 mRNA expression in the lacrimal gland, and reduce the pro-inflammatory microenvironment observed in a model of murine DED.

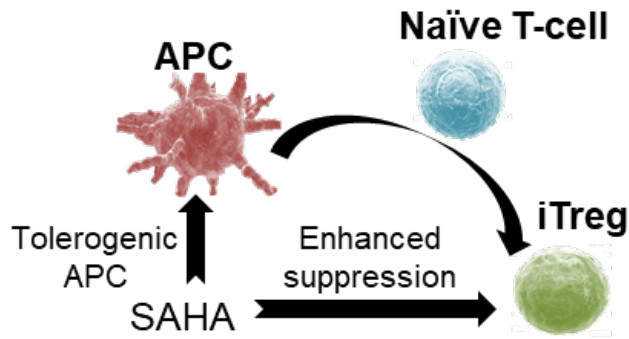


Figure 30. A tolerogenic antigen presenting cell (APC) can activate a naïve T effector (Teff) and under the treatment of an HDACi this can lead to non-polarizing conditions resulting in the induction of Tregs and can directly enhance the suppressive function of Tregs.

4.2 MATERIALS AND METHODS

In the following experiments, we aimed to assess the efficacy of SAHA microspheres for the prevention of pathological signs of DED. Moreover, we also aimed to determine whether the SAHA microspheres were able to reduce the pro-inflammatory ocular microenvironment.

4.2.1 Fabrication of HDACi Microspheres

HDACi microspheres were fabricated using a single-emulsion evaporation technique due to the hydrophobic nature of SAHA. Specifically, 200 mg of Poly (lactic-co-glycolic) acid (PLGA-65:35 lactide:glycolide, acid terminated) (MW:7,000-17,000) (viscosity: 0.16-0.24 dL/g, 0.1 % (w/v) (Sigma Aldrich, MO) and 40 mg of SAHA (Selleck Chem, TX) in 2.68 ml of dichloromethane and 1.32 ml of methanol then sonicated for 1 hour. Subsequently, this emulsion was then mixed with 60 ml of 2% polyvinyl-alcohol (PVA, MW ~25,000, 98% hydrolyzed; PolySciences) and homogenized (L4RT-A, Silverson, procured through Fisher Scientific) at 3,500 rpm for 1 min. Subsequently, homogenized mixtures were added to 80 ml of 1% PVA on stir plate and left for approximately 1.5 hours in order for the organic solvent to evaporate. After 1.5 hours, the microspheres were centrifuged (200 g, 5 min, 4 °C), washed 4 times with deionized water, and lyophilized for 48 hours (Virtis Benchtop K freeze dryer, Gardiner, NY).

4.2.2 Characterization of HDACi Microspheres

The morphology of the microspheres were characterized using scanning electron microscopy (SEM) (JEOL, JSM-6330F, Peabody, MA) and volume impedance measurements were performed on a Beckman Coulter Counter (Multisizer-3, Beckman Coulter, Fullerton, CA). In order to determine the release kinetics of the SAHA microspheres, 10 mg of the fabricated microspheres with drug (SAHA) or unloaded microspheres (composed of no drug only polymer-as a control) were added to 1ml of 0.2% Tween 80 in PBS (Sigma Aldrich, St. Louis, MO), which was placed onto a rotator at 37°C. The supernant was sampled daily and the release profile was determined using a NanoDrop 2000 Spectrophotometer (ThermoFisher Scientific, MA).

4.2.3 Mice

Balb/c, female mice aged 6-8 weeks were utilized in this study. (Charles Rivers Laboratories, Wilmington, MA). All murine experiments were approved by the Institutional Animal Care and Use Committee, University of Pittsburgh, Pittsburgh, Pa.

4.2.4 Murine Model

10 mg/ml of Concanavalin A (ConA) (Sigma Aldrich, St. Louis, MO) in phosphate buffered saline solution (PBS) was injected into the lacrimal glands with a 28.5 gauge needle using a dissecting microscope in order to induce an inflammatory-murine model of DED. (10 mg/ml of either Blank MS or SAHA MS were simultaneously administered at the same time as ConA).^[222,337]

4.2.5 Tear Production

In order to measure tear production, phenol red cotton threads were utilized. (Oasis Medical, San Dimas, CA). Specifically, the phenol red thread was placed in the lateral canthus of the eye for a period of 60 seconds, and the amount of tears absorbed onto the thread (when tears are absorbed onto the thread a color change occurs from yellow to red) was measured using a dissecting microscope (Olympus SZX10, Waltham, MA).

4.2.6 Corneal Fluorescein Staining

Approximately 1µl of fluorescein (1% solution in PBS) was applied to the conjunctival sac. Subsequently, the ocular surface was examined using a dissecting microscope (Olympus SZX10, Waltham, MA) to identify punctate staining. The scoring of staining was completed by a masked ophthalmologist, and scored 0 for no staining, score 1 for a quarter of staining, score of 2 for less than a half, score of 3 for half, and 4 for more than half of the eye.

4.2.7 Ocular Histology

At the end of the one-week study, murine eyes were exenterated and fixed in 10% neutral buffered formalin solution for a period of 48 hours. Then paraffin embedded sections were cut at approximately 5µm and stained with Periodic Acid Schiff (PAS). These histological sections were scanned and the goblet cell density was quantified using a Zeiss Axio Scan. Z1 (Thornwood, NY) and Pannoramic Viewer software (3D HISTECH Ltd.).

4.2.8 qRT-PCR

Total RNA was extracted from excised lacrimal glands using TRI-reagent (Molecular Research Center, Cincinnati, OH), and quantified using a NanoDrop 2000 (Thermo Scientific). For the reverse transcriptase assay, 2 µg RNA was converted to cDNA using a QuantiTect Reverse Transcription Kit (Qiagen, Valencia, CA). Quantitative real-time PCR was then performed using VeriQuest Probe qPCR Mastermix (Affymetrix, Santa Clara, CA), (Thermo Scientific) specific for (IFN-γ:Mm01168134_m1, FAM-MGB dye), (IL-12: Mm01288989_m1, FAM-MGB dye),

(IL-6:Mm00446190_m1, FAM-MGB dye),(FoxP3: Mm00475162_m1, FAM-MGB dye) and (Gusb: Mm01197698_m1, VIC-MGB PL dye, endogenous control). Duplex reactions (target gene + GUSB) were run and analyzed on a StepOnePlus Real-Time PCR System (Applied Biosystems, Carlsbad, CA). Relative fold changes of IFN- γ , IL-12, IL-6, and FoxP3 expression were calculated and normalized based upon the $2^{-\Delta\Delta C_t}$ method, with the Saline group as the untreated control.

4.2.9 Suppression Assay

Lymphocytes were isolated from Balb/c spleens and stained with antibodies against CD4, CD25, and CD45RB (eBioscience, San Diego, CA). Flow activated cell sorting (FACS) was performed (FACS Aria, BD Bioscience) to obtain Teff (CD4⁺CD25⁻CD45RB^{hi}) and Treg (CD4⁺CD25⁻CD45RB^{lo}). Teff and Treg were labeled with CellTrace CFSE or CellTrace Far Red, respectively (Invitrogen, Carlsbad, CA). Teff were cultured in round-bottom 96 well plates (5 x 10⁴ cells/well) with Dynabeads Mouse T-Activator CD3/CD28 (Gibco, Gaithersburg, MD) stimulation (1 Dynabead: 4 Teff) and 0:1, 1:1, 1:2, or 1:4 ratios of Treg:Teff. T cells were cultured in RPMI media (Corning, Corning, NY) containing either 0, 50, or 200 nM SAHA (Selleck Chem, Houston, Texas) for 72 hours. T cells were stained with Fixable Viability Dye (eBioscience, San Diego, CA) and CFSE dilution was analyzed by flow cytometry.

4.2.10 Statistical Analysis

Data expressed as mean \pm S.D. Comparisons between multiple treatment groups were performed using one-way ANOVA, followed by Bonferroni multiple comparisons, and $p \leq 0.05$ was considered statistically significant. For PCR data, a Grubb's test was performed to determine any significant outliers. Any significant outlier identified ($p > 0.05$) was excluded from the statistical analysis. If an assumption of the One-Way ANOVA was not met a non-parametric test was performed. Statistical tests were performed using GraphPad Prism Software 6.0 (GraphPad Prism, San Diego, CA).

4.3 RESULTS

4.3.1 Characterization of SAHA Microspheres

Scanning electron micrographs (SEM) (**Figure 31A**) illustrate that individual, polymer particles are spherical with average diameter of $\sim 17 \mu\text{m}$ (Blank Microspheres) and $\sim 17 \mu\text{m}$ (SAHA Microspheres), which was confirmed with a Coulter Counter (representative plots of volume impedance measurements shown below in **Figure 31B**). Additionally, the release kinetics were characterized using a NanoDrop (UV-vis spectrophotometer) through detection of the absorbance of SAHA, which demonstrates a cumulative release of approximately 50 ng/mg of microspheres over the course of 5-6 days shown in **Figure 32**.

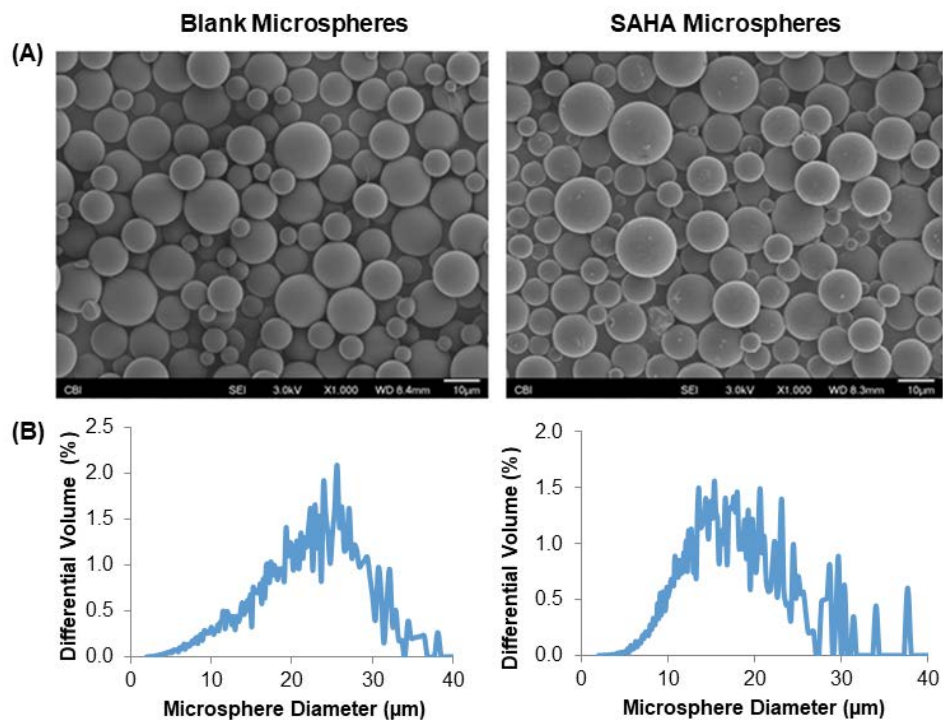


Figure 31. Characterization of SAHA Microspheres. (A) Representative scanning electron microscopy (SEM) images (1000X) (B) Volume Impedance Measurements (Coulter Counter) of Blank Microspheres and SAHA Microspheres.

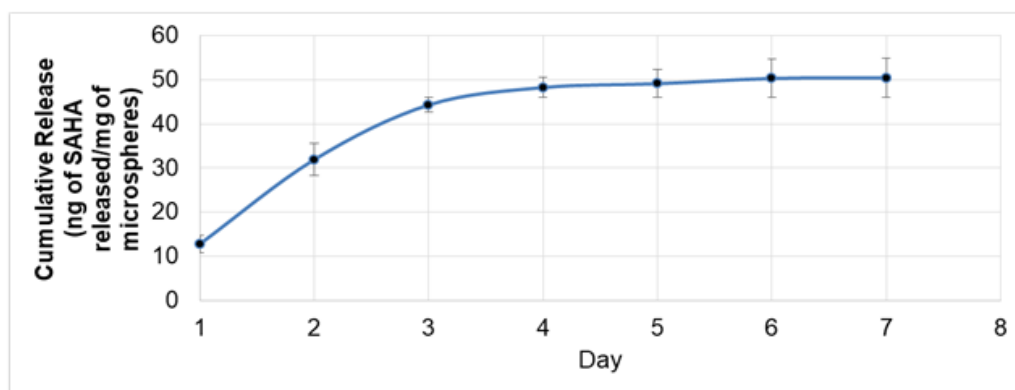


Figure 32. Cumulative Release of SAHA Microspheres.

4.3.2 Aqueous Tear Production is Restored by SAHA Microsphere Treatment

To determine whether SAHA MS were capable of preventing key signs of DED, aqueous tear secretion was examined using phenol red threads at the conclusion of the experimental study.^[222]

The lacrimal gland injection of ConA with or without Blank MS significantly reduced tear production, compared to saline (non-diseased) injected mice as shown in **Figure 33**. Notably, the loss of tear production was prevented by the administration of SAHA MS as compared to the ConA (alone) group as shown below in **Figure 33**.

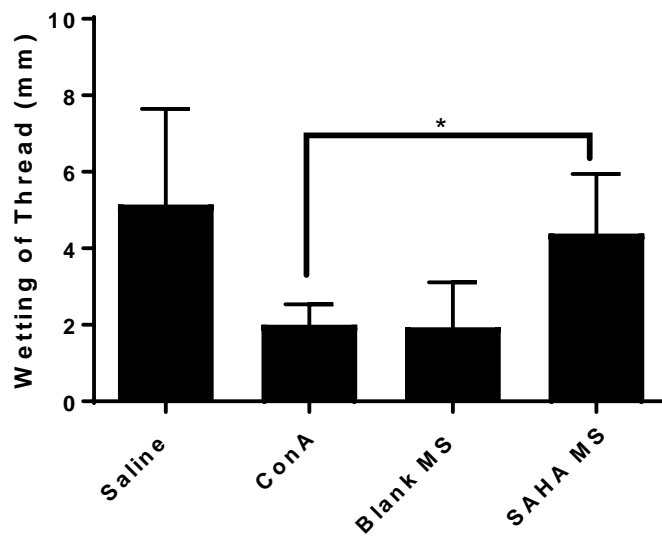


Figure 33. Tear Production is maintained with the administration of SAHA MS shown as mean \pm S.D (n=4-5 per group) Saline (non-diseased), ConA (diseased), Blank MS (diseased + unloaded microspheres), SAHA MS (diseased + SAHA microspheres). * $p \leq 0.05$

4.3.3 The Administration of SAHA Microspheres Prevents Loss of Goblet Cell Density

Goblet cells are located within the stratified columnar conjunctival epithelial cells, and play an integral role in producing, mucin, a key component of tears.^[363] Moreover, goblet cells also produce MUC5AC, which acts as a gel layer to trap pollen and allergens.^[301,364] A state of chronic inflammation (e.g. from DED) often results in depletion of these goblet cells, which in turn can lead to conjunctival epithelial squamous metaplasia and an abnormal tear film.^[364] Thus, Periodic Acid Schiff (PAS) staining of the ocular tissue was used to determine whether SAHA MS could prevent the loss of goblet cells (pink/purple cells, **Figure 34**) in the conjunctiva, resulting from ConA-induced inflammation. Notably, there was a significant preservation of goblet cell density with the administration of SAHA MS as compared to the ConA alone group. Although, SAHA MS prevented some ConA-induced loss of goblet cells, there were still fewer goblet cells than in the non-diseased saline control as shown in **Figure 34**.

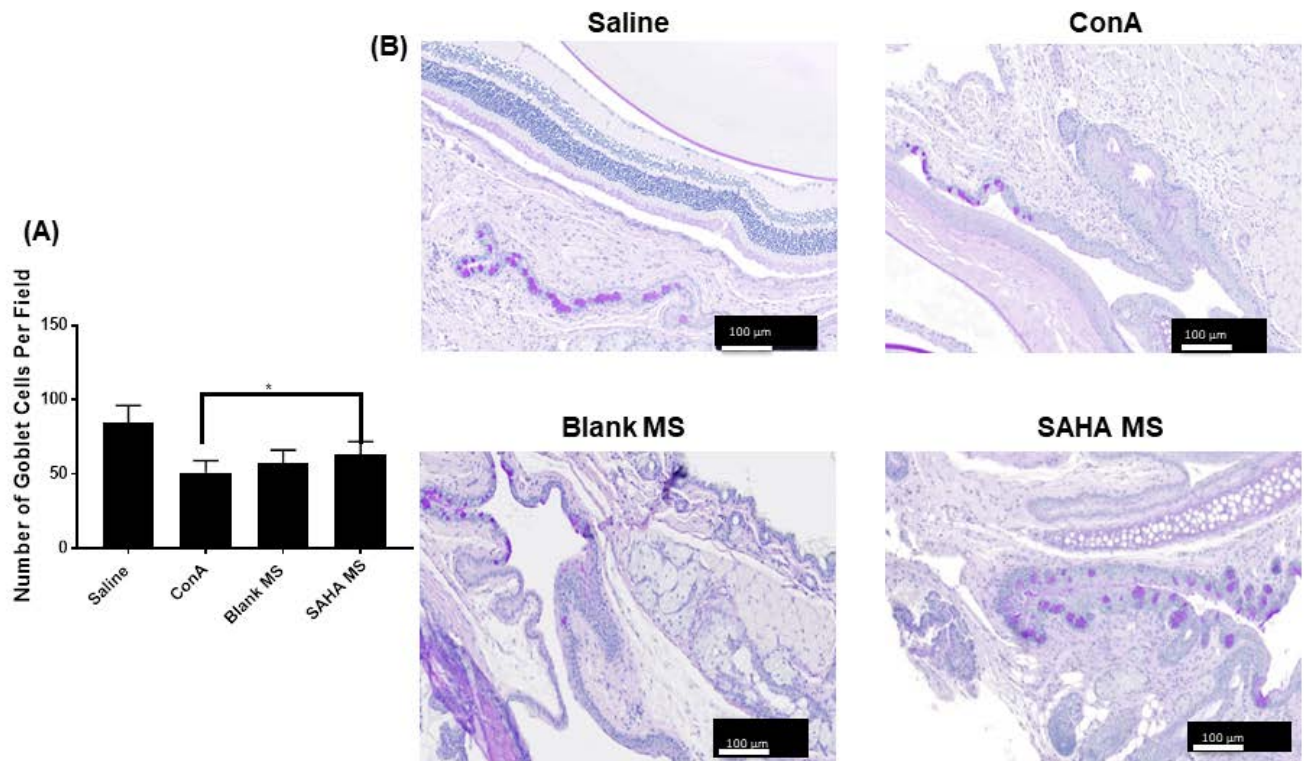


Figure 34. SAHA MS Preserve Goblet Cell Density in the Conjunctival Epithelial Layer.
(A) Quantification of the Number of Goblet Cells per field shown as mean ± S.D (n=5-8 per group).
(B) Representative Histological Images of the goblet cells in the conjunctiva (10X) of Saline (non-diseased), ConA (diseased), Blank MS (diseased + unloaded microspheres), SAHA MS (diseased + SAHA microspheres) * p ≤ 0.05

4.3.4 SAHA Microspheres Decrease Corneal Fluorescein Staining

A hallmark of DED is an increase in permeability of the corneal epithelial layer of the ocular tissue.^[342] Fluorescein staining, used to identify regions of the ocular surface damage, is a standard diagnostic measurement/indicator for dry eye disease severity.^[342] Representative corneal fluorescein images were captured using a fluorescent dissecting microscope and scored by a masked ophthalmologist on a scale of 0 to 4, with 0 corresponding to no staining, and 4 corresponding to staining on more than 50% of the cornea, as seen in **Figure 35**. Compared to the ConA alone and ConA + Blank MS groups, uptake of fluorescein by the cornea was significantly lower in the Saline (non-diseased) and SAHA MS (preventative therapy) groups. Ultimately, the preventative therapy involving local administration of SAHA MS to lacrimal glands was able to reduce fluorescein scores by approximately 25% compared to mice with ConA-induced dry eye disease.

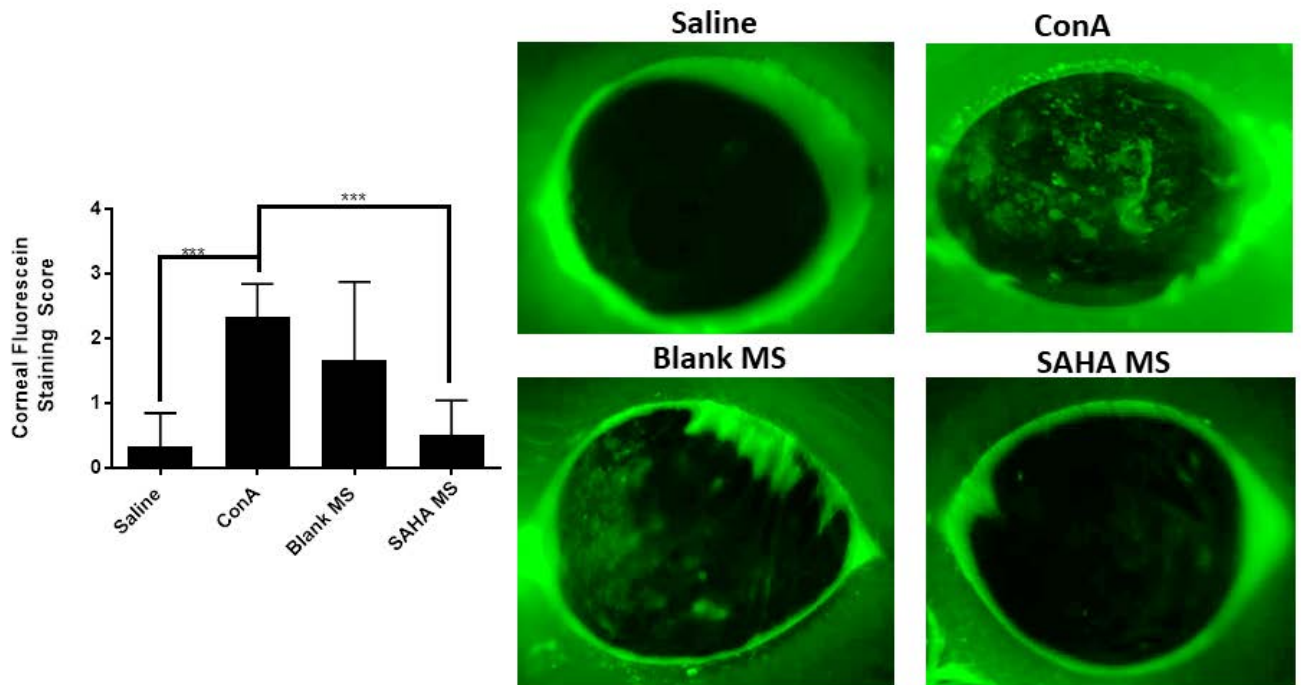


Figure 35. Corneal Fluorescein Staining is Reduced with the Administration of SAHA MS.
(A) Corneal Fluorescein Staining scored on a scale of (0-4) shown as mean \pm S.D. (n=6). (B) Representative Corneal Fluorescein Images of Saline (non-diseased), ConA (diseased), Blank MS (diseased + unloaded microspheres), SAHA MS (diseased + SAHA microspheres) * $p \leq 0.05$; ** $p \leq 0.01$; * $p \leq 0.001$**

4.3.5 mRNA Expression Altered in the Lacrimal Gland with SAHA Microspheres

Inflammation in the lacrimal gland is associated with an infiltration of lymphocytes and an increase in pro-inflammatory cytokines.^[309,365] Thus, mRNA expression levels were measured in the lacrimal gland tissue after ConA-induced inflammation. Data from qRT-PCR analyses indicate that IL-12, IFN- γ , and IL-6 induced by ConA (diseased control) were significantly reduced in the lacrimal glands of SAHA MS-treated as shown in **Figure 36**.^[337] Additionally, the level of FoxP3 (Treg-specific transcription factor) mRNA expression was significantly higher in the lacrimal glands of SAHA MS-treated mice, compared to the diseased (ConA) control shown in **Figure 36**.^[366] Together, these data suggest that the SAHA MS were able to reduce the pro-inflammatory microenvironment initiated by ConA and enhance the expression levels of FoxP3, reflecting either an increase in Treg number in the lacrimal gland, or greater FoxP3 expression by Tregs.

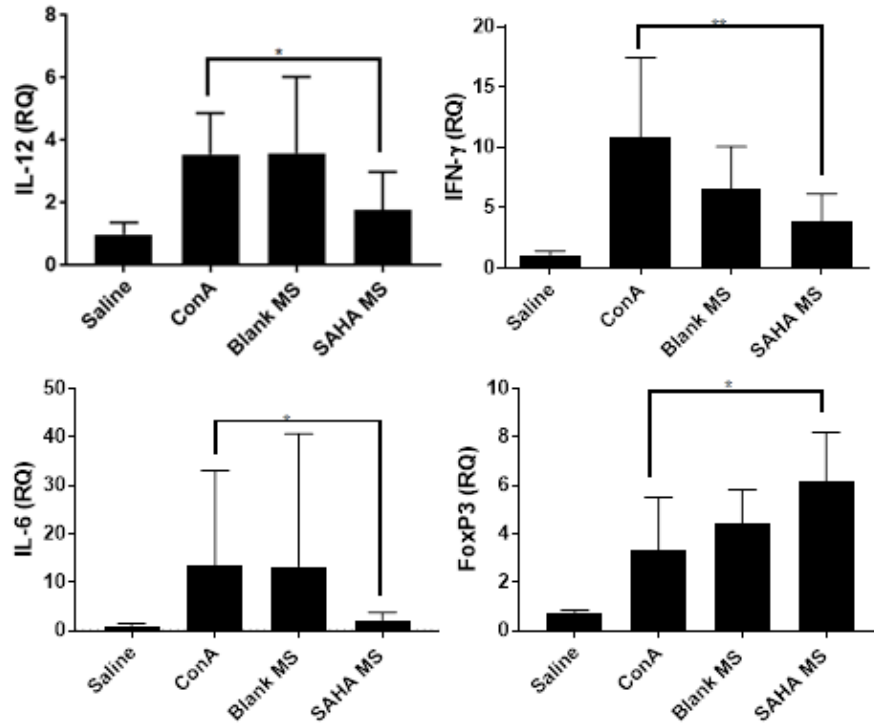


Figure 36. mRNA Expression is Altered in the Lacrimal Gland Tissue with the administration of SAHA MS shown as mean \pm S.D (n=4). * $p \leq 0.05$

4.3.6 Lymphocyte Suppression Assay

Various mechanisms by which SAHA can influence the Treg-Teff balance have been proposed including direct suppression of Teff proliferation and enhancement of Treg function.^[358,359,367–369]In order to gain insight into the mechanism of inflammation reduction in our model of murine DED, CFSE labeled Teff alone or CFSE labeled Teff co-cultured with Tregs were treated with SAHA and proliferation was assessed by CFSE dilution. It was observed that Teff alone, treated with 200 nM SAHA, exhibited significantly reduced proliferation compared to Teff alone that were not treated with SAHA (Figure 7A). Teff co-cultured with Tregs exhibited less proliferation, and this was further reduced in a dose-dependent manner by the addition of SAHA as shown in Figure 7B. Although 200nM SAHA inhibited the proliferation of Teff alone by 18% and a 1:1 Teff:Treg ratio (SAHA not treated) inhibited proliferation by 27%, the combination of 200nM SAHA and a 1:1 Treg:Teff ratio inhibited T cell proliferation by 66%. Overall, the impact of SAHA alone on solely T effector cells appears to be smaller compared to the co-culture of Tregs and Teff cells.

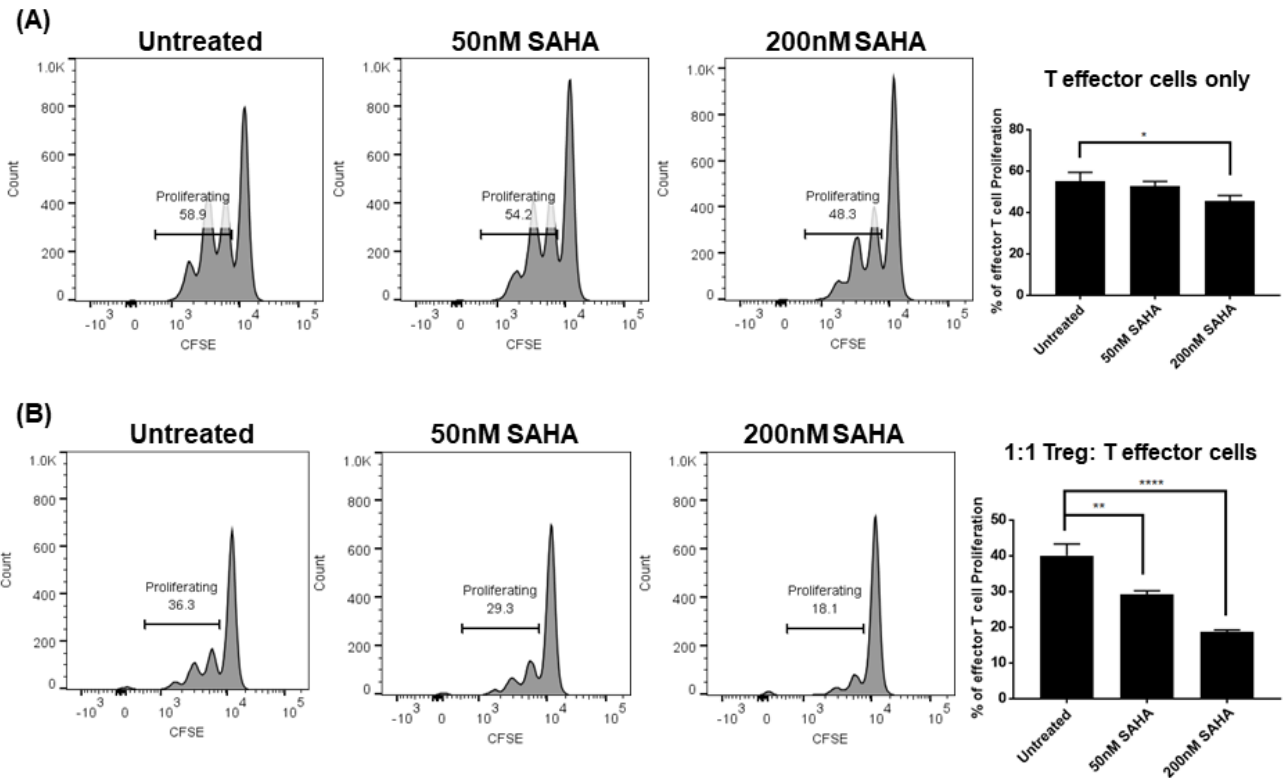


Figure 37. Lymphocyte Suppression Assay. (A) Representative Flow Cytometry Histograms of T effector cells only untreated (no SAHA) and cells treated with 50nM and 200nM SAHA and bar graphs shown as mean \pm S.D. (B) Representative Flow Cytometry Histograms of 1:1 Treg: T effector cells untreated (no SAHA) and cells treated with 50nM and 200nM SAHA and bar graphs shown as mean \pm S.D. * $p \leq 0.05$; ** $p \leq 0.01$; * $p \leq 0.001$**

4.4 DISCUSSION

Recently, immunosuppressive agents such as corticosteroids, such as cyclosporine (calcineurin inhibitor) or doxycycline (antibiotic) (as discussed in Chapter 1) have been investigated as a therapeutic to reduce inflammation associated with DED.^{36,37} However, long-term topical use of corticosteroids has been implicated in conditions such as glaucoma and retinopathy.³⁸ As an alternative to non-specific corticosteroids and associated side effects, a histone deacetylase inhibitor (HDACi) was utilized to alter the adaptive immune response to restore immunological homeostasis. Specifically, the HDACi, SAHA, was selected due to its ability to cause epigenetic modifications that regulate gene expression and protein function to modulate the function of immune cells such as T lymphocytes.^{18,19} In particular, SAHA and other HDACi can stimulate thymic production of anti-inflammatory Tregs, enhance Treg suppressive function, and promote the peripheral conversion of CD4⁺ naïve T cells into Tregs.^{19,35} Although, these HDACi have shown promising immunomodulatory effects on T lymphocytes, this class of small molecules possess a narrow therapeutic window (both efficacy and toxicity).³⁹ Thus, being able to locally and sustainably deliver the HDACi would permit a much lower dosage and ultimately would reduce the amount of injections as compared to daily systemic administration for pre-clinical inflammatory models which can require 0.1 mg/kg/d.¹⁷ In this study, a controlled release system was fabricated to provide local administration of SAHA to the lacrimal gland in an inflammatory murine model of DED. These SAHA MS formulations maintained therapeutic levels over several days, ultimately reducing the total amount of HDACi required for therapeutic efficacy and minimizing toxicity concerns.^{17,40}

SAHA releasing microspheres (MS) were fabricated using the biodegradable and biocompatible polymer poly (lactic-co-glycolic) acid (PLGA), and showed the ability to release SAHA over the course of approximately five days (as shown in **Figure 32**) with the intention of altering the local microenvironment in the ocular tissue.^[334,370] Notably, the data suggest that local administration of SAHA MS in the ocular tissue prevented several clinical signs of DED. For instance, a common clinical sign of DED is a reduction of overall tear production, which subsequently can lead to ocular dryness and irritation.^[351] While aqueous tear secretion was significantly reduced in diseased (ConA ± Blank MS), as expected,^[222,329,337] SAHA MS treatment prevented ConA-induced loss of aqueous tear secretion as can be seen in **Figure 33**. In addition to preserving aqueous tear production, effective therapeutics should also maintain the composition of tears by protecting gel-forming, mucin-producing goblet cells.^[340] These goblet cells are located on the apical surface of the conjunctiva and produce important non-aqueous components of tears.^[301,341] Interestingly, loss of goblet cells in ocular tissue in DED is reportedly due to an increase in the pro-inflammatory milieu.^[301] Thus, in this study, histological sections of the conjunctiva were examined to determine whether SAHA MS treatment preserved mucin-producing goblet cells. Indeed, there was a significantly greater goblet cell density in SAHA MS-treated mice, compared to diseased (ConA) mice as shown in **Figure 34**. Although, the preservation of goblet cell density was not as profound as other measurements (ex: corneal fluorescein staining) there was a statistically significant decrease in goblet cell numbers in the SAHA MS as compared to the ConA (diseased) group as can be seen in **Figure 34**. These results are in agreement with a previous report by DeZoeten *et al.*, which demonstrated that administration of an HDACi from the same class as SAHA, led to preservation of intestinal goblet cells in an inflammatory colitis model.^[371]

Since loss of aqueous tear production and/or mucin-producing goblet cells in DED ultimately leads to damage of the ocular surface,^[372–374] it was investigated whether SAHA MS, which prevented both of these pathological features, also maintained integrity of the corneal epithelium. Corneal integrity was assessed with fluorescein,^[342,375] a dye that stains dead epithelial cells and can diffuse into areas where cellular tight junctions are compromised.^[354] Punctate staining was observed in mice with DED induced by ConA (with or without Blank MS), as shown in **Figure 35**. Notably, there was a 4-fold reduction in the average fluorescein staining score in the SAHA MS group, compared to ConA alone, suggesting that the HDACi was able to prevent damage to the ocular tissue initiated by ConA.

In order to demonstrate that the prevention of clinical signs of DED was attributed to changes in the underlying T cell mediated immune response, the lacrimal gland microenvironment was evaluated using PCR analysis. The underlying pathogenesis of DED involves effector T cells that infiltrate the ocular tissue and secrete pro-inflammatory cytokines, which can directly affect the health of the ocular microenvironment.^[304,305,376,377] Since increases in pro-inflammatory cytokines have been found in inflamed lacrimal gland tissues of mice, the microenvironment of the tissue was investigated to determine whether the SAHA MS-mediated prevention of clinical signs of DED was due to a reduced pro-inflammatory milieu in the ocular tissue.^[352,378,379] Specifically, mRNA expression levels of pro-inflammatory cytokines (IL-12, IFN- γ , and IL-6) in lacrimal gland tissue were evaluated by qRT-PCR. Expression of IL-12 and IFN- γ was induced by ConA injection, relative to saline controls, as shown in **Figure 36**. This is likely attributed to ConA acting as a T-cell mitogen, ultimately leading to the production of Th1 cytokines.^[286,356] Both of these findings in the ConA-induced murine model of DED are consistent with clinical reports that IL-12 and IFN- γ are upregulated in tears of patients with

DED.^[351,363,378] In addition to increases in IL-12 and IFN- γ in the lacrimal gland, IL-6 was also significantly elevated by ConA, which is consistent with other reports of increased IL-6 production in lacrimal glands of DED murine models.^[273,337] Importantly, treatment with SAHA MS significantly inhibited ConA-induced expression of IL-12, IFN- γ , and IL-6 as shown in **Figure 36**. These reductions in the expression levels of pro-inflammatory cytokines prompted the question of whether SAHA MS were altering the immunological microenvironment by increasing anti-inflammatory Tregs. Previous studies have demonstrated that HDACi can expand FoxP3⁺ Tregs *in vitro* and *in vivo*.^[359,367] Interestingly, we observed a significant increase in FoxP3 mRNA expression in the lacrimal gland tissue of SAHA MS-treated mice as shown in **Figure 36**, suggesting that the reduction of signs of DED and pro-inflammatory microenvironment in the lacrimal gland may be due to Tregs suppressing ocular inflammation. Future studies will be needed to determine whether increased FoxP3 expression in lacrimal glands of SAHA MS-treated mice is due to an increase in the number of Tregs in the tissue, or enhanced expression of FoxP3 by Tregs, which is associated with greater suppressive function.^[380]

In vitro experiments suggest, however, that SAHA may enhance Treg function in addition to directly inhibiting Teff as can be seen in **Figure 37**. Notably, neither Treg induction, nor increased expression of FoxP3 by Tregs was observed with SAHA treatment *in vitro* in our hands (data not shown). It is possible that this discrepancy between *in vitro* and *in vivo* results regarding FoxP3 expression is due to the fact that increased FoxP3 mRNA in the lacrimal gland may not necessarily correspond to increases in FoxP3 protein, as was measured *in vitro* experiments. Alternatively, enhanced FoxP3 expression *in vivo* could be due to the effects of dendritic cells (DCs) and other antigen-presenting cells on T cells *in vivo*.^[358] In addition to

direct effects on T cells, SAHA has also been shown to cause DCs to reduce costimulatory molecule expression and increase IDO production, both of which can promote Treg induction.^[381] Due to the ubiquitous nature of histone acetylation and the dynamic nature of epigenetic regulation, it is not surprising that HDACi shift the Teff-Treg balance through multiple direct and indirect mechanisms. The results presented here are consistent with several previous reports of SAHA directly inhibiting Teff proliferation and enhancing the suppressive function of Tregs.^[358,367,369,382]

In summary, administration of SAHA MS preserved aqueous tear production and mucin-producing goblet cells and prevented damage to ocular tissue by reducing the pro-inflammatory milieu in the lacrimal gland and enhancing numbers and/or function of FoxP3⁺ Tregs in an inflammatory murine model of DED. Given these encouraging results, future studies will be needed to fabricate SAHA MS with potentially longer release kinetics. Additionally, future studies will test the efficacy of SAHA MS in a larger pre-clinical rabbit model of DED, and potentially develop a novel topical formulation for ocular delivery for potential translation as a treatment for DED. Ultimately, the controlled delivery of SAHA may also have pharmacological benefits for other inflammation-based conditions (based on previous literature reports)^[360,367,382,383] by locally inducing FoxP3⁺ Tregs and suppressing the pro-inflammatory milieu.

5.0 CONCLUSIONS AND FUTURE WORK

The three aims presented in this thesis were to develop and utilize first-of-their-kind acellular systems that were designed to (1) recruit the body's own endogenous Tregs, (2) induce the body's own endogenous Tregs *in situ* or (3) induce/enhance the immunosuppressive function of the body's own endogenous Tregs without the use of live cell therapy (without *ex vivo* expanded, live cells) for the prevention of DED. Particularly, this modulation in Treg function and prevalence in the lacrimal gland (*in situ*) possesses the ability to regulate the function of pro-inflammatory cells, leading to re-establishment of immunological homeostasis in the ocular tissue and prevention of DED.

In order to promote immunological homeostasis in the ocular tissue, and prevent the rapid diffusion of soluble drugs/biologics out of the lacrimal gland (reducing therapeutic efficacy as shown in Chapter 2), a local synthetically engineered sustained release system would be required to cause the recruitment/induction of Tregs to/at the site of inflammation to resolve destructive tissue damage. Moreover, local delivery is important, as it has been demonstrated that establishment of a concentration gradient is critical in order to direct lymphocytes to local sites of inflammation due to the short *in vivo* half-life of proteins.^[290,384] Therefore, due to the advantages of a synthetically engineered sustained release system, formulations were fabricated using a biodegradable polymer, poly (lactic-co-glycolic) acid, in order to prevent the symptoms of DED in a murine model of ConA-induced DED.

Our data suggest that our Treg-based formulations were able to prevent clinical signs of DED. Specifically, Treg-recruiting microspheres were able to shift the ratio of Tregs to effector T cells in the lacrimal gland thereby preventing ocular tissue damage. In addition, to our strategy to recruit endogenous Tregs to the ocular tissue, we also examined bolstering the pool of Tregs by inducing peripheral naïve CD4⁺ T cells into Tregs. Notably, these formulations can induce naïve CD4⁺ T cells into Tregs through the sustained simultaneous presence of IL-2, TGF- β , and rapamycin (rapa) in the local ocular microenvironment.^[334] However, when either the individual microsphere formulations alone (ex: Rapa, TGF- β , IL-2) or the combination of two microsphere formulations (ex: Rapa + TGF- β ; Rapa + IL-2; TGF- β + IL-2) were administered, clinical signs of disease were not prevented. Therefore, the data suggests the combination of all three microspheres formulations (TRI MS) were required to shift the pro-inflammatory microenvironment and prevent clinical outcomes associated with DED pathogenesis. Although, TRI MS were effective in preventing clinical signs of disease, a more translational approach would be to utilize one small molecule as opposed to a combination of biologics/small molecule for the treatment of DED.

In an attempt to potentially enhance the clinical safety and reduce regulatory concerns surrounding the usage of biologicals and or the combination of biologicals/small molecules, a controlled release formulation of a clinically used small molecule was investigated as a potential treatment in a murine model of DED. Specifically, a class of histone deacetylase inhibitors (HDACi-known as SAHA), was chosen due to its ability to increase the expression of FoxP3 *in vivo* and enhance the suppressive function of Tregs.^[360] Therefore, a controlled release formulation of HDACi microspheres was developed encapsulating SAHA in order to investigate whether this particular small molecule could prevent signs of DED and reduce the pro-

inflammatory milieu in the lacrimal gland. Notably, SAHA MS were able to prevent clinical signs of DED, reduce the pro-inflammatory ocular microenvironment, and enhance FoxP3⁺ expression in the lacrimal gland tissue. Given these encouraging results, future work will be performed to examine the efficacy of these particular formulations in a pre-established model of DED in addition to the ConA model (preventative) utilized.

Although, the ConA model was effective in studying the effects of these treatment on the downstream T-cells over a relatively short-period of time, the ConA-induced murine DED model does not intend to replicate the natural induction of DED in humans (i.e. desiccating stress induced tissue damage). Accordingly, future work will utilize a controlled environmental chamber (CEC-resembles the induction of DED in humans via desiccating stress) mouse model of DED to evaluate the efficacy of Treg-recruiting/inducing formulations. Using this model, it will become possible to determine whether these formulations can ultimately reduce the pro-inflammatory microenvironment in the ocular tissue and improve the overall clinical symptoms of DED such as tear production, corneal lymphangiogenesis, goblet cell density, and corneal fluorescein staining. This model will also allow for the determination of the duration of effect (post administration) as well as optimizing administration for use in a therapeutic format.

In addition to examining the efficacy of our therapeutic formulations in a pre-established CEC model for future studies, we also plan on investigating the efficacy of these formulations in a larger animal model (more closely resembling the physiology and size of human eyes compared to mice) to facilitate translation. Specifically, a lapine DED model will be utilized to investigate the translatability of our Treg-based formulations (injected into the lacrimal gland) due to their large ocular surface (more similar to the size of a human eye compared to mice) as well as similarities in the composition of proteins in human and rabbit tears.^[385–387] Some of the

tests which will be performed utilizing the lapine model include: Shirmer test, corneal fluorescein staining, goblet cell density, and conjunctival impression cytology. We will also perform flow cytometry to determine the state of the immune homeostasis by analyzing T-cell populations of Th1 (CD4⁺IFN- γ ⁺), Treg (CD4⁺Foxp3⁺), Tc1 (CD8⁺IFN- γ ⁺) and antigen presenting cells (CD11c⁺MHCII^{Hi}CD86^{Hi}) populations in the lacrimal glands. The tear compositions of rabbits (with or without DED) will also be compared with the composition of human tears (with or without DED) to correlate key markers of DED to determine whether a decrease (in both humans and rabbits) in these key biomarkers markers (ex: relative levels of proteins such as IL-2, IL-4, IL-6, IFN- γ , IL-1 β , TNF- α , MMP-9) are a sign of disease resolution. Furthermore, this model will afford us the ability to determine feasibility of additional routes of administration.^[388]

Although lacrimal gland injection itself could be possible from a translational perspective, (ex: superior temporal injection near the lacrimal gland or an inferior fornix injection near the eye subconjunctivally), a non-invasive, topical-based, long-acting eye drop formulation comprised of the Treg-inducing microsphere formulation and a thermo-responsive hydrogel could be a desirable alternative to lacrimal gland injection.^[389] Moreover, this formulation can safely retain controlled release microspheres in the lower fornix of the eye, and has shown efficacy as a long term glaucoma drug delivery system and may be a potential future translational method of ocular delivery for DED.^[389,390]

Once the method of delivery (ex: topical gel, subconjunctival injection) is determined, pharmacokinetic studies on the distribution of these three factors (two cytokines and one small molecule) will be investigated for work focused upon optimization and translation of our treatment. Specifically, this study will be performed in a larger, pre-clinical rabbit model (ocular

size more similar to humans). Additionally, since it is challenging to detect the relative small quantities (nanogram to picogram) of these three factors being released in the tissue (and delineate the between the endogenous cytokines (ex: IL-2 and TGF- β) and those released from the microspheres) new controlled release formulations will need to be developed that would include radio-labelled proteins. These radiolabeled drugs will also need to be tested to ensure similar loading and release profiles as the current microsphere formulations. Ultimately, in order to facilitate the translation of our formulations these dose dependent toxicity studies will be performed within an IND protocol (Investigational New Drug Application) enabling the ability to determine whether the small molecule/protein is reasonably safe for use in humans, and if it demonstrates pharmacological efficacy for commercialization.

Finally, future testing and clinical evaluation of these controlled release formulations fabricated and utilized herein, could be repurposed for other ocular diseases involving inflammation (ex: AMD and Uveitis). Moreover, this engineered drug delivery system could serve as an easily modifiable platform to incorporate other types of biologics (ex: DNA) or small molecules with as little as picograms-to-nanograms of active agent for local delivery. Overall, the future translations of these new modern interdisciplinary engineered approaches are a novel therapeutic field, which aims to mimic the natural system of immuno-regulation, the human body.

APPENDIX A

ONE –STEP SYNTHESIS OF FLUORESCENTLY LABELLED, SINGLE-WALLED CARBON NANOTUBES

Michelle L. Guaragno, Riccardo Gottardi, Morgan V. Fedorchak, Abhijit Roy, Prashant N. Kumta and Steven R. Little. One-step synthesis of fluorescently labelled, single-walled carbon nanotubes. *Chemical Communications*. 2015, 51, 17233-17236. Reproduced by permission of The Royal Society of Chemistry.
<http://pubs.rsc.org/en/content/articlelanding/2015/cc/c5cc05573c#!divAbstract>

Single-walled carbon nanotubes (SWNTs) are a tubular allotrope of carbon whose hallmark is the sp² hybridized structure.^[391] Carbon nanotubes possess excellent mechanical, thermal and electrical properties, which have been widely studied for biomedical applications.^[392–394] Specifically, SWNTs have been investigated for use in drug delivery, molecular sensing, and diagnostic imaging when conjugated to fluorophores, which can increase the aqueous solubility and endow the SWNTs with fluorescent properties.^[395,396] Currently, the procedures used to attach fluorophores involve either non-covalent interactions or the formation of a covalent bond. Non-covalent functionalization occurs via π - π interactions.^[397] For instance, PEGylated fluorescein has been non-covalently attached to carbon nanotubes by simple sonication of the mixture, creating fluorescent SWNTs for imaging or pH sensing.^[397] Alternatively, covalent

functionalization requires local alterations of the nanotube sidewalls and preferentially starts at the defect sites of the SWNT.^[398] Covalent functionalization methods often exploit the hydrophilic carboxyl groups on carbon nanotubes, via several different esterification methods.^[399] For example, carboxylic acids (COOH) can be converted to an acid chloride (COCl) through refluxing the carbon nanotubes in thionyl chloride (SOCl₂), which is then reacted to covalently couple to a compound in order to form an ester.^[400] Another method used to complete an esterification reaction of a fluorophore to a carbon nanotube includes a three-step process, which is necessary when the fluorophore of interest does not possess a primary reactive alcohol group.^[401] The reaction begins by functionalizing the fluorophore with a compound containing an alcohol group followed by esterification to an acid chloride-functionalized carbon nanotube.^[401]

Yet to date, covalent functionalization of a fluorophore to a carbon nanotube via an esterification reaction has been achieved utilizing multiple-step syntheses. These decrease the overall weight yield and often require modification of the fluorophore in order to undergo an esterification reaction.^[401] In fact, some fluorophores such as fluorescein do not possess a primary alcohol group. Therefore, the development of a new one-step esterification process to react the phenol group on a fluorophore and with the carboxylic acid on carbon nanotubes would be a desirable, straightforward approach to functionalize SWNTs with fluorophores with a potentially higher percentage weight yield.

For this reason, we have developed a one-step reaction using boron trifluoride etherate to covalently attach the, fluorescein, to a carbon nanotube via a phenol group through an esterification reaction. This one-step synthetic process requires approximately 5 days due to the lower reactivity of the phenol, which is longer than other multi-step esterification

methods.^[401,402] However; our one-step synthesis does not require modification of fluorescein. Our results suggest that the fluorescent characteristics are not affected and that the process has a 95% overall weight yield. Effective functionalization and maintenance of the SWNT structure was confirmed using FT-IR, Raman, UV-vis-NIR and TGA. To our knowledge, this is the first description of a simple, one-step covalent esterification linkage to attach a fluorophore to a SWNT, with a corresponding high percentage weight yield.

Single-walled carbon nanotubes (P3) (SWNT purified with nitric acid and contains 1.1 atomic percentage of COOH groups, as assessed by Boehm titration were purchased from Carbon Solutions, Inc. (Riverside, CA).^[403] The SWNTs were functionalized with fluorescein via an esterification reaction. Briefly, 50mg of (P3) SWNTs and 120mg of fluorescein free acid were mixed with 4ml of boron trifluoride etherate ($\geq 46\%$ BF₃ basis), Sigma Aldrich (St. Louis, MO), which acts as a catalyst. Nitrogen gas was bubbled for five minutes to degas the reaction. The reaction mixture was heated at 60°C in a silicone oil bath to maintain consistent heating and stirring for the duration. After five days, the reaction was cooled and transferred to a centrifuge tube. Then 10ml of diethyl ether etherate (Fisher Scientific, USA) was added to the reaction and centrifuged (Hettich Rotina 38/38R) at 23,760 G (11,000 rpm) for 10 minutes at 24°C. This served as a purification step to help ensure there was no remaining unreacted fluorescein. The centrifugation process was repeated until the supernatant was clear upon visual inspection. The remaining supernatant was then decanted and the product was dried in a desiccator for 24 hours at room temperature.

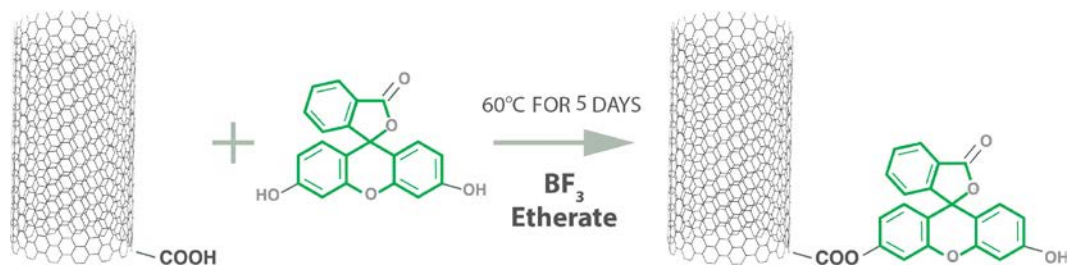


Figure 38. The reaction scheme of the Single-Walled Carbon Nanotubes reacted with fluorescein in the presence of boron trifluoride etherate. The reaction starting materials are SWNT functionalized with carboxylic acid groups (1.1% atomic weight) and fluorescein free acid (green compound), which is reacted via esterification reaction using a Lewis acid catalyst (boron trifluoride etherate).

The SWNT or functionalized SWNT were dispersed in deionized water (1mg/20ml) and bath sonicated (Branson 1510) for two hours. After sonication, the samples were transferred to a 2ml quartz cuvette and scanned between 400nm and 1400nm with a UV-vis-NIR spectrophotometer (Varian Cary 5000). This spectral range was chosen to include the maximum peak intensity for the fluorescein (496nm) and the distinct signatures of the S11 and M11 peaks of the carbon nanotubes.

Raman spectroscopy was completed using dried films of SWNT or functionalized carbon nanotubes. Suspensions of the SWNT and functionalized nanotubes were prepared as described above for UV-vis-NIR studies. Approximately 50 μ l of each suspension was pipetted onto a quartz microscope slide and dried at room temperature. Raman spectra were collected using a Raman microscope (Renishaw inVia) with a HeNe laser at excitation wavelength of 633nm. Samples were scanned between 100 cm^{-1} and 3000 cm^{-1} in order to examine the radial breathing mode (RBM), and the tangential modes (G and D band) intensities. The spectra were collected with a 10s exposure time and 20 scans were averaged for each sample.

Approximately (1-2mg) of SWNTs were mixed with 100mg of KBr (Sigma, St. Louis, USA) and grinded using a mortar and pestle until all the nanotubes were evenly dispersed in the KBr and the resulting powder was formed into a pellet using a pellet press. The collection of the spectrum was completed between 500 cm^{-1} and 3500 cm^{-1} using a Nicolet IR200 FT-IR spectrometer.

The Thermogravimetric analyses (TGA) of the carbon nanotubes were carried out in a STA 409 PC thermal analyzer (NETZSCH Instruments) under argon atmosphere employing a heating rate of 10 $^{\circ}\text{C min}^{-1}$.

The aforementioned techniques were employed in order to develop and characterize a new one-step synthetic process to attach a fluorophore moiety to a SWNT with a high weight percentage yield as shown in **Figure 38**. To that end, we employed a Lewis acid catalyst, enabling the nanotubes to remain in suspension throughout the reaction. SWNTs were functionalized with fluorescein via an esterification reaction using boron trifluoride etherate as a catalyst, and the product was isolated using centrifugation. Notably, this process results in a 95% overall weight percentage yield of the product.

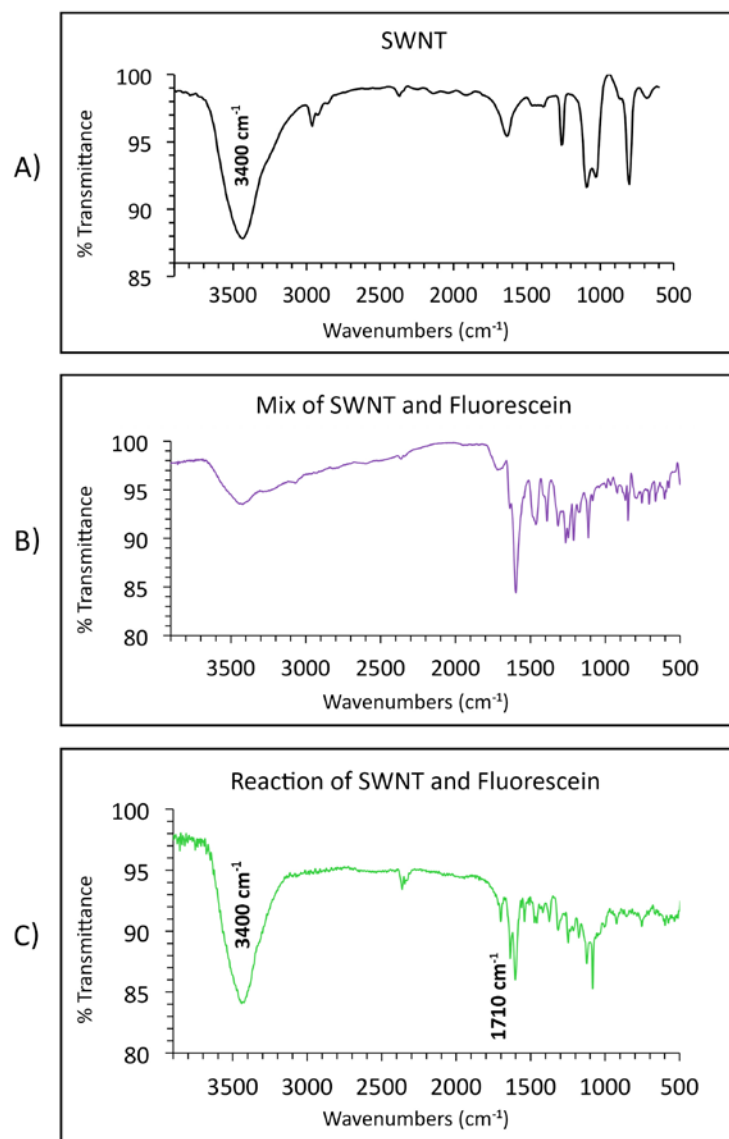


Figure 39. FT-IR spectra of functional groups contained on the starting materials and reaction of SWNT and fluorescein (A) (P3) SWNT starting material (B) SWNT mechanically ground with fluorescein as a physical mixture (1:4 ratio), and (C) the reaction product of SWNT and fluorescein (1:4 ratio) after esterification.

The starting materials and the product were analysed via several approaches to determine functionalization and ensure that the structure of the nanotube was maintained. One method in particular, which was used to determine whether the fluorophore was indeed covalently conjugated to the carbon nanotube was FT-IR. **Figure 39** represents the spectra of 1) P3-SWNT (shown in **Figure 39A**), 2) a mixture of SWNT and fluorescein prior to their reaction as shown in **Figure 39B** and 3) the SWNT and fluorescein mixture after 5 days of reaction time represented in **Figure 39C** were obtained and compared. P3 SWNTs purchased through Carbon Solutions, Inc., have approximately 1-3% lattice defects resulting in COOH groups on the nanotube surface. Each spectrum presented a broad peak at $\sim 3400\text{ cm}^{-1}$, which is likely due to the O-H stretching modes of the bonds of the carboxylic acid group, while the peak in the 1600 cm^{-1} region likely corresponds to a carboxylic acid C=O stretching vibration.^[404] The spectrum of the SWNT fluorescein mixture prior to the reaction as shown in **Figure 39B** has several additional peaks as compared to the spectra of SWNT alone shown in **Figure 39A**, which can be attributed to the bonds found in the free acid of fluorescein. After the functionalization reaction, a new sharp peak at $\sim 1710\text{ cm}^{-1}$ appears in the fluorescein functionalized SWNT spectrum represented in **Figure 39C**, which represents evidence of the formation of an ester bond. The comparatively lesser intensity of the ester bond peak is dependent upon the percentage of available COOH groups on the P3 carbon nanotubes and the remaining carbonaceous impurities specifically the amorphous carbon, which results in a relatively lower theoretical level of possible functionalization.^[405]

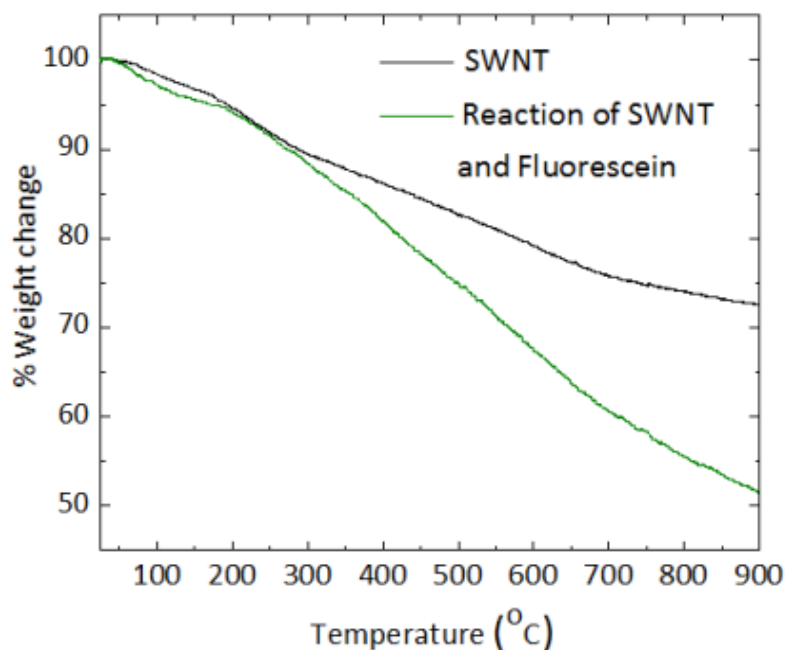


Figure 40. Thermogravimetric Analysis (TGA) compares the stability of the (P3) SWNT (black) and the Reaction of SWNT and Fluorescein (green). The (P3) SWNTs have a higher thermal stability compared to the reaction of fluorescein SWNTs. The total weight loss difference between the SWNT and functionalized SWNT is 22%.

We examined the characteristic weight loss of the SWNT compared to the fluorescein functionalized SWNT using TGA. The process of sidewall functionalization to the nanotubes can result in a lower thermal stability causing the functionalized SWNT to oxidize more rapidly than SWNT alone.^[406,407] Over the 30°C to 900°C temperature range, the weight loss for SWNT was approximately 28% whereas for the fluorescein functionalized SWNT was nearly 50% as shown in **Figure 40**. Thus, the faster degradation rate concomitant with higher weight loss of

functionalized nanotubes further confirms that SWNT are functionalized with fluorescein. We assumed that the difference of weight loss in the TGA data was primarily due to the pyrolysis of the functionalized groups. Therefore, we estimated that approximately one fluorescein molecule for every 98 carbons atoms, equivalent to about 1.02%, was functionalized to the SWNT. This result, compared with the 1.1 atomic percentage of COOH groups per nanotube, suggests the conversion of ~92.7% of the carboxylic acid groups.^[408,409]

In order to assess the integrity of the SWNTs, we compared the spectra of unmodified SWNT and functionalized SWNT via Raman spectroscopy. This analysis suggested that the inherent structure of the SWNT was maintained through the functionalization process. Notably, multiple step processes can increase the probability of changes in the structure of the SWNTs, leading to the creation of Stone-Walls defects to the nanotubes sidewalls during reaction.^[410] In **Figure 41**, the tangential modes (G and D bands at $\sim 1590\text{cm}^{-1}$ and at $\sim 1390\text{cm}^{-1}$, respectively) and the radial breathing mode (RBM) are clearly visible both in the SWNT (black line) and functionalized (green line) SWNT. Specifically, the presence of the RBM, typical of the thermal contractile nature of the nanotube, demonstrates the maintenance of the SWNT tubular structure.^[411,412] Furthermore, the G/D band ratio does not show any noticeable significant increase after functionalization, from $G/D=1.19$ for SWNT and $G/D= 1.20$ for reaction of SWNT and fluorescein, suggesting that the reaction process did not increase the amount of sidewall defects.

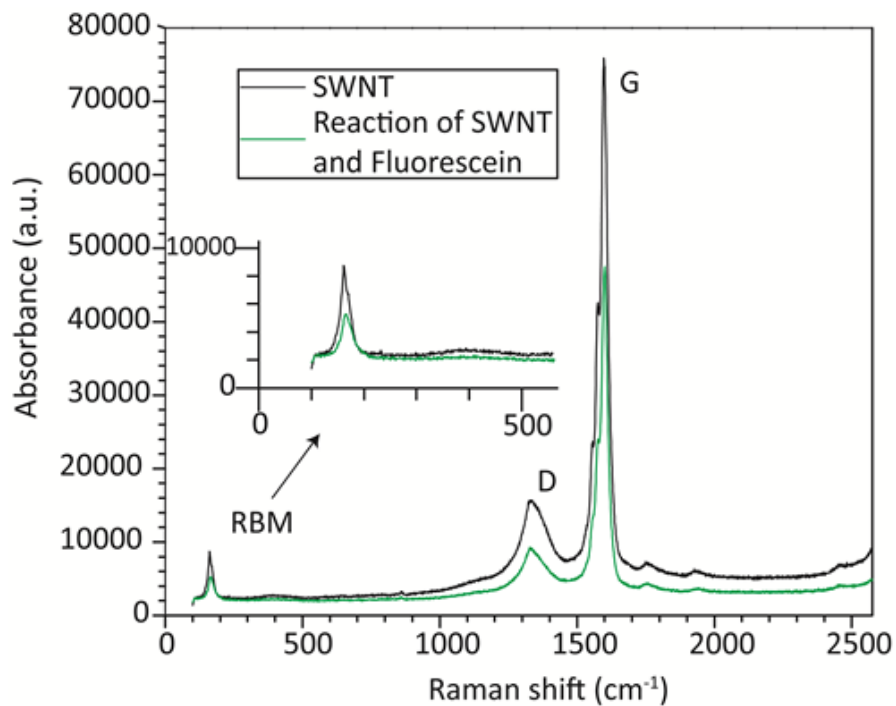


Figure 41. Raman spectrum examines the inherent structure and possible defects of (P3) SWNT (black) and reaction of SWNT and fluorescein (green). The 1590 cm⁻¹ peak typical of the graphene band (G band) and the 1390 cm⁻¹ peak typical of defect band (D band) are marked as well as the radial breathing mode (RBM) typical of thermal contractile nature of the nanotube, which is also highlighted in the insert.

After examining the functionalization and structure of SWNT, UV-vis-NIR spectroscopy was used to investigate the fluorescent properties of the functionalized nanotubes as shown in **Figure 42**. Comparisons were performed on the individual components (fluorescein and SWNT), their mixture, and their reaction product. The fluorescein free acid is characterized by a peak at $\lambda_{\text{max}}/496\text{nm}$ (red line), which is not affected by the presence of SWNT in the suspension (blue line). Chemical conjugation of SWNTs with fluorescein can also affect the spectrophotometric properties of the fluorescein molecule. Similarly, fluorescein absorption is only slightly red shifted after the reaction as shown in **Figure 42**, green line), which is not unexpected after conjugation through the C=O group.^[413,414] We also investigated the physical structure of the nanotube, using UV-vis-NIR spectroscopy. The two characteristic peaks of SWNT are the M_{11} metallic $\lambda_{\text{max}}/(600\text{nm}-800\text{nm})$ and the S_{11} semiconducting $\lambda_{\text{max}}/(830\text{nm}-1200\text{nm})$ peaks (black line).^[415] The fluorescein functionalized SWNT spectra suggests that the inherent electronic structure (M_{11} and S_{11}) of the nanotube is maintained after functionalization and exhibits a distinctive shift in the absorbance wavelength of fluorescein as shown in **Figure 42** (green line).

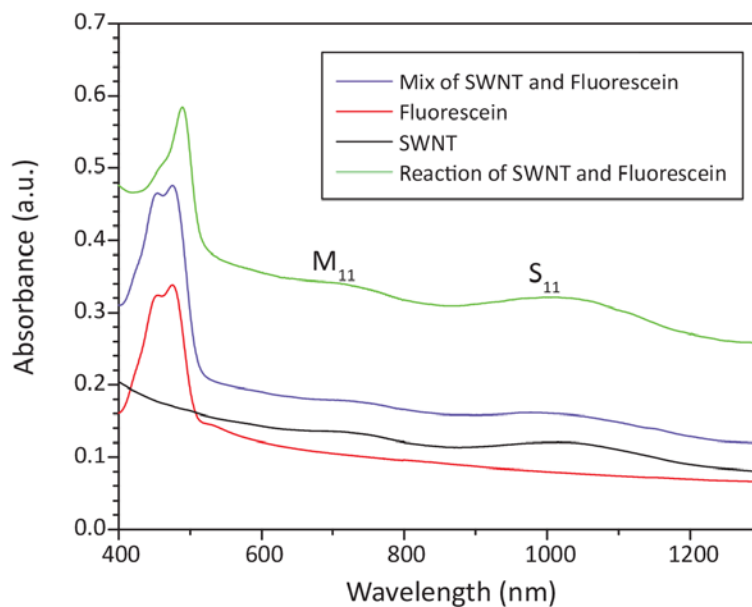


Figure 42. UV-vis-NIR spectrum demonstrates the fluorescent properties of the (P3) SWNT (black), fluorescein (red), mixture of SWNT and fluorescein (1:4 ratio) (purple) and the reaction product of SWNT and fluorescein (green). The SWNT exhibit the signatures of the M₁₁ (metallic) and S₁₁ (semiconducting) bands. The fluorescein exhibits a peak corresponding to $\lambda_{max}/496\text{nm}$. The reaction of SWNT and fluorescein produces the signature bands of nanotubes and a slight shift in the fluorescence of fluorescein.

Overall, the FT-IR and TGA data suggest that SWNT can be successfully functionalized with fluorescein using a one-step esterification reaction employing a Lewis acid catalyst. Furthermore, UV-vis-NIR and Raman spectroscopy demonstrate that the SWNT and the fluorescein structure were not significantly altered during the functionalization process. This process, notably, does require a five-day reaction period due to the low reactivity of the phenol and the carboxylic acid, compared to the shorter reaction time period of an esterification reaction using an acid chloride functionalized nanotube.^[416] The reaction time is longer than other reactions of primary alcohol groups and could be potentially shortened by using a microwave reactor as reported with other SWNT reactions.^[417] Also, the extent of functionalization on the nanotube could be enhanced by increasing the amount of carboxylic acid groups attached to the SWNT. This could potentially enhance the intensity of the fluorescence, enable additional fluorophores to be functionalized to the SWNT, or allow for attachment of another fluorophore moiety with similar chemical functionality. Lastly, the method described herein represents a one-step, straightforward and potentially scalable process with a 95% overall weight yield that does not require any modification to the starting materials prior to initiating the reaction.

In conclusion, we have developed a new method to functionalize SWNTs with a commonly used fluorophore, fluorescein. The process occurs via a one-step esterification reaction under mild conditions, with no significant creation of defects to the structure of the nanotube. The esterification process enables a straightforward preparation, which can be further scaled and exploited for other biologically relevant fluorophores currently used as contrast agents for in vivo diagnostic imaging, pH sensors, and optical fluorescent imaging.^[418-420]

BIBLIOGRAPHY

- [1] N. J. D. Gower, R. J. Barry, M. R. Edmunds, L. C. Titcomb, A. K. Denniston, *BMC Ophthalmol.* **2016**, *16*, 11.
- [2] N. J. Friedman, *Curr. Opin. Ophthalmol.* **2010**, *21*, 310.
- [3] U. Chakravarthy, T. Y. Wong, A. Fletcher, E. Pault, C. Evans, G. Zlateva, R. Buggage, A. Pleil, P. Mitchell, *BMC Ophthalmol.* **2010**, *10*, 31.
- [4] J. R. Smith, A. J. Stempel, A. Bharadwaj, B. Appukuttan, *Clin. Transl. Immunol.* **2016**, *5*, e63.
- [5] M. Hessen, E. K. Akpek, *J. Ophthalmic Vis. Res.* **2014**, *9*, 240.
- [6] J. El Annan, S. K. Chauhan, T. Ecoiffier, Q. Zhang, D. R. Saban, R. Dana, *Invest. Ophthalmol. Vis. Sci.* **2009**, *50*, 3802.
- [7] A. Kauppinen, J. J. Paterno, J. Blasiak, A. Salminen, K. Kaarniranta, *Cell. Mol. Life Sci.* **2016**, *73*, 1765.
- [8] H. R. Coleman, C. Chan, F. L. F. Iii, E. Y. Chew, *Lancet* **2009**, *372*, 1835.
- [9] G. N. Lemp, Michael A, Foulks, *Ocul. Surf.* **2007**, *Dry Eye Wo*, 75.
- [10] P. Kulkarni, *J. Ocul. Pharmacol. Ther.* **2001**, *17*, 181.
- [11] Y. Wang, V. M. Wang, C.-C. Chan, *Eye* **2011**, *25*, 127.
- [12] J. D. Nelson, H. Helms, R. Fiscella, Y. Southwell, J. D. Hirsch, *Adv. Ther.* **2000**, *17*, 84.
- [13] R. J. Barry, Q. D. Nguyen, R. Wlee, P. Imurray, A. K. Denniston, *Clin. Ophthalmol.* **2014**, *8*, 1891.
- [14] Yi Wei et al., *Eye Contact Lens* **2014**, *40*, 248.
- [15] T. Larson, R. B. Nussenblatt, H. N. Sen, *Expert Opin. Emerg. Drugs* **2011**, *16*, 309.
- [16] J. F. Fangueiro, F. Veiga, A. M. Silva, E. B. Souto, *Curr. Pharm. Des.* **2016**, *22*, 1135.

- [17] A. Urtti, *Adv. Drug Deliv. Rev.* **2006**, 58, 1131.
- [18] K. Cholkar, S. P. Patel, A. D. Vadlapudi, A. K. Mitra, *J. Ocul. Pharmacol. Ther.* **2013**, 29, 106.
- [19] S. A. Molokhia, S. C. Thomas, K. J. Garff, K. J. Mandell, B. M. Wirostko, *J. Ocul. Pharmacol. Ther.* **2013**, 29, 92.
- [20] P. Baranowski, B. Karolewicz, M. Gajda, J. Pluta, *Sci. World J.* **2014**, 2014, DOI 10.1155/2014/861904.
- [21] N. Kuno, S. Fujii, *Polymers (Basel)*. **2011**, 3, 193.
- [22] K. Cholkar, S. P. Patel, A. D. Vadlapudi, A. K. Mitra, *J. Ocul. Pharmacol. Ther.* **2013**, 29, 106.
- [23] C. C. Peng, J. Kim, A. Chauhan, *Biomaterials* **2010**, 31, 4032.
- [24] R. Gaudana, H. K. Ananthula, A. Parenky, A. K. Mitra, **2010**, 12, 348.
- [25] A. G. M. Jünemann, T. Chorągiewicz, M. Ozimek, P. Grieb, R. Rejdak, *Ophthalmol. J.* **2016**, 1, 29.
- [26] Q. Xu, S. Kambhampati, R. Kannan, *Middle East Afr. J. Ophthalmol.* **2013**, 20, 26.
- [27] J. Araújo, E. Gonzalez, M. A. Egea, M. L. Garcia, E. B. Souto, *Nanomedicine Nanotechnology, Biol. Med.* **2009**, 5, 394.
- [28] A. Guzman-Aranguez, B. Fonseca, G. Carracedo, A. Martin-Gil, A. Martinez-Aguila, J. Pintor, *Eye Contact Lens Sci. Clin. Pract.* **2015**, 42, 1.
- [29] J. Kim, A. Conway, A. Chauhan, *Biomaterials* **2008**, 29, 2259.
- [30] F. A. Maulvi, T. G. Soni, D. O. Shah, *Drug Deliv.* **2016**, 7544, 1.
- [31] C. C. Peng, A. Chauhan, *J. Control. Release* **2011**, 154, 267.
- [32] H. J. Jung, M. Abou-Jaoude, B. E. Carbia, C. Plummer, A. Chauhan, *J. Control. Release* **2013**, 165, 82.
- [33] C. L. Schultz, T. R. Poling, J. O. Mint, *Clin. Exp. Optom.* **2009**, 92, 343.
- [34] M. Yang, Y. Yang, M. Lei, C. Ye, C. Zhao, J. Xu, K. Wu, M. Yu, *Drug Deliv.* **2016**, 23, 3538.
- [35] J. Kim, C. C. Peng, A. Chauhan, *J. Control. Release* **2010**, 148, 110.
- [36] D. Gulsen, C. Anuj, *IOVS* **2004**, 45, 2342.

- [37] U. B. Kompella, R. S. Kadam, V. H. Lee, *Ther. Deliv.* **2010**, *1*, 435.
- [38] C. Gupta, A. Chauhan, *J. Control. Release* **2011**, *150*, 70.
- [39] V. K. Yellepeddi, R. Sheshala, H. McMillan, C. Gujral, D. Jones, T. Raghu Raj Singh, *Drug Discov. Today* **2015**, *20*, 884.
- [40] N. Gooch, S. A. Molokhia, R. Condie, R. M. Burr, B. Archer, B. K. Ambati, B. Wirostko, *Pharmaceutics* **2012**, *4*, 197.
- [41] U. B. Kompella, R. S. Kadam, V. H. L. Lee, *Ther. Deliv.* **2010**, *1*, 435.
- [42] S. H. Boddu, H. Gupta, S. Patel, *Recent Pat. Drug Deliv. Formul.* **2014**, *8*, 27.
- [43] L. R. Schopf, A. M. Popov, E. M. Enlow, J. L. Bourassa, W. Z. Ong, P. Nowak, H. Chen, *Transl. Vis. Sci. Technol.* **2015**, *4*, 11.
- [44] P. W. Morrison, V. V. Khutoryanskiy, *Ther. Deliv.* **2014**, *5*, 1297.
- [45] K. Cholkar, A. Patel, A. D. Vadlapudi, A. K. Mitra, *Recent Pat. Nanomed.* **2014**, *2*, 82.
- [46] Y. C. Kim, B. Chiang, X. Wu, M. R. Prausnitz, *J. Control. Release* **2014**, *190*, 172.
- [47] J. Cunha-Vaz, F. B. Marques, R. Fernandes, C. Alves, T. Velpandian, **2016**, 37.
- [48] J. Lee, R. M. Pelis, *Drug Metab. Dispos.* **2016**, *44*, 1675.
- [49] U. B. Kompella, A. C. Amrite, R. Pacha Ravi, S. A. Durazo, *Prog. Retin. Eye Res.* **2013**, *36*, 172.
- [50] A. Shapiro, *Retin. Today* **2016**, 1.
- [51] H. F. Edelhauser, C. L. Rowe-Rendleman, M. R. Robinson, D. G. Dawson, G. J. Chader, H. E. Grossniklaus, K. D. Rittenhouse, C. G. Wilson, D. A. Weber, B. D. Kuppermann, K. G. Csaky, T. W. Olsen, U. B. Kompella, V. M. Holers, G. S. Hageman, B. C. Gilger, P. A. Campochiaro, S. M. Whitcup, W. T. Wong, *Invest. Ophthalmol. Vis. Sci.* **2010**, *51*, 5403.
- [52] P. J. Rosenfeld, D. M. Brown, J. S. Heier, D. S. Boyer, P. K. Kaiser, C. Y. Chung, R. Y. Kim, MARINA Study Group, *N. Engl. J. Med.* **2006**, *355*, 1419.
- [53] E. W. M. Ng, D. T. Shima, P. Calias, E. T. Cunningham, D. R. Guyer, A. P. Adamis, *Nat. Rev. Drug Discov.* **2006**, *5*, 123.
- [54] C. Wang, H. Hou, K. Nan, M. J. Sailor, W. R. Freeman, L. Cheng, *Exp. Eye Res.* **2014**, *129*, 74.
- [55] W. Chen, X. Zhang, J. Li, Y. Wang, Q. Chen, C. Hou, Q. Garrett, *Investig. Ophthalmol. Vis. Sci.* **2013**, *54*, 6287.

- [56] S. S. Shah, L. V Denham, J. R. Elison, P. S. Bhattacharjee, C. Clement, T. Huq, J. M. Hill, *Expert rev Ophthalmol* **2010**, *5*, 75.
- [57] E. M. del Amo, A. Urtti, *Drug Discov. Today* **2008**, *13*, 135.
- [58] R. S. Hunter, A.-M. Lobo, *Clin. Ophthalmol.* **2011**, *5*, 1613.
- [59] D. S. Boyer, J. Posalski, *Am. J. Ophthalmol.* **1999**, *127*, 349.
- [60] S. S. Lee, P. Hughes, A. D. Ross, M. R. Robinson, *Pharm. Res.* **2010**, *27*, 2043.
- [61] J. P. Bertram, S. M. Jay, S. R. Hynes, R. Robinson, J. M. Criscione, E. B. Lavik, *Acta Biomater.* **2009**, *5*, 2860.
- [62] A. P. Acharya, J. S. Lewis, B. G. Keselowsky, *Biomaterials* **2013**, *34*, 3422.
- [63] A. Kumari, S. K. Yadav, S. C. Yadav, *Colloids Surfaces B Biointerfaces* **2010**, *75*, 1.
- [64] H. K. Makadia, S. J. Siegel, *Polymers (Basel)*. **2011**, *3*, 1377.
- [65] D. J. Lee, *J. Funct. Biomater.* **2015**, *6*, 650.
- [66] P. Calvo, A. Ferreras, F. Al Adel, Y. Wang, M. H. Brent, *Br. J. Ophthalmol.* **2014**, *1*.
- [67] S. N. Rothstein, W. J. Federspiel, S. R. Little, *J. Mater. Chem.* **2008**, *18*, 1873.
- [68] S. N. Rothstein, W. J. Federspiel, S. R. Little, *Biomaterials* **2009**, *30*, 1657.
- [69] S. N. Rothstein, S. R. Little, *J. Mater. Chem.* **2011**, *21*, 29.
- [70] A. A. Moshfeghi, G. A. Peyman, *Adv. Drug Deliv. Rev.* **2005**, *57*, 2047.
- [71] F. Ramazani, C. Hiemstra, R. Steendam, F. Kazazi-Hyseni, C. F. Van Nostrum, G. Storm, F. Kiessling, T. Lammers, W. E. Hennink, R. J. Kok, *Eur. J. Pharm. Biopharm.* **2015**, *95*, 368.
- [72] N. Elsaid, T. L. Jackson, Z. Elsaid, A. Alqathama, S. Somavarapu, *Mol. Pharm.* **2016**, *13*, 2923.
- [73] M. A. Kamaledin, *Nanomedicine Nanotechnology, Biol. Med.* **2017**, *0*.
- [74] H. A. Salama, M. Ghorab, A. A. Mahmoud, M. Abdel Hady, *AAPS PharmSciTech* **2017**, DOI 10.1208/s12249-017-0710-8.
- [75] Q. Pan, Q. Xu, N. J. Boylan, N. W. Lamb, D. G. Emmert, J. C. Yang, L. Tang, T. Heflin, S. Alwadani, C. G. Eberhart, W. J. Stark, J. Hanes, *J. Control. Release* **2015**, *201*, 32.
- [76] B. G. Short, *Toxicol. Pathol.* **2008**, *36*, 49.

- [77] T. Yasukawa, Y. Ogura, Y. Tabata, H. Kimura, P. Wiedemann, Y. Honda, *Prog. Retin. Eye Res.* **2004**, *23*, 253.
- [78] D. Moinard-Chécot, Y. Chevalier, S. Briançon, L. Beney, H. Fessi, *J. Colloid Interface Sci.* **2008**, *317*, 458.
- [79] C. Wischke, S. P. Schwendeman, *Int. J. Pharm.* **2008**, *364*, 298.
- [80] V. Andrés-Guerrero, M. Zong, E. Ramsay, B. Rojas, S. Sarkhel, B. Gallego, R. De Hoz, A. I. Ramirez, J. J. Salazar, A. Trivino, J. M. Ramirez, E. M. Del Amo, N. Cameron, B. De-Las-Heras, A. Urtti, G. Mihov, A. Dias, R. Herrero-Vanrell, *J. Control. Release* **2015**, *211*, 105.
- [81] T. Peters, S.-W. Kim, V. Castro, K. Stingl, T. Strasser, S. Bolz, U. Schraermeyer, G. Mihov, M. Zong, V. Andres-Guerrero, R. Herrero Vanrell, A. A. Dias, N. R. Cameron, E. Zrenner, *Biomaterials* **2017**, *124*, 157.
- [82] Y. S. Chen, C. R. Green, K. Wang, H. V. Danesh-Meyer, I. D. Rupenthal, *Eur. J. Pharm. Biopharm.* **2014**, *95*, 378.
- [83] T. R. Thrimawithana, S. Young, C. R. Bunt, C. Green, R. G. Alany, *Drug Discov. Today* **2011**, *16*, 270.
- [84] M. V. Fedorchak, I. P. Conner, C. A. Medina, J. B. Wingard, J. S. Schuman, S. R. Little, *Exp. Eye Res.* **2014**, *125*, 210.
- [85] M. L. Ratay, A. J. Glowacki, S. C. Balmert, A. P. Acharya, J. Polat, L. P. Andrews, M. V. Fedorchak, J. S. Schuman, D. A. A. Vignali, S. R. Little, *J. Control. Release* **2017**, DOI 10.1016/j.jconrel.2017.05.007.
- [86] Y. He, Y. Liu, Y. Liu, J. Wang, X. Zhang, W. Lu, Z. Ma, X. Zhu, Q. Zhang, *Investig. Ophthalmol. Vis. Sci.* **2006**, *47*, 3983.
- [87] M. V. Fedorchak, I. P. Conner, A. Cugini, J. S. Schuman, S. R. Little, *Sci. Rep.* **2017**, *7*, 8639.
- [88] S. Day, K. Acquah, P. P. Lee, P. Mruthyunjaya, F. A. Sloan, *Am. J. Ophthalmol.* **2011**, *152*, 1014.
- [89] J. L. Gottlieb, *JAMA Ophthalmology* **2002**, *288*, 2233.
- [90] M. Singer, *F1000Prime Rep* **2014**, *6*, 29.
- [91] R. D. Jager, W. F. Mieler, J. W. Miller, *N. Engl. J. Med.* **2008**, *358*, 2606.
- [92] A.-R. E. D. S. Group, *Arch. Ophthalmol.* **2001**, *119*, 1417.

- [93] C. M. Stanton, J. R. W. Yates, A. I. den Hollander, J. M. Seddon, A. Swaroop, D. Stambolian, S. Fauser, C. Hoyng, Y. Yu, K. Atsuhiko, K. Branham, M. Othman, W. Chen, E. Kortvely, K. Chalmers, C. Hayward, A. T. Moore, B. Dhillon, M. Ueffing, A. F. Wright, *Invest. Ophthalmol. Vis. Sci.* **2011**, *52*, 8828.
- [94] J. Roychoudhury, J. M. Herndon, J. Yin, R. S. Apte, T. A. Ferguson, *Investig. Ophthalmol. Vis. Sci.* **2010**, *51*, 3560.
- [95] S. L. Doyle, M. Campbell, E. Ozaki, R. G. Salomon, A. Mori, P. F. Kenna, G. J. Farrar, A. Kiang, M. M. Humphries, C. Ed, *Nat. Med.* **201AD**, *18*, 791.
- [96] P. A. Campochiaro, A. K. Lauer, E. H. Sohn, T. A. Mir, S. Naylor, M. C. Anderton, M. Kelleher, R. Harrop, S. Ellis, K. A. Mitrophanous, *Hum. Gene Ther.* **2016**, *28*, 99.
- [97] N. G. Kolosova, N. A. Muraleva, A. A. Zhdankina, N. A. Stefanova, A. Z. Fursova, M. V. Blagosklonny, *Am. J. Pathol.* **2012**, *181*, 472.
- [98] L. He, A. G. Marneros, *J. Biol. Chem.* **2014**, *289*, 8019.
- [99] T. Iwase, J. Fu, T. Yoshida, D. Muramatsu, A. Miki, N. Hashida, L. Lu, B. Oveson, R. Lima E Silva, C. Seidel, M. Yang, S. Connelly, J. Shen, B. Han, M. Wu, G. L. Semenza, P. A. Campochiaro, J. Hanes, *J Control Release* **2013**, *172*, DOI 10.1016/j.jconrel.2013.10.008.
- [100] T. C. R. Group, *N. Engl. J. Med.* **2011**, *364*, 1897.
- [101] P. A. Campochiaro, Q. D. Nguyen, S. M. Shah, M. L. Klein, E. Holz, R. N. Frank, D. A. Saperstein, A. Gupta, J. T. Stout, J. Macko, R. Dibartolomeo, L. L. Wei, *Hum. Gene Ther.* **2006**, *17*, 167.
- [102] and C. S. Peter F. Ziipfel Nadine Lauer, *Adv. Exp. Med. Biol.* **2010**, *703*, 9.
- [103] S. L. Doyle, F. J. Lopez, L. Celkova, K. Brennan, K. Mulfaul, E. Ozaki, P. F. Kenna, E. Kurali, N. Hudson, T. Doggett, T. A. Ferguson, P. Humphries, P. Adamson, M. Campbell, *Investig. Ophthalmol. Vis. Sci.* **2015**, *56*, 5424.
- [104] S. D. Schwartz, C. D. Regillo, B. L. Lam, D. Elliott, P. J. Rosenfeld, N. Z. Gregori, J. Hubschman, J. L. Davis, G. Heilwell, M. Spirn, J. Maguire, R. Gay, J. Bateman, R. M. Ostrick, D. Morris, M. Vincent, E. Anglade, L. V Del Priore, R. Lanza, L. V. Del Priore, *Lancet* **2014**, *6736*, 1.
- [105] G. De Wert, C. Mummery, *Hum. Reprod.* **2003**, *18*, 672.
- [106] M. Fields, H. Cai, J. Gong, L. Del Priore, *Cells* **2016**, *5*, 44.
- [107] C. E. Thomas, A. Ehrhardt, M. a Kay, *Nat. Rev. Genet.* **2003**, *4*, 346.

- [108] S. Sodha, K. Wall, S. Redenti, H. Klassen, M. J. Young, S. L. Tao, *J. Biomater. Sci. Polym. Ed.* **2011**, *22*, 443.
- [109] E. B. Lavik, H. Klassen, K. Warfvinge, R. Langer, M. J. Young, *Biomaterials* **2005**, *26*, 3187.
- [110] S. R. Hynes, E. B. Lavik, *Graefe's Arch. Clin. Exp. Ophthalmol.* **2010**, *248*, 763.
- [111] J. D. Fisher, A. P. Acharya, S. R. Little, *Clin. Immunol.* **2015**, *160*, 24.
- [112] H. D. Perry, R. Solomon, E. D. Donnenfeld, A. R. Perry, J. R. Wittpenn, H. E. Greenman, H. E. Savage, *Arch. Ophthalmol.* **2008**, *126*, 1046.
- [113] C. A. Cox, J. Amaral, R. Salloum, L. Guedez, T. W. Reid, C. Jaworski, M. John-aryankalayil, K. A. Freedman, M. M. Campos, A. Martinez, S. P. Becerra, D. A. Carper, *Ophthalmology* **2010**, *117*, 1782.
- [114] L. He, A. G. Marneros, *J. Biol. Chem.* **2014**, *289*, 8019.
- [115] R. L. Avery, D. J. Pieramici, M. D. Rabena, A. A. Castellarin, M. A. Nasir, M. J. Giust, *Am. Acad. Ophthalmol.* **2006**, *113*, DOI 10.1016/j.opthta.2005.11.019.
- [116] B. D. Kelly, S. F. Hackett, K. Hirota, Y. Oshima, Z. Cai, S. Berg-Dixon, A. Rowan, Z. Yan, P. A. Campochiaro, G. L. Semenza, *Circ. Res.* **2003**, *93*.
- [117] P. J. Rosenfeld, D. M. Brown, J. S. Heier, D. S. Boyer, P. K. Kaiser, C. Y. Chung, R. Y. Kim, *N. Engl. J. Med.* **2006**, *355*, 1419.
- [118] S. M. Cashman, L. Bowman, J. Christofferson, R. Kumar-Singh, *Investig. Ophthalmol. Vis. Sci.* **2006**, *47*, 3496.
- [119] K. Binley, P. S. Widdowson, M. Kelleher, J. de Belin, J. Loader, G. Ferrige, M. Carlucci, M. Esapa, D. Chipchase, D. Angell-Manning, S. Ellis, K. Mitrophanous, J. Miskin, V. Bantsev, T. M. Nork, P. Miller, S. Naylor, *Hum Gene Ther* **2012**, *23*, 980.
- [120] M. Gemenetzi, A. J. Lotery, *Eye* **2016**, *30*, 1.
- [121] B. Lu, C. Malcuit, S. Wang, S. Girman, P. Francis, L. Lemieux, R. Lanza, R. Lund, *Stem Cells* **2009**, *27*, 2126.
- [122] A. Trounson, N. D. DeWitt, *Nat. Rev. Mol. Cell Biol.* **2016**, *17*, 194.
- [123] M. D. de Smet, S. R. J. Taylor, B. Bodaghi, E. Miserocchi, P. I. Murray, U. Pleyer, M. Zierhut, T. Barisani-Asenbauer, P. LeHoang, S. Lightman, *Prog. Retin. Eye Res.* **2011**, *30*, 452.
- [124] Q. D. Nguyen, P. T. Merrill, W. L. Clark, A. S. Banker, C. Fardeau, P. Franco, P. LeHoang, S. Ohno, S. R. Rathinam, S. Thurau, A. Abraham, L. Wilson, Y. Yang, N. Shams, *Ophthalmology* **2016**, *123*, 2413.

- [125] J. S. Kim, J. E. Knickelbein, R. B. Nussenblatt, N. Sen, *Int Ophthalmol Clin* **2015**, *55*, 79.
- [126] N. R. Acharya, V. M. Tham, E. Esterberg, D. S. Borkar, J. V. Parker, A. C. Vinoya, A. Uchida, *JAMA Ophthalmol.* **2013**, *131*, 1405.
- [127] S. Mérida, E. Palacios, A. Navea, F. Bosch-Morell, *Int. J. Mol. Sci.* **2015**, *16*, 18778.
- [128] P. H. Papotto, E. B. Marengo, L. R. Sardinha, A. C. Goldberg, L. V. Rizzo, *Autoimmun. Rev.* **2014**, *13*, 909.
- [129] P. Lin, *Curr. Ophthalmology Rep.* **2015**, *3*, 170.
- [130] H. Takase, Y. Futagami, T. Yoshida, K. Kamoi, S. Sugita, Y. Imai, M. Mochizuki, *Investig. Ophthalmol. Vis. Sci.* **2006**, *47*, 1557.
- [131] R. R. Caspi, *J. Clin. Invest.* **2010**, *120*, 3073.
- [132] R. K. Agarwal, R. R. Caspi, *Methods Mol Med* **2004**, *102*, 395.
- [133] M. D. Becker, G. Adamus, M. P. Davey, J. T. Rosenbaum, *Ocul. Immunol. Inflamm.* **2000**, *8*, DOI 10.1076/0927-3948(200006)8.
- [134] E. S. Sen, A. D. Dick, A. V Ramanan, *Nat. Rev. Rheumatol.* **2015**, DOI 10.1038/nrrheum.2015.20.
- [135] R. R. Caspi, *Investig. Ophthalmol. Vis. Sci.* **2011**, *52*, 1873.
- [136] G. Palareti, C. Legnani, B. Cosmi, E. Antonucci, N. Erba, D. Poli, S. Testa, A. Toso, *Int. J. Lab. Hematol.* **2016**, *38*, 42.
- [137] Y. Sakoda, T. Nagai, S. Murata, Y. Mizuno, H. Kurosawa, H. Shoda, N. Morishige, R. Yanai, K.-H. Sonoda, K. Tamada, *J. Immunol.* **2016**, *196*, 2947.
- [138] J. Chen, H. Qian, R. Horai, C. C. Chan, Y. Falick, R. R. Caspi, *PLoS One* **2013**, *8*, DOI 10.1371/journal.pone.0072161.
- [139] M. Chen, D. A. Copland, J. Zhao, J. Liu, J. V. Forrester, A. D. Dick, H. Xu, *Am. J. Pathol.* **2012**, *180*, 235.
- [140] C. M. Samson, N. Waheed, S. Baltatzis, C. S. Foster, *Ophthalmology* **2001**, *6420*, 1134.
- [141] D. Doycheva, M. Zierhut, G. Blumenstock, N. Stuebiger, C. Deuter, *Graefe's Arch. Clin. Exp. Ophthalmol.* **2011**, *249*, 1235.
- [142] S. Al-Khatib, E. Suhler, A. Djalilian, H. Sen, R. Nussenblatt, R. Buggage, *Invest. Ophthalmol. Vis. Sci.* **2002**, *43*, 4278.
- [143] K. Kitahara, S. Kawai, *Curr. Opin. Rheumatol.* **2007**, *19*, 238.

- [144] A. T. Vitale, A. Rodriguez, C. S. Foster, F. Acs, *Ophthalmology* **1996**, *103*, 365.
- [145] R. O. Kaçmaz, J. H. Kempen, C. Newcomb, E. Daniel, S. Gangaputra, R. B. Nussenblatt, J. T. Rosenbaum, E. B. Suhler, J. E. Thorne, D. A. Jabs, G. A. Levy-Clarke, C. S. Foster, *Ophthalmology* **2010**, *117*, 576.
- [146] T. B. Abud, F. Amparo, U. S. Saboo, A. Di Zazzo, T. H. Dohlman, J. B. Ciolino, P. Hamrah, R. Dana, *Ophthalmology* **2016**, *123*, 1449.
- [147] C. C. Murphy, *Arch. Ophthalmol.* **2005**, *123*, 634.
- [148] A. C. Hogan, C. E. McAvoy, A. D. Dick, R. W. J. Lee, *Ophthalmology* **2007**, *114*, DOI 10.1016/j.ophtha.2007.01.026.
- [149] J. N. Kruh, P. Yang, A. M. Suelves, C. S. Foster, *Ophthalmology* **2014**, *121*, 358.
- [150] I. Tugal-Tutkun, A. Mudun, M. Urgancioglu, S. Kamali, E. Kasapoglu, M. Inanc, A. Gu, *Arthritis Rheum.* **2005**, *52*, 2478.
- [151] S. Yeh, K. Wroblewski, R. Buggage, Z. Li, S. K. Kurup, H. Nida, S. Dahr, P. Sran, G. F. Reed, R. Robinson, J. A. Ragheb, T. A. Waldmann, R. B. Nussenblatt, *J. Autoimmun.* **2008**, *31*, 91.
- [152] A. D. Dick, I. Tugal-Tutkun, S. Foster, M. Zierhut, S. H. Melissa Liew, V. Bezlyak, S. Androudi, *Ophthalmology* **2013**, *120*, 777.
- [153] S. Schwartzman, *Best Pract. Res. Clin. Rheumatol.* **2016**, *30*, 304.
- [154] S. Pasadhika, **2010**, 1.
- [155] N. Kenawy, G. Cleary, D. Mewar, N. Beare, A. Chandna, I. Pearce, **n.d.**, DOI 10.1007/s00417-010-1523-6.
- [156] G. J. Jaffe, C. H. Yang, H. Guo, J. P. Denny, C. Lima, P. Ashton, *Invest. Ophthalmol.* **2000**, *41*, 3569.
- [157] G. J. Jaffe, R. M. McCallum, B. Branchaud, C. Skalak, Z. Butuner, P. Ashton, *Ophthalmology* **2005**, *112*, 1192.
- [158] I.-M. Fang, C.-P. Lin, C.-H. Yang, B.-L. Chiang, C.-M. Yang, L.-Y. Chau, M.-S. Chen, *J. Ocul. Pharmacol. Ther.* **2005**, *21*, 420.
- [159] J. J. Servat, K. A. Mears, E. H. Black, J. J. Huang, *Expert Opin. Biol. Ther.* **2012**, *12*, 311.
- [160] A. Srivastava, M. Rajappa, J. Kaur, *Clin. Chim. Acta* **2010**, *411*, 1165.
- [161] C. You, H. F. Sahawneh, L. Ma, B. Kubaisi, A. Schmidt, C. S. Foster, *Clin. Ophthalmol.* **2017**, *11*, 257.

- [162] S. Gangaputra, C. W. Newcomb, T. L. Liesegang, R. O. Kaçmaz, D. A. Jabs, G. A. Levy-Clarke, R. B. Nussenblatt, J. T. Rosenbaum, E. B. Suhler, J. E. Thorne, C. S. Foster, J. H. Kempen, *Ophthalmology* **2009**, *116*, 2188.
- [163] A. C. Allison, *Lupus* **2005**, *14*, s2.
- [164] J. E. Thorne, D. A. Jabs, F. A. Qazi, Q. D. Nguyen, J. H. Kempen, J. P. Dunn, *Ophthalmology* **2005**, *112*, 1472.
- [165] N. P. Chanaud, B. P. Vistica, E. Eugui, R. B. Nussenblatt, A. C. Allison, I. Gery, *Exp. Eye Res.* **1995**, *61*, 429.
- [166] K. Siepmann, M. Huber, N. Stübiger, C. Deuter, M. Zierhut, *Graefe's Arch. Clin. Exp. Ophthalmol.* **2006**, *244*, 788.
- [167] L. Sobrin, W. Christen, C. S. Foster, *Ophthalmology* **2008**, *115*, 1416.
- [168] S. Il Gum, Y.-H. Kim, J.-C. Jung, I. G. Kim, J. S. Lee, K. W. Lee, Y. J. Park, *Biochem. Biophys. Res. Commun.* **2016**, *482*, 1148.
- [169] S. H. Lee, H. Chung, H. G. Yu, *Korean J. Ophthalmol.* **2012**, *26*, 21.
- [170] C. Isnard Bagnis, *J. Am. Soc. Nephrol.* **2002**, *13*, 2962.
- [171] B. D. Myers, R. Sibley, L. Newton, S. J. Tomlanovich, C. Boshkos, E. Stinson, J. a Luetscher, D. J. Whitney, D. Krasny, N. S. Coplon, *Kidney Int.* **1988**, *33*, 590.
- [172] C. M. Sloper, R. J. Powell, H. S. Dua, *Ophthalmology* **1999**, *106*, 723.
- [173] C. M. Sloper, R. J. Powell, H. S. Dua, *Ophthalmology* **1999**, *106*, 723.
- [174] R. W. J. Lee, R. Greenwood, H. Taylor, R. Amer, S. Biester, J. Heissigerova, J. V. Forrester, A. D. Dick, *Ophthalmology* **2012**, *119*, 1223.
- [175] S. Hale, S. Lightman, *Cytokine* **2006**, *33*, 231.
- [176] M. Cordero-Coma, L. Sobrin, *Surv. Ophthalmol.* **2015**, *60*, 575.
- [177] M. Busch, D. Bauer, M. Hennig, S. Wasmuth, S. Thanos, *IOVS* **2013**, *54*, 39.
- [178] J. Braun, J. Brandt, J. Listing, A. Zink, R. Alten, G. Burmester, W. Golder, H. Kellner, M. Schneider, H. So, *Arthritis Rheum.* **2003**, *48*, 2224.
- [179] W. Reinisch, G. Van Assche, R. Befrits, W. Connell, G. D. Haens, S. Ghosh, P. Michetti, T. Ochsenkühn, R. Panaccione, S. Schreiber, M. S. Silverberg, D. Sorrentino, C. J. Van Der Woude, S. Vermeire, J. Panes, *J. Crohn's Colitis* **2012**, *6*, 248.
- [180] K. E. Hostettler, M. Tamm, H. Brutsche, *Respiration* **2012**, *83*, 218.

- [181] S. Sukumaran, K. Marzan, B. Shaham, A. Reiff, *ISRB Rheumatol.* **2012**, DOI 10.5402/2012/765380.
- [182] F. Gasparin, B. S. Takahashi, M. R. Scolari, F. Gasparin, L. S. Pedral, F. M. Damico, *Arq Bras Oftalmol* **2012**, 75, 143.
- [183] F. Vincenti, R. Kirkman, S. Light, G. Bumgardner, M. Pescovitz, P. Halloran, J. Neylan, A. Wilkinson, H. Ekberg, R. Gaston, L. Backman, J. Burdick, *N. Engl. J. Med.* **1998**, 338, 161.
- [184] G. Vlad, E. K. Ho, E. R. Vasilescu, J. Fan, Z. Liu, J. W. Cai, Z. Jin, E. Burke, M. Deng, M. Cadeiras, R. Cortesini, S. Itescu, C. Marboe, D. Mancini, N. Suciufoca, *Transpl. Immunol.* **2007**, 18, 13.
- [185] J. C. Mullen, E. J. Kuurstra, A. Oreopoulos, M. J. Bentley, S. Wang, *Transplant. Res.* **2014**, 3, 1.
- [186] S. B. Rasaiah, J. A. Light, T. M. Sasaki, C. B. Currier, A. Light, T. M. Sasaki, *Clin. Transplant.* **2000**, 14, 409.
- [187] E. M. Yoshida, P. J. Marotta, P. D. Greig, N. M. Kneteman, D. Marleau, M. Cantarovich, K. M. Peltekian, L. B. Lilly, C. H. Scudamore, V. G. Bain, W. J. Wall, A. Roy, *Liver Transplant.* **2005**, 11, 1064.
- [188] J. C. Mullen, A. Oreopoulos, D. C. Lien, M. J. Bentley, D. L. Modry, K. Stewart, T. L. Winton, K. Jackson, *J. Hear. Lung Transplant.* **2003**, 26, 504.
- [189] G. N. Papaliadis, D. Chu, C. S. Foster, *Ophthalmology* **2003**, 110, 786.
- [190] R. B. Nussenblatt, J. S. Peterson, C. S. Foster, *Ophthalmology* **2005**, 112, 764.
- [191] R. B. Nussenblatt, D. J. S. Thompson, Z. Li, J. S. Peterson, R. R. Robinson, R. S. Shames, S. Nagarajan, M. T. Tang, M. Mailman, G. Velez, C. Roy, G. A. Levy-clark, E. B. Suhler, A. Djalilian, H. N. Sen, S. Al-khatib, R. Ursea, S. Srivastava, A. Bamji, S. Mellow, P. Sran, T. A. Waldmann, R. R. Buggage, *J. Autoimmun.* **2003**, 21, 283.
- [192] D. D. Patel, D. M. Lee, F. Kolbinger, C. Antoni, *Ann Rheum Dis* **2013**, 72 Suppl 2, ii116.
- [193] J. R. Maya, M. A. Sadiq, L. J. Zapata, M. Hanout, S. Sarwar, N. Rajagopalan, K. E. Guinn, Y. J. Sepah, Q. D. Nguyen, *J. Ophthalmol.* **2014**.
- [194] B. Strober, A. B. Gottlieb, B. Sherif, P. Mollon, I. Gilloteau, L. McLeod, T. Fox, M. Mordin, A. Gnanasakthy, C. Papavassilis, M. G. Lebwohl, *J. Am. Acad. Dermatol.* **2017**, DOI 10.1016/j.jaad.2016.11.043.

- [195] W. Hueber, D. D. Patel, T. Dryja, A. M. Wright, I. Koroleva, G. Bruin, C. Antoni, Z. Draelos, M. H. Gold, P. Durez, P. P. Tak, J. J. Gomez-Reino, S. C. Foster, R. Y. Kim, M. C. Samson, N. S. Falk, D. S. Chu, Q. Callanan, Q. D. Nguyen, K. Rose, A. Haider, F. Di Padova, *Am. J. Ophthalmol.* **2010**, 2, DOI 10.1016/0002-9394(82)90197-0.
- [196] E. Letko, S. Yeh, C. S. Foster, U. Pleyer, M. Brigell, C. L. Grosskreutz, A. S. Group, *OPHTHA* **2015**, 122, 939.
- [197] P. Lin, E. B. Suhler, J. T. Rosenbaum, *Ophthalmology* **2014**, 121, 365.
- [198] S. Pasadhika, J. T. Rosenbaum, *Biol. Target Ther.* **2014**, 20, 67.
- [199] F. Zulian, M. Balzarini, F. Falcini, G. Martini, M. Alessio, R. Cimaz, L. Cimino, M. E. Zannin, *Arthritis Care Res.* **2010**, 62, 821.
- [200] N. Kenawy, G. Cleary, D. Mewar, N. Beare, A. Chandna, I. Pearce, *Graefe's Arch. Clin. Exp. Ophthalmol.* **2011**, 249, 297.
- [201] J.-Y. Driot, G. D. Novack, K. D. Rittenhouse, C. Milazzo, P. A. Pearson, *J. Ocul. Pharmacol. Ther.* **2004**, 20, 269.
- [202] G. J. Jaffe, J. Ben-nun, H. Guo, J. P. Dunn, P. Ashton, *Ophthalmology* **2000**, 107, 2024.
- [203] D. A. Mohammad, B. V. Sweet, S. G. Elner, *Ann. Pharmacother.* **2007**, 41, 449.
- [204] J. Hsu, *Curr. Opin. Ophthalmol.* **2007**, 18, 235.
- [205] Y. He, J.-C. Wang, Y.-L. Liu, Z.-Z. Ma, X.-A. Zhu, Q. Zhang, *J. Ocul. Pharmacol. Ther.* **2006**, 22, 121.
- [206] F. Lallemand, O. Felt-Baeyens, K. Besseghir, F. Behar-Cohen, R. Gurny, *Eur. J. Pharm. Biopharm.* **2003**, 56, 307.
- [207] E. Wolska, M. Sznitowska, *Int. J. Pharm.* **2013**, 441, 449.
- [208] P. Trittibach, S. E. Barker, C. A. Broderick, M. Natkunarajah, Y. Duran, S. J. Robbie, J. W. Bainbridge, A. J. Smith, G. M. Sarra, A. D. Dick, R. R. Ali, *Gene Ther.* **2008**, 15, 1478.
- [209] W. Stevenson, S. K. Chauhan, R. Dana, *Arch. Ophthalmology* **2012**, 130, 90.
- [210] M. Rolando, M. Zierhut, *Surv. Ophthalmol.* **2001**, 45 Suppl 2, S203.
- [211] F. Brewitt H. Sistani, *Surv. Ophthalmol.* **2001**, 45, 199.
- [212] J. L. Gayton, *Clin. Ophthalmol.* **2009**, 3, 405.
- [213] J. Yu, C. V Asche, C. J. Fairchild, *Cornea* **2011**, 30, 379.

- [214] M. A. Lemp, *Am. J. Ophthalmol.* **2008**, *146*, 350.
- [215] C. Baudouin, P. Aragona, E. M. Messmer, A. Tomlinson, M. Calonge, K. G. Boboridis, Y. A. Akova, G. Geerling, M. Labetoulle, M. Rolando, *Ocul. Surf.* **2013**, *11*, 246.
- [216] M.-C. Tai, C. B. Cosar, E. J. Cohen, C. J. Rapuano, P. R. Laibson, *Cornea* **2002**, *21*, 135.
- [217] N. Jehangir, G. Bever, S. M. J. Mahmood, M. Moshirfar, *J. Ophthalmol.* **2016**, *2016*, DOI 10.1155/2016/9312340.
- [218] L. Tong, R. Beuerman, S. Simonyi, D. A. Hollander, M. E. Stern, *Ocul. Surf.* **2016**, *14*, 233.
- [219] C. Clouzeau, D. Godefroy, L. Riancho, W. Rostène, C. Baudouin, F. Brignole-Baudouin, *Mol. Vis.* **2012**, *18*, 851.
- [220] S. C. Pflugfelder, A. Solomon, M. E. Stern, D. Ph, *Cornea* **2000**, *19*, 644.
- [221] M. E. Stern, J. Gao, K. F. Siemasko, R. W. Beuerman, S. C. Pflugfelder, *Exp. Eye Res.* **2004**, *78*, 409.
- [222] M. J. Lee, A. Y. Ko, J. H. Ko, H. J. Lee, M. K. Kim, W. R. Wee, S. I. Khwarg, J. Y. Oh, *Mol. Ther.* **2014**, *1*.
- [223] M. E. Stern, C. S. Schaumburg, R. Dana, M. Calonge, J. Y. Niederkorn, S. C. Pflugfelder, *Mucosal Immunol.* **2010**, *3*, 425.
- [224] M. E. Stern, C. S. Schaumburg, S. C. Pflugfelder, *Int. Rev. Immunol.* **2013**, *32*, 19.
- [225] J. Y. Niederkorn, M. E. Stern, S. C. Pflugfelder, C. S. De Paiva, R. M. Corrales, J. Gao, K. Siemasko, *J. Immunol.* **2006**, *176*, 3950.
- [226] S. K. Chauhan, J. El Annan, T. Ecoiffier, S. Goyal, Q. Zhang, D. R. Saban, R. Dana, *J. Immunol.* **2009**, *182*, 1247.
- [227] Y. Chen, S. K. Chauhan, H. S. Lee, D. R. Saban, R. Dana, *Mucosal Immunol.* **2014**, *7*, 38.
- [228] V. L. Perez, S. C. Pflugfelder, S. Zhang, A. Shojaei, R. Haque, *Ocul. Surf.* **2016**, *14*, DOI 10.1016/j.jtos.2016.01.001.
- [229] E. Chang, A. J. McClellan, W. J. Farley, D. Li, C. Stephen, *J. Clin. Exp. Ophthalmology* **2013**, *2*, 1.
- [230] A. Lim, M. R. Wenk, L. Tong, *Trends Mol. Med.* **2015**, *21*, 1.
- [231] S. Rashid, Y. Jin, T. Ecoiffier, S. Barabino, D. a Schaumberg, M. R. Dana, *Arch. Ophthalmol.* **2008**, *126*, 219.
- [232] A. J. Bron, P. Argueso, M. Irkec, F. V. Bright, *Prog. Retin. Eye Res.* **2015**, *44*, 36.

- [233] A. R. Thode, R. A. Latkany, *Drugs* **2015**, *75*, 1177.
- [234] S. S. Lane, H. B. DuBiner, R. J. Epstein, P. H. Ernest, J. V. Greiner, D. R. Hardten, E. J. Holland, M. a. Lemp, J. E. McDonald, D. I. Silbert, C. a. Blackie, C. a. Stevens, R. Bedi, *Cornea* **2012**, *31*, 396.
- [235] C. A. Blackie, C. A. Coleman, E. J. Holland, *Clin. Ophthalmol.* **2016**, *10*, 1385.
- [236] Y. Zhao, A. Veerappan, S. Yeo, D. M. Rooney, R. U. Acharya, J. H. Tan, L. Tong, *Eye Contact Lens Sci. Clin. Pract.* **2016**, *0*, 1.
- [237] A. G. Kabat, J. W. Sowka, *Rev. Optom.* **2010**, 109.
- [238] D. E. Perry, D. Henry and Donnenfeld, *Curr. Opin. Ophthalmology* **2004**, *15*, 299.
- [239] P. J. Barnes, *Eur. J. Pharmacol.* **2006**, *533*, 2.
- [240] Z. Zhang, W. Z. Yang, Z. Z. Zhu, Q. Q. Hu, Y. F. Chen, H. He, Y. X. Chen, Z. G. Liu, *Investig. Ophthalmol. Vis. Sci.* **2014**, *55*, 2963.
- [241] C. S. De Paiva, R. M. Corrales, A. L. Villarreal, W. J. Farley, D. Q. Li, M. E. Stern, S. C. Pflugfelder, *Exp. Eye Res.* **2006**, *83*, 526.
- [242] J. P. Kersey, D. C. Broadway, *Eye* **2006**, *20*, 407.
- [243] D. Stevenson, J. Tauber, B. L. Reis, *Ophthalmology* **2000**, *107*, 967.
- [244] S. Goyal, S. K. Chauhan, Q. Zhang, R. Dana, *Arch. Ophthalmol.* **2009**, *127*, 882.
- [245] H. Kang, K. H. Cha, W. Cho, J. Park, H. J. Park, B. K. Sun, S. M. Hyun, S. J. Hwang, *Int. J. Nanomedicine* **2016**, *11*, 2921.
- [246] W. C. M. Duivenvoorden, E. Seidlitz, H. W. Hirte, R. G. Tozer, G. Singh, *Cancer Res.* **2002**, *62*, 1588.
- [247] J. Stechmiller, L. Cowan, G. Schultz, *Biol. Res. Nurs.* **2010**, *11*, 336.
- [248] D.-Q. Li, Z. Chen, X. J. Song, L. Luo, S. C. Pflugfelder, *Invest. Ophthalmol. Vis. Sci.* **2004**, *45*, 4302.
- [249] C. P. Moore, J. B. McHugh, J. G. Thorne, T. E. Phillips, *Investig. Ophthalmol. Vis. Sci.* **2001**, *42*, 653.
- [250] C. W. Roberts, P. E. Carniglia, B. G. Brazzo, *Cornea* **2007**, *26*, 805.
- [251] A. Okanobo, S. K. Chauhan, M. H. Dastjerdi, S. Kodati, R. Dana, *Am. J. Ophthalmol.* **2012**, *154*, 63.

- [252] F. A. Maulvi, A. A. Shaikh, D. H. Lakdawala, A. R. Desai, M. M. Pandya, S. S. Singhanian, R. J. Vaidya, K. M. Ranch, B. A. Vyas, D. O. Shah, *Acta Biomater.* **2017**, 1.
- [253] C. A. Dinarello, J. W. M. van der Meer, *Semin. Immunol.* **2013**, 25, 469.
- [254] C. Antoni, J. Braun, *Clin. Exp. Rheumatol.* **2002**.
- [255] S. C. Pflugfelder, M. Stern, S. Zhang, A. Shojaei, *J. Ocul. Pharmacol. Ther.* **2016**, 33, 5.
- [256] A. H. Krauss, R. M. Corrales, F. S. A. Pelegrino, J. Tukler-Henriksson, S. C. Pflugfelder, C. S. de Paiva, *Investig. Ophthalmol. Vis. Sci.* **2015**, 56, 5888.
- [257] J. D. Sheppard, G. L. Torkildsen, J. D. Lonsdale, F. A. D'Ambrosio, E. B. McLaurin, R. A. Eiferman, K. S. Kennedy, C. P. Semba, *Ophthalmology* **2014**, 121, 475.
- [258] Q. Tang, J. a Bluestone, *Nat. Immunol.* **2008**, 9, 239.
- [259] S. Jhunjhunwala, G. Raimondi, A. J. Glowacki, S. J. Hall, D. Maskarinec, S. H. Thorne, A. W. Thomson, S. R. Little, *Adv. Mater.* **2012**, 24, 4735.
- [260] D. A. A. Vignali, L. W. Collison, C. J. Workman, *Nat. Rev. Immunol.* **2008**, 8, DOI 10.1038/nri2343.
- [261] M. I. Christodoulou, N. M. Moutsopoulos, H. M. Moutsopoulos, *Am. J. Pathol.* **2008**, 173, 1389.
- [262] M. Yadav, S. Stephan, J. A. Bluestone, *Front. Immunol.* **2013**, 4, 1.
- [263] M. Miyara, S. Sakaguchi, *Trends Mol. Med.* **2007**, 13, 108.
- [264] J. Stein-Streilein, A. W. Taylor, *J. Leukoc. Biol.* **2007**, 81, 593.
- [265] S. Sakaguchi, T. Yamaguchi, T. Nomura, M. Ono, *Cell* **2008**, 133, 775.
- [266] J. M. Stewart, B. G. Keselowsky, *Adv. Drug Deliv. Rev.* **2017**, 1.
- [267] A. Yagci, C. Gurdal, *Int. Ophthalmol.* **2014**, 34, 1291.
- [268] J. L. Riley, C. H. June, B. R. Blazar, *Immunity* **2009**, 30, 656.
- [269] A. J. Glowacki, R. Gottardi, S. Yoshizawa, F. Cavalla, G. P. Garlet, C. Sfeir, S. R. Little, *Ann. Biomed. Eng.* **2015**, 43, 593.
- [270] K. F. Siemasko, J. Gao, V. L. Calder, R. Hanna, M. Calonge, S. C. Pflugfelder, J. Y. Niederkorn, M. E. Stern, *Invest. Ophthalmol. Vis. Sci.* **2008**, 5434.
- [271] R. Baluna, E. S. Vitetta, *Immunopharmacology* **1997**, 37, 117.

- [272] K. Kim, S. W. Park, J. H. Kim, S. H. Lee, D. Kim, T. Koo, K. E. Kim, J. H. Kim, J. S. Kim, *Genome Res.* **2017**, *27*, 419.
- [273] B. Xiao, Y. Wang, P. S. Reinach, Y. Ren, J. Li, S. Hua, H. Lu, W. Chen, *PLoS One* **2015**, *10*, 1.
- [274] B. H. Nelson, *J. Immunol.* **2004**, *172*, 3983.
- [275] M. Vulcano, C. Albanesi, A. Stoppacciaro, R. Bagnati, G. D'Amico, S. Struyf, P. Transidico, R. Bonecchi, a D. Prete, P. Allavena, L. P. Ruco, C. Chiabrande, G. Girolomoni, A. Mantovani, S. Sozzani, *Eur. J. Immunol.* **2001**, *31*, 812.
- [276] H. Ghadially, X.-L. Ross, C. Kerst, J. Dong, A. B. Reske-Kunz, R. Ross, *J. Immunol.* **2005**, *174*, 5620.
- [277] A. C. laudia Araujo-Pires, A. E. spindola Vieira, C. F. avaro Francisconi, C. C. ristina Bigueti, A. Glowacki, S. Yoshizawa, A. P. aula Campanelli, A. P. aula F. Trombone, C. S. Sfeir, S. R. Little, G. P. ompermaier Garlet, *J. bone Miner. Res.* **2015**, *30*, 412.
- [278] A. W. Mailloux, M. R. I. Young, *J. Immunol.* **2009**, *182*, 2753.
- [279] S. Jhunjunwala, G. Raimondi, A. J. Glowacki, S. J. Hall, D. Maskarinec, S. H. Thorne, A. W. Thomson, S. R. Little, *Adv. Mater.* **2012**, *24*, 4735.
- [280] A. J. Glowacki, S. Yoshizawa, S. Jhunjunwala, A. E. Vieira, G. P. Garlet, C. Sfeir, S. R. Little, *Proc. Natl. Acad. Sci. U. S. A.* **2013**, *110*, 18525.
- [281] T. J. Curiel, G. Coukos, L. Zou, X. Alvarez, P. Cheng, P. Mottram, M. Evdemon-Hogan, J. R. Conejo-Garcia, L. Zhang, M. Burow, Y. Zhu, S. Wei, I. Kryczek, B. Daniel, A. Gordon, L. Myers, A. Lackner, M. L. Disis, K. L. Knutson, L. Chen, W. Zou, *Nat. Med.* **2004**, *10*, 942.
- [282] J. Montane, L. Bischoff, G. Soukhatcheva, D. L. Dai, G. Hardenberg, M. K. Levings, P. C. Orban, T. J. Kieffer, R. Tan, C. B. Verchere, *J. Clin. Invest.* **2011**, *121*, 3024.
- [283] J. M. Eby, H.-K. Kang, S. T. Tully, W. E. Bindeman, D. S. Peiffer, S. Chatterjee, S. Mehrotra, I. C. Le Poole, *J. Invest. Dermatol.* **2015**, *135*, 1.
- [284] J. M. Anderson, M. S. Shive, *Adv. Drug Deliv. Rev.* **2012**, *64*, 72.
- [285] K.-C. Yoon, K.-Y. Ahn, W. Choi, Z. Li, J.-S. Choi, S.-H. Lee, S.-H. Park, *Invest. Ophthalmol. Vis. Sci.* **2011**, *52*, 7267.
- [286] F. Gantner, M. Leist, A. W. Lohse, P. G. Germann, G. Tiegs, *Hepatology* **1995**, *21*, 190.
- [287] D. Dursun, M. Wang, D. Monroy, D.-Q. Li, B. L. Lokeshwar, M. E. Stern, S. C. Pflugfelder, *Invest. Ophthalmol. Vis. Sci.* **2002**, *43*, 632.

- [288] S. C. Pflugfelder, C. S. De Paiva, Q. L. Moore, E. A. Volpe, D.-Q. Li, K. Gumus, M. L. Zaheer, R. M. Corrales, *Investig. Ophthalmology Vis. Sci.* **2015**, *56*, 7545.
- [289] D. Coe, S. Begom, C. Addey, M. White, J. Dyson, J. G. Chai, *Cancer Immunol. Immunother.* **2010**, *59*, 1367.
- [290] Y. Wang, D. J. Irvine, *Biomaterials* **2011**, *32*, 4903.
- [291] Y. Wang, D. J. Irvine, *Integr. Biol.* **2013**, *5*, 481.
- [292] X. Zhao, S. Jain, H. B. Larman, S. Gonzalez, D. J. Irvine, *Biomaterials* **2005**, *26*, 5048.
- [293] Y. Gao, K. Min, Y. Zhang, J. Su, M. Greenwood, K. Gronert, *J. Immunol.* **2015**, *195*, 3086.
- [294] S. Létourneau, E. M. M. van Leeuwen, C. Krieg, C. Martin, G. Pantaleo, J. Sprent, C. D. Surh, O. Boyman, *Proc. Natl. Acad. Sci. U. S. A.* **2010**, *107*, 2171.
- [295] L. M. Wakefield, T. S. Winokur, R. S. Hollands, K. Christopherson, A. D. Levinson, M. B. Sporn, *J. Clin. Invest.* **1990**, *86*, 1976.
- [296] P. Hillyer, D. Male, *Immunol. Cell Biol.* **2005**, *83*, 375.
- [297] and G. A. K. Xin Zhou, Maren S. Fragala, Janet E. McElhaney, *Curr Opin Clin Nutr Metab Care* **2010**, *13*, 541.
- [298] R. D. William Stevenson, Sunil K. Chauhan, *Arch. Ophthalmology* **2012**, *130*, 90.
- [299] M. E. Stern, J. Gao, T. A. Schwalb, M. Ngo, D. D. Tieu, C. Chan, B. L. Reis, S. M. Whitcup, D. Thompson, J. A. Smith, *Investig. Ophthalmol. Vis. Sci.* **2002**, *43*, 2609.
- [300] X. Zhang, W. Chen, C. S. De Paiva, R. M. Corrales, E. A. Volpe, A. J. McClellan, W. J. Farley, D. Q. Li, S. C. Pflugfelder, *Investig. Ophthalmol. Vis. Sci.* **2011**, *52*, 6279.
- [301] Z. Zhang, W. Z. Yang, Z. Z. Zhu, Q. Q. Hu, Y. F. Chen, H. He, Y. X. Chen, Z. G. Liu, *Investig. Ophthalmol. Vis. Sci.* **2014**, *55*, 2963.
- [302] M. E. Stern, C. S. Schaumburg, R. Dana, M. Calonge, J. Y. Niederkorn, S. C. Pflugfelder, *Mucosal Immunol.* **2010**, *3*, 425.
- [303] K. S. Kunert, A. S. Tisdale, I. K. Gipson, *Arch. Ophthalmol.* **2002**, *120*, 330.
- [304] T. G. Coursey, N. B. Gandhi, E. A. Volpe, S. C. Pflugfelder, C. S. De Paiva, *PLoS One* **2013**, *8*, DOI 10.1371/journal.pone.0078508.
- [305] J. El Annan, S. K. Chauhan, T. Ecoiffier, Q. Zhang, D. R. Saban, R. Dana, *Invest. Ophthalmol. Vis. Sci.* **2009**, *50*, 3802.

- [306] M. G. Ritt, B. A. Lindborg, T. D. O'Brien, J. Bisignano, J. F. Modiano, *Vet. Sci.* **2015**, *2*, 43.
- [307] D. R. Saban, *Ocul. Surf.* **2014**, *12*, 87.
- [308] B. D. Singer, L. S. King, F. R. D'Alessio, *Front. Immunol.* **2014**, *5*, 1.
- [309] Driss Zoukhri, *Exp. Eye Res.* **2006**, *82*, 885.
- [310] J. Van Loosdregt, Y. Vercoulen, T. Guichelaar, Y. Y. J. Gent, J. M. Beekman, O. Van Beekum, A. B. Brenkman, D. J. Hijnen, T. Mutis, E. Kalkhoven, B. J. Prakken, P. J. Coffey, *Blood* **2010**, *115*, 965.
- [311] S. K. Chauhan, J. El Annan, T. Ecoiffier, S. Goyal, Q. Zhang, D. R. Saban, R. Dana, *J. Immunol.* **2009**, *182*, 1247.
- [312] A. Schmidt, N. Oberle, P. H. Krammer, *Front. Immunol.* **2012**, *3*, 1.
- [313] and P. A. A. Yi Wei, *Eye Contact Lens* **2014**, *40*, 248.
- [314] S. You, L. Poulton, S. Cobbold, C. P. Liu, M. Rosenzweig, D. Ringler, W. H. Lee, B. Segovia, J. F. Bach, H. Waldmann, L. Chatenoud, *PLoS One* **2009**, *4*, 1.
- [315] J. Shimizu, S. Yamazaki, T. Takahashi, Y. Ishida, S. Sakaguchi, *Nat. Immunol.* **2002**, *3*, 135.
- [316] B. J. Kim, Z. Li, R. N. Fariss, D. F. Shen, S. P. Mahesh, C. Egwuagu, C.-R. Yu, C. N. Nagineni, C.-C. Chan, R. B. Nussenblatt, *Invest. Ophthalmol. Vis. Sci.* **2004**, *45*, 3170.
- [317] G. T. S. Kirby, L. J. White, C. V. Rahman, H. C. Cox, F. R. A. J. Rose, D. W. Huttmacher, K. M. Shakesheff, M. A. Woodruff, *Eur. Cells Mater.* **2011**, *22*, 24.
- [318] M. Ye, S. Kim, K. Park, *J. Control. Release* **2010**, *146*, 241.
- [319] S. E. Reinhold, K. G. H. Desai, L. Zhang, K. F. Olsen, S. P. Schwendeman, *Angew. Chemie - Int. Ed.* **2012**, *51*, 10800.
- [320] K. F. Siemasko, J. Gao, V. L. Calder, R. Hanna, M. Calonge, S. C. Pflugfelder, J. Y. Niederkorn, M. E. Stern, *Invest. Ophthalmol. Vis. Sci.* **2008**, 5434.
- [321] S. Kodati, S. K. Chauhan, Y. Chen, T. H. Dohlman, P. Karimian, D. Saban, R. Dana, *Invest. Ophthalmol. Vis. Sci.* **2014**, *55*, 5871.
- [322] S. C. and R. D. Stefano Barabino, Yihe Chen, *Prog. Retin. Eye Res.* **2013**, *31*, 271.
- [323] F. J. Montoya, C. E. Riddell, R. Caesar, S. Hague, *Eye (Lond)*. **2002**, *16*, 705.
- [324] R. L. Avery, D. J. Pieramici, M. D. Rabena, A. A. Castellarin, M. A. Nasir, M. J. Giust, *Am. Acad. Ophthalmol.* **2006**, *113*, DOI 10.1016/j.opthta.2005.11.019.

- [325] K. Ziahosseini, Z. Al-Abbadi, R. Malhotra, *Eye* **2015**, 29, 656.
- [326] M. Y. Avila, *Cornea* **2014**, 33, 18.
- [327] M. V. Fedorchak, I. P. Conner, C. A. Medina, J. B. Wingard, J. S. Schuman, S. R. Little, *Exp. Eye Res.* **2014**, 125, 210.
- [328] Y. Bin Choy, S. R. Patel, J. H. Park, B. E. McCarey, H. F. Edelhauser, M. R. Prausnitz, *Investig. Ophthalmol. Vis. Sci.* **2011**, 52, 2627.
- [329] M. L. Ratay, A. J. Glowacki, S. C. Balmert, A. P. Acharya, J. Polat, L. P. Andrews, M. V. Fedorchak, J. S. Schuman, D. A. A. Vignali, S. R. Little, *J. Control. Release* **2017**, 258, 208.
- [330] S. Sakaguchi, K. Wing, Y. Onishi, P. Prieto-Martin, T. Yamaguchi, *Int. Immunol.* **2009**, 21, 1105.
- [331] D. A. Horwitz, S. G. Zheng, J. Wang, J. D. Gray, *Eur. J. Immunol.* **2008**, 38, 912.
- [332] H. L. and B. Shi, *Cell. Mol. Immunol.* **2015**, 12, 24.
- [333] D. a Vignali, L. W. Collison, C. J. Workman, *Nat. Rev. Immunol.* **2009**, 8, 523.
- [334] S. Jhunjhunwala, S. C. Balmert, G. Raimondi, E. Dons, E. E. Nichols, A. W. Thomson, S. R. Little, *J. Control. release* **2012**, 159, 78.
- [335] V. L. Perez, S. C. Pflugfelder, S. Zhang, A. Shojaei, R. Haque, *Ocul. Surf.* **2016**, 14, DOI 10.1016/j.jtos.2016.01.001.
- [336] J. Hou, S. a Townson, J. T. Kovalchin, A. Masci, O. Kiner, Y. Shu, B. M. King, E. Schirmer, K. Golden, C. Thomas, K. C. Garcia, G. Zarbis-Papastoitis, E. S. Furfine, T. M. Barnes, *Proc. Natl. Acad. Sci. U. S. A.* **2013**, 110, 3913.
- [337] M. J. Lee, D. H. Kim, J. S. Ryu, A. Y. Ko, J. H. Ko, M. K. Kim, W. R. Wee, S. I. Khwarg, J. Y. Oh, *Investig. Ophthalmol. Vis. Sci.* **2015**, 56, 5175.
- [338] S. C. Balmert, A. C. Zmolek, A. J. Glowacki, T. D. Knab, S. N. Rothstein, J. M. Wokpetah, M. V. Fedorchak, S. R. Little, *J. Mater. Chem. B* **2015**, 3, 4723.
- [339] E. Pisani, C. Ringard, V. Nicolas, E. Raphaël, V. Rosilio, L. Moine, E. Fattal, N. Tsapis, *Soft Matter* **2009**, 5, 3054.
- [340] M. Rolando, M. Zierhut, *Surv. Ophthalmol.* **2001**, 45 Suppl 2, S203.
- [341] C. Baudouin, P. Aragona, E. M. Messmer, A. Tomlinson, M. Calonge, K. G. Boboridis, Y. A. Akova, G. Geerling, M. Labetoulle, M. Rolando, *Ocul. Surf.* **2013**, 11, 246.
- [342] Z. Lin, X. Liu, T. Zhou, Y. Wang, L. Bai, H. He, Z. Liu, *Mol. Vis.* **2011**, 17, 257.

- [343] A. D. Cohen, D. A. Schaer, C. Liu, Y. Li, D. Hirschhorn-Cymerman, S. C. Kim, A. Diab, G. Rizzuto, F. Duan, M. A. Perales, T. Merghoub, A. N. Houghton, J. D. Wolchok, *PLoS One* **2010**, *5*, DOI 10.1371/journal.pone.0010436.
- [344] and C. S. de P. Pflugfelder, Stephen C. Rosa M. Corrales, *Exp. Eye Res.* **2013**, *117*, 520.
- [345] N. J. Friedman, *Curr. Opin. Ophthalmol.* **2010**, *21*, 310.
- [346] M. a Lemp, *Am. J. Ophthalmol.* **2008**, *146*, 350.
- [347] M. Guzmán, I. Keitelman, F. Sabbione, A. S. Trevani, M. N. Giordano, J. G. Galletti, *Clin. Exp. Immunol.* **2015**, *184*, 248.
- [348] M. T. Brady, J. M. Yanni, *J. Ocul. Pharmacol. Ther.* **2005**, *21*.
- [349] C. Baudouin, *Surv. Ophthalmol.* **2001**, *45*, S211.
- [350] F. Brewitt H. Sistani, *Surv. Ophthalmol.* **2001**, *45*, 199.
- [351] J. M. Tiffany, *Eye (Lond)*. **2003**, *17*, 923.
- [352] S. C. Pflugfelder, R. M. Corrales, C. S. de Paiva, *Exp. Eye Res.* **2013**, *117*, 118.
- [353] C. S. De Paiva, A. L. Villarreal, R. M. Corrales, H. T. Rahman, V. Y. Chang, W. J. Farley, M. E. Stern, J. Y. Niederkorn, D.-Q. Li, S. C. Pflugfelder, *Invest. Ophthalmol. Vis. Sci.* **2007**, *48*, 2553.
- [354] A. J. Bron, P. Argueso, M. Irkec, F. V. Bright, *Prog. Retin. Eye Res.* **2015**, *44*, 36.
- [355] C. S. De Paiva, R. M. Corrales, A. L. Villarreal, W. J. Farley, D. Q. Li, M. E. Stern, S. C. Pflugfelder, *Exp. Eye Res.* **2006**, *83*, 526.
- [356] R. Palacios, *J. Immunol.* **1982**, *128*, 337.
- [357] K. Ververis, A. Hiong, T. C. Karagiannis, P. V. Licciardi, *Biol. Targets Ther.* **2013**, *7*, 47.
- [358] T. Akimova, U. H. Beier, Y. Liu, L. Wang, W. W. Hancock, *Blood* **2012**, *119*, 2443.
- [359] R. Tao, E. F. de Zoeten, E. Ozkaynak, C. Chen, L. Wang, P. M. Porrett, B. Li, L. a Turka, E. N. Olson, M. I. Greene, A. D. Wells, W. W. Hancock, *Nat. Med.* **2007**, *13*, 1299.
- [360] C. Chen, L. Wang, P. M. Porrett, B. Li, R. Tao, E. F. De Zoeten, O. Engin, L. A. Turka, E. N. Olson, M. I. Greene, A. D. Wells, W. W. Hancock, *Nat. Med.* **2007**, *13*, 1299.
- [361] B. Li, A. Samanta, X. Song, K. T. Iacono, K. Bembas, R. Tao, S. Basu, J. L. Riley, W. W. Hancock, Y. Shen, S. J. Saouaf, M. I. Greene, H. T. N-terminal, *Proc. Natl. Acad. Sci. U. S. A.* **2007**, *104*, 4571.

- [362] Y. Sun, Y. E. Chin, E. Weisiger, C. Malter, I. Tawara, T. Toubai, E. Gatza, P. Mascagni, C. A. Dinarello, P. Reddy, *J. Immunol.* **2009**, *182*, 5899.
- [363] T. G. Coursey, J. T. Henriksson, F. L. Barbosa, C. S. de Paiva, S. C. Pflugfelder, *Am. J. Pathol.* **2016**, *186*, 1.
- [364] Gangaraju Vamsi K. Lin Haifan, *Curr. Opin. Clin. Immunol.* **2014**, *14*, 467.
- [365] M. E. Stern, J. Gao, K. F. Siemasko, R. W. Beuerman, S. C. Pflugfelder, *Exp. Eye Res.* **2004**, *78*, 409.
- [366] Q. Tang, J. a Bluestone, *Nat. Immunol.* **2008**, *9*, 239.
- [367] J. Johnson, A. Pahuja, M. Graham, B. Hering, W. W. Hancock, P. Bansal-Pakala, *Transplant. Proc.* **2008**, *40*, 459.
- [368] F. Blanchard, C. Chipoy, *Drug Discov. Today* **2005**, *10*, 197.
- [369] T. Akimova, G. Ge, T. Golovina, T. Mikheeva, L. Wang, J. L. Riley, W. W. Hancock, *Clin. Immunol.* **2010**, *136*, 348.
- [370] X. Rong, W. Yuan, Y. Lu, X. Mo, *Int. J. Nanomedicine* **2014**, *9*, 3057.
- [371] and W. W. H. Edwin F. De Zoeten, Liqing Wang, Hong Sai, Wolfgang H. Dillmann, *Gastroenterology* **2010**, *138*, 583.
- [372] E. Badaro, E. A. Novais, F. M. Penha, M. Maia, M. E. Farah, E. B. Rodrigues, S. Paulo, *Curr. Eye Reseach* **2014**, 1.
- [373] D. Zoukhri, A. Fix, J. Alroy, C. L. Kublin, *Investig. Ophthalmol. Vis. Sci.* **2008**, *49*, 4399.
- [374] J. D. Nelson, H. Helms, R. Fiscella, Y. Southwell, J. D. Hirsch, *Adv. Ther.* **2000**, *17*, 84.
- [375] S. Goyal, S. K. Chauhan, Q. Zhang, R. Dana, *Arch. Ophthalmol.* **2009**, *127*, 882.
- [376] Y. Chen, S. K. Chauhan, H. S. Lee, D. R. Saban, R. Dana, *Mucosal Immunol.* **2014**, *7*, 38.
- [377] M. E. Stern, C. S. Schaumburg, S. C. Pflugfelder, *Int. Rev. Immunol.* **2013**, *32*, 19.
- [378] M. L. Massingale, X. Li, M. Vallabhajosyula, D. Chen, Y. Wei, P. A. Asbell, *Cornea* **2009**, *28*, 1023.
- [379] K. S. Na, J. W. Mok, J. Y. Kim, C. R. Rho, C. K. Joo, *Investig. Ophthalmol. Vis. Sci.* **2012**, *53*, 5443.
- [380] S. K. Chauhan, D. R. Saban, H. K. Lee, R. Dana, *J. Immunol.* **2009**, *182*, 148.
- [381] J. Frikeche, Z. Peric, E. Brissot, M. Grégoire, B. Gaugler, M. Mohty, *Exp. Hematol.* **2012**, *40*, 783.

- [382] J. L. Lucas, P. Mirshahpanah, E. Haas-Stapleton, K. Asadullah, T. M. Zollner, R. P. Numerof, *Cell. Immunol.* **2009**, *257*, 97.
- [383] L. Wang, E. F. de Zoeten, M. I. Greene, W. W. Hancock, *Nat. Rev. Drug Discov.* **2009**, *8*, 969.
- [384] K. Fu, a M. Klibanov, R. Langer, *Nat. Biotechnol.* **2000**, *18*, 24.
- [385] S. D'Souza, L. Tong, *Eye Vis.* **2014**, *1*, 6.
- [386] L. Tong, L. Zhou, R. Beuerman, S. Simonyi, D. A. Hollander, M. E. Stern, *Ocul. Surf.* **2016**, *1*.
- [387] and C. D. Lei Ahou, Ruihua Wei, Ping Zhao, Siew Kwan Koh, Roger W Beuerman, *Mol. Vis.* **2013**, *13*, 2469.
- [388] M. V. Fedorchak, I. P. Conner, J. S. Schuman, A. Cugini, S. R. Little, *Sci. Rep.* **2017**, *7*, 8639.
- [389] M. V. Fedorchak, I. P. Conner, A. Cugini, J. S. Schuman, S. R. Little, *Sci. Rep.* **2017**, *7*, DOI 10.1038/s41598-017-09379-8.
- [390] J. E. Mealy, M. V Fedorchak, S. R. Little, *Acta Biomater.* **2014**, *10*, 87.
- [391] W. Linert, I. Lukovits, *J. Chem. Inf. Model.* **2007**, *47*, 887.
- [392] K. Kamalasanan, R. Gottardi, S. Tan, Y. Chen, B. Godugu, S. Rothstein, A. C. Balazs, A. Star, S. R. Little, *Angew. Chem. Int. Ed. Engl.* **2013**, *52*, 11308.
- [393] R. H. Baughman, A. a Zakhidov, W. a de Heer, *Science* **2002**, *297*, 787.
- [394] M. Prato, K. Kostarelos, *Acc. Chem. Res.* **2008**, *41*, 60.
- [395] R. Gottardi, B. Douradinha, *J. Nanobiotechnology* **2013**, *11*, 30.
- [396] W. Yang, P. Thordarson, J. J. Gooding, S. P. Ringer, F. Braet, *Nanotechnology* **2007**, *18*, 412001.
- [397] N. Nakayama-ratchford, S. Bangsaruntip, X. Sun, K. Welsher, S. U. V, *JACS* **2006**, *129*, 2448.
- [398] N. Karousis, N. Tagmatarchis, D. Tasis, *Chem. Rev.* **2010**, *110*, 5366.
- [399] S. Banerjee, T. Hemraj-Benny, S. S. Wong, *Adv. Mater.* **2005**, *17*, 17.
- [400] V. Mittal, *Surf. Modif. Nanotub. Fill.* **2011**.
- [401] G. Ghini, C. Trono, a. Giannetti, G. L. Puleo, L. Luconi, J. Amadou, G. Giambastiani, F. Baldini, *Sensors Actuators B Chem.* **2013**, *179*, 163.

- [402] M. a. Hamon, H. Hui, P. Bhowmik, H. M. E. Itkis, R. C. Haddon, *Appl. Phys. A Mater. Sci. Process.* **2002**, *74*, 333.
- [403] H. Hu, P. Bhowmik, B. Zhao, M. a Hamon, M. E. Itkis, R. C. Haddon, *Chem. Phys.* **2001**, *345*, 25.
- [404] F. Pompeo, D. E. Resasco, *Nano Lett.* **2002**, *2*, 369.
- [405] M. E. Itkis, D. E. Perea, S. Niyogi, S. M. Rickard, M. A. Hamon, H. Hu, B. Zhao, R. C. Haddon, *Nano Lett.* **2003**, *3*, 309.
- [406] D. Bom, R. Andrews, D. Jacques, J. Anthony, *Nano Lett.* **2002**, *2*, 615.
- [407] E. Hirata, C. Ménard-Moyon, E. Venturelli, H. Takita, F. Watari, A. Bianco, A. Yokoyama, *Nanotechnology* **2013**, *24*, 435101.
- [408] J. Lejosne, G. Mercier, V. Mamane, Y. Fort, J. F. Marêché, E. McRae, F. Valsaque, B. Vigolo, *Carbon N. Y.* **2011**, *49*, 3010.
- [409] H. Peng, L. B. Alemany, J. L. Margrave, V. N. Khabashesku, *J. Am. Chem. Soc.* **2003**, *125*, 15174.
- [410] X. Lu, Z. Chen, P. V. R. Schleyer, *J. Am. Chem. Soc.* **2005**, *127*, 20.
- [411] G. Cao, X. Chen, J. W. Kysar, *J. Mech. Phys. Solids* **2006**, *54*, 1206.
- [412] V. M. Irurzun, M. P. Ruiz, D. E. Resasco, *Carbon N. Y.* **2010**, *48*, 2873.
- [413] P. C. Pinheiro, A. L. Daniel-da-Silva, D. S. Tavares, M. P. Calatayud, G. F. Goya, T. Trindade, *Materials (Basel)*. **2013**, *6*, 3213.
- [414] a Jimeno, S. Goyanes, a Eceiza, G. Kortaberria, I. Mondragon, M. a Corcuera, *J. Nanosci. Nanotechnol.* **2009**, *9*, 6222.
- [415] Z. Shi, Y. Lian, F. Liao, X. Zhou, Z. Gu, Y. Zhang, S. Iijima, *Solid State Commun.* **1999**, *112*, 35.
- [416] J. L. Bahr, J. M. Tour, *J. Mater. Chem.* **2002**, *12*, 1952.
- [417] F. G. Brunetti, M. A. Herrero, J. D. M. Mun, A. Di, J. Alfonsi, M. Meneghetti, M. Prato, E. Va, S. Farmaceutiche, V. Uni, *J. Am. Chem. Soc.* **2008**, *130*, 8094.
- [418] S. K. Smart, a. I. Cassady, G. Q. Lu, D. J. Martin, *Carbon N. Y.* **2006**, *44*, 1034.
- [419] M. a Hahn, A. K. Singh, P. Sharma, S. C. Brown, B. M. Moudgil, *Anal. Bioanal. Chem.* **2011**, *399*, 3.
- [420] K. Welsher, Z. Liu, S. P. Sherlock, J. T. Robinson, Z. Chen, D. Daranciang, H. Dai, *Nat. Nanotechnol.* **2009**, *4*, 773.